The role of microbial CO_2 fixation for belowground carbon cycling and its influence on carbon isotopic signatures

Dissertation

To Fulfill the

Requirements for the Degree of

„doctor rerum naturalium“ (Dr. rer. nat.)

Submitted to the Council of the

Faculty of Biology and Pharmacy

of the Friedrich Schiller University Jena

by Martin Nowak

born on 10.09.1983 in Mikołow

Gutachter:

1. Prof. Susan Trumbore, PhD
   Max Planck Institut für Biogeochemie Jena

2. Prof. Dr. Erika Kothe
   Institut für Mikrobielle Kommunikation, Friedrich Schiller Universität Jena

3. Prof. Dr. Marcus Horn
   Institut für Mikrobiologie, Leibniz Universität Hannover

Tag der Verteidigung: 30 März 2017

Acknowledgements

There are many people who helped me during the course of my PhD time at the Max Planck Institute for Biogeochemistry in Jena.

First of all, I want to thank my supervisors Prof. Susan Trumbore and Prof. Dr. Kirsten Küsel. I would like to thank you for giving me the opportunity to conduct my PhD under your supervision, for guiding me through my PhD time, for fruitful discussions about data and research, revision of my manuscripts and encouraging me during writing this thesis.

The funding from the DFG Research Training Group GRK 1257 "Alteration and element mobility at the microbe- mineral interface" and the International Max-Planck Research School for Global Biogeochemical Cycles (IMPRS gBGC) is kindly acknowledged.

I thank Thomas Behrendt for support and advice regarding samples, measurements and the great time in Brazil.

I thank Stefen Rühlow for advising me in HPLC-IRMS measurements, Heike Geilmann for isotope measurements of bulk carbon and nitrogen, Steffen Knabe and Michael Rothe for gas measurements, Ines Hilke and Birgit Fröhlich for C and N measurements and Heike Machts and Axel Steinhof for radiocarbon analyses. Special thanks goes to the student helpers Christian Seiffet and Sandy Laschke for their big efforts in the laboratory.

Professor Riccardo Krüger is acknowledged for the support and valuable discussions during my research stay at the Department of Cell Biology, University of Brasilia.

I thank Beto Quesada, Reiner Ditz, Steffan Wolf and Ana Maria Yanez Serrano for field and lab support in Manaus and the ATTO site.

I thank my colleagues and friends from the GRK research training school and IMPRS for the cooperation and friendship, especially Ashish Malik, Emily Solly, Saadat Malghani, Stefan Karlowsky, Carsten Simon, Somak Chowdhury, Huei Ying Gan, Zhang Haiyang and Jenia Singh.

I also want to thank all the co-authors of the papers for good collaboration and valuable input and comments on the manuscripts.

My greatest thank goes to my family, my parents Damian and Hermine Nowak, my brothers Dominik and Alexander as well as my mother in law Christine. Our meetings and calls were always a big source of strength and moral support. My biggest gratitude goes to my wife Caroline. Thank you for always being there for me and supporting me in any kind of situation.

1 Introduction

1.1 Background

The concentration of carbon dioxide (CO_2) in the atmosphere has increased from approximately 277 parts per million (ppm) in 1750, the beginning of the industrial era, to 397 ppm in 2014, mainly caused by anthropogenic emissions derived from fossil fuel burning and land use change (Le Quere et al., 2015). Anthropogenic emissions occur on top of an active natural carbon cycle that circulates carbon between the atmosphere, ocean, and terrestrial biosphere reservoirs on timescales from days to millennia.

Rising CO_2 concentrations are perturbing this global carbon cycle as well as climate through radiative forcing and complex feedback processes between ecosystems and climate (Heimann and Reichstein, 2008). Predicting the extent of the perturbations and their influence on global climate remains a difficult task, although earth observations and global models improved in recent years. Predictions contain huge uncertainties, mainly because biological processes behind the climate-ecosystem feedbacks are poorly constraint (Friedlingstein et al., 2006; Heimann and Reichstein, 2008).

Within the global carbon cycle, C migrates through the reservoirs atmosphere (CO_2 and methane), land (soil organic matter), biomass (plants), oceans (bicarbonate and dissolved CO_2) and other aquatic systems like lakes or groundwater (carbonates, bicarbonate and dissolved CO_2) as well as sediments and rocks (carbonates, coal, gas or oil).

Understanding the global carbon cycle as well as the exchange and transformation of C between its compartments is key for understanding the fate of carbon within the different pools and its impact on climate.

Soils are the biggest carbon pool within terrestrial ecosystems and are a crucial part of the global carbon cycle (Amundson, 2001). Stocks of soil organic matter are estimated up to 1550 Pg in the upper 1 meter, which is three times more than either in the atmosphere or plant biomass, and increase to more than 2330 Pg, if the carbon stocks down to 3 meter depth are taken into account (Jobbagy

and Jackson, 2000). The importance of soil organic matter is not only constituted by its size, but also by its fast interaction with atmospheric CO_2 through soil respiration (Trumbore and Czimczik, 2008). Although short-term fluxes of carbon between biosphere, soil and atmosphere are well constraint, high uncertainty exists in our understanding about the origin and long-term fate of soil organic matter (Torn et al., 1997).

The concepts of soil carbon formation and stabilization changed in recent years, challenging your understanding of how interactions between soil and atmosphere might act under a changing climate (Trumbore and Czimczik, 2008).

New concepts highlight that soil microorganisms play a key role in soil carbon stabilization and formation (Ekschmitt et al., 2008). They do not only control soil carbon cycling through their growth and activity, but also through their diversity and different carbon utilization (Schimel and Schaeffer, 2012). The microbial diversity in soil is high and numbers of archaea, bacteria and fungi can reach many thousands of individual taxa (Schimel and Schaeffer, 2012). However, the functional significance of this great diversity remains largely unknown, rising the question, who is there, who is active and who is doing what.

Although chemical recalcitrance and physical isolation from decomposers (e.g. in soil aggregates) have been regarded as main stabilization factors, recent studies revealed a mismatch between the intrinsic stability of soil organic matter compounds and its persistence in soils (Schmidt et al., 2011). A concept that addresses this mismatch is that plant carbon is processed by soil microorganisms, which either respire it as CO_2 or transform and stabilize it as soil organic matter (Kogel-Knabner, 2002; Miltner et al., 2012). The generated carbon can be recycled by other microorganisms many times, leading to a decoupling of the molecules age from its molecular composition (Gleixner, 2013).

A microbial process that can contribute to carbon recycling is microbial CO_2 fixation, i.e. the utilization of CO_2 as a building block for newly synthesised organic carbon. CO_2 fixation has been shown to be a common process in soils (Miltner et al., 2005; Santruckova et al., 2005; Yuan et al., 2012). However, its contribution to soil carbon and influence on soil geochemical parameters like isotope signatures is little constraint.

CO_2 fixation is not only a process that is acting in soils but might also be a significant process in groundwater.

Groundwater is immediately connected with soils and together they are part of the so called "Critical Zone". The Critical Zone includes the land surface and extends through the pedosphere, unsaturated vadose zone and saturated groundwater zone. Interactions between the compartments of the Critical Zone determine the availability of nearly every life-sustaining resource (NRC, 2001). Soils are recharging groundwater aquifers and strongly determine their physicochemical and biological properties. If carbon input from soils to the aquifer is limited, microbial communities might rely on other, subsurface derived carbon sources (Küsel et al., 2016). CO_2 fixing microorganisms might play an important role in these habitats as primary producers for other organisms leading to a decoupling of the subsurface carbon cycle from the surface. However, their contribution for subsurface carbon cycling is still very poorly constraint (Alfreider et al., 2003; Simkus et al., 2016).

This thesis aims at improving our knowledge about the contribution of microbial CO_2 fixation for carbon formation in the subsurface, its contribution to carbon recycling and its influence on the carbon isotopic composition of carbon in soils and groundwater.

1.2 Carbon cycling in soils

Organic matter is an important resource, which plays a key role in determining the physical, chemical and biological properties of soils (Trumbore and Czimczik, 2008; Young and Crawford, 2004). Soil organic matter is a heterogeneous mixture of materials that range at different stages of decomposition, ranging from unaltered plant materials to highly decomposed humus (Kogel-Knabner, 2002). Plants are a major source of carbon to soils. Plant inputs are broken down by soil microorganisms, transformed and respired as CO_2 (Trumbore and Czimczik, 2008). One part of the carbon gets assimilated by soil microorganisms, which generate microbial biomass and microbial by-products like extracellular polymeric substances (EPS) or exoenzymes (Schimel and Schaeffer, 2012). Some

of this carbon can get recycled to form new microbial biomass (Gleixner et al., 2002).

Although recalcitrant substances like pyrogenic constituents might accumulate, because they are hard to decompose, most of soil organic matter is made of simple molecules that organize through interactions with reactive surfaces and with each other (Trumbore and Czimczik, 2008). An important new concept includes the idea that soil microorganisms are a major source and stabilization factor for soil organic matter (Miltner et al., 2012). Most organic matter is therefore derived from dead microbial cell fragments (i.e. necromass), which can get recycled or stabilized in the soil. This concept also implies that there might be other sources of soil organic matter than plant material, since microorganisms are metabolically versatile and able to recycle soil organic matter or to use other substrates like CO_2 as a carbon source (Malik and Gleixner, 2013; Miltner et al., 2005).

1.3 Carbon cycling in groundwater

Dissolved inorganic carbon (DIC) consists of the species $H_2CO_3^*$, HCO_3^- and CO_3^{-2}. DIC is an important constituent in the carbon cycle of groundwater systems and a useful tool for studying carbon cycling in aquatic and hydrogeological systems (Barth and Veizer, 1999; Bethke and Johnson, 2008). The starting point for the groundwater carbon cycle are weathering reactions through dissolved CO_2 derived from the soil of the recharge area. Most groundwaters start as meteoric waters and percolate through the soils into the subsurface. Dissolved inorganic carbon is gained by dissolution of CO_2 and carbonate weathering. Groundwater is usually in equilibrium with calcite, which controls pH and equilibrium of carbonate species.

Another carbon source is dissolved organic carbon (DOC). Oxidation of DOC is accomplished by aerobic bacteria, which consume oxygen. If all O_2 is depleted, then anaerobic bacteria will consume the remaining organic matter using terminal electron acceptors such as NO_3^-, Fe^{3+} or SO_4^{2-}.

Different carbon pools are linked through acid-base and redox reactions, which are most often mediated by bacteria. Recent research highlighted that aquifer

foodwebs might be more independent from the surface than thought previously, feeding on in situ formed carbon, e.g. from autotrophic microorganisms (Hutchins et al., 2016).

1.4 Microbial CO_2 fixation

Microorganisms that solely depend on CO_2 as carbon source are called autotrophs. They are important primary producers in different ecosystems (Berg, 2011) (figure 1.1). Autotrophs can either use the energy of light (phototrophs) or reduced inorganic compounds (chemolithoautotrophs) to gain energy for CO_2 fixation. Photoautotrophy and chemolithoautotrophy are the only two pathways on earth, which allow generation of new organic carbon. They are therefore the backbone of the carbon cycle. CO_2 is a ubiquitous carbon source, which can be converted from an oxidation state of +4 to an average oxidation state of 0 (reduced cellular carbon). These reactions require reducing equivalents and energy. Energy is provided by ATP hydrolysis and reducing equivalents are NADPH or reduced ferredoxin (Fuchs, 2011). An enzyme links either CO_2 or HCO_3^- with an organic acceptor molecule, which must be regenerated in the following steps of the pathway. Each autotrophic pathway produces a product, from which carbohydrates, proteins, nucleic acids or lipids can be derived (Fuchs, 2011). Key enzymes, which catalyse the carboxylation reaction can appear in large amounts within the cell. Eukaryotic CO_2 fixation through plants is only possible through the Calvin Benson Cycle, whereas prokaryotic CO_2 fixation can be accomplished through six possible metabolic pathways, (1) the Calvin Benson Cycle, (2) the Reverse Citric Acid Cycle, (3) the Reductive Acetyl CoA Cycle, (4) the Hydroxypropionat Cycle, (5) Dicarboxylate/4-Hydroxybutyrate Cycle and (6) 3-Hydroxypropionate/4-Hydroxybutyrate Cycle (Fuchs, 2011) (figure 1.1).

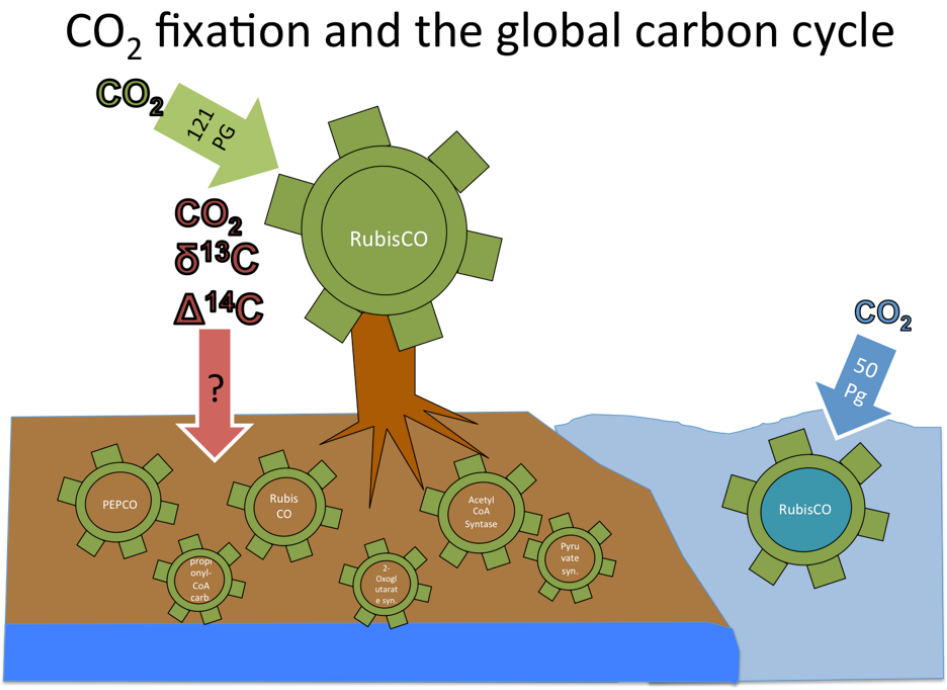

Figure 1-1: RubisCO is the most abundant enzyme in the world and is an important part of the global carbon cycle. It allows plants and marine algae to act as primary producers in terrestrial and marine ecosystems. However, also microorganisms in soil and groundwater have the capability to fix CO_2. Since they are metabolically versatile they have also other enzymes for CO_2 assimilation. However, little is known about the importance of CO_2 fixing microbes in the subsurface and their influence on geochemical parameters like isotope signatures.

1.4.1 The Calvin Benson Cycle

The Calvin Benson Cycle is the most common CO_2 fixation pathway used by many photoautotrophs and chemolitoautotrophs (Fuchs, 2011; Yuan et al., 2012). The Calvin Benson cycle has a high robustness to molecular oxygen (Berg, 2011). The fixation pathway can be subdivided into three stages, a fixation, reduction and regeneration stage. It requires NADPH and ATP as well as the key enzymes Ribulosebiphosphat-Carboxylase (RubisCO) and Phosphoribulose-Kinase (Berg, 2011).

The first step is catalysed by RubisCO, which binds CO_2 on Ribulose-1,5-biphosphate. The product disintegrates to two molecules of 3-phosphoglycerate. 3-phosphoglycerate gets reduced to glycerinaldehyd 3-phosphate, which is an intermediate of glycolysis, the stepwise degradation of glucose. From this stage, glucose can be formed by converting two molecules triosephosphate to fructose-

1,6-biphosphate. The following steps regenerate ribulose-1,5-biphosphate for further CO_2 fixation. The Calvin Benson cycle can not only function as an CO_2 fixation pathway but also as an electron sink for some bacteria, which grow photoheterotrophic on substrates which are more reduced than cell carbon (Berg, 2011).

RubisCO exists in four distinct forms (I, II, III and IV) (Badger and Bek, 2008). These forms have different structure, catalytic activity and O_2 sensitivity. RubisCO is not able to discriminate between the two molecules CO_2 and O_2 (Badger and Bek, 2008). The evolution of the different forms is a consequence of adaptation to different environmental conditions (Berg, 2011). RubisCO enzymes participating in CO_2 fixation are form I and form II. Form I consists of eight large and eight small subunits, whereas form II contains only the large subunit. Form I has usually lower catalytic turnover rate and efficiency, but a higher CO_2 specificity to CO_2 than form II RubisCO. Bacteria possessing form II RubisCO grow preferentially under anoxic or microoxic conditions, where the high affinity of form II to O_2 is not a problem (Alfreider et al., 2012).

For fixing six molecules of CO_2 via the Calvin Benson Cycle, 12 molecules of NADPH are required and 18 ATP are consumed. The Calvin Benson cycle has therefore a high energy demand. The fixation via the Calvin Benson Cycle is the most important autotrophic pathway in the biosphere. It is used by plants and algae, cyanobacteria, anoxygenic phototrophic bacteria and chemolithoautotrophic bacteria.

1.4.2 Acetyl CoA pathway

Chemolithoauotrophic methanogens, sulphidogens and acetogens use the reductive acetyl-CoA pathway for CO_2 fixation (Saini et al., 2011). Two moles of CO_2 are converted to acetyl-CoA. In contrast to other CO_2 fixation pathways, the acetyl-CoA pathway is noncyclic. One CO_2 gets reduced to a carbonyl group and the other one to a methyl group. Both groups are aggregated at the end of the cycle to form acetyl-CoA (Ragsdale and Pierce, 2008). The acetyl CoA pathway is the most common pathway under anaerobic conditions (Berg, 2011). It is preferred by microorganisms which live close to the thermodynamic limit, like

acetogens or methanogens (Berg, 2011). It is the only autotrophic pathway that can simultaneously fix CO_2 and generate ATP by converting acetyl CoA to acetate and may act therefore also for energy conservation . The reductive acetyl CoA pathway is used by acetogenic bacteria, sulphate reducing bacteria, methanogenic archaea as well as some denitrifiers (Berg, 2011). The pathway can further be used for the assimilation of C1 compounds like CO, formaldehyde and methanol. Acetoclastic methanogenic archaea disproportionate acetate through the pathway into methane plus CO_2, and hydrogenotrophic methanogens use the methyl branch for methane formation in addition to autotrophic CO_2 fixation (Saini et al., 2011). The pathway requires strict anoxic conditions, since some of its enzymes are highly oxygen sensitive, which restricts organisms using the acetyl-CoA pathway to anoxic environments (Berg, 2011).

1.4.3 Reductive citric acid cycle

The reductive citric acid cycle is a reversal of the citric acid cycle, generating acetyl-CoA from 2 CO_2 rather than inversely oxidizing acetyl-CoA. The pathway acts under anaerobic conditions. Several irreversible steps of the citric cycle need to be modified to turn the cycle into the reductive direction (Berg, 2011). Two enzymes, which are coupled to ferredoxin, catalyse the reductive fixation of CO_2. These are the carboxylation of succinyl-CoA to 2-oxoglutarate and the carboxylation of acetyl CoA to pyruvate. Although some biochemical adaptations to oxic conditions are known, this pathway involves enzymes that are sensitive to oxygen and is therefore mainly found in anaerobes and microaerophiles (Alfreider and Vogt, 2012).

The reductive citric acid cycle was first found in the green sulphur bacteria *Chlorobium limicola*, in Delta-Proteobacteria and in members of *Aquificae* (Berg, 2011).

1.4.4 3-hydroxypropionate cycle

The phototrophic green nonsulfur bacterium *Chloroflexus aurantiacus* and related *Chloroflexi* use the 3-hydroxypropionate cycle for autotrophic CO_2

fixation under aerobic conditions. The pathway includes the carboxylation of acetyl-CoA and propionyl-CoA. Key enzymes are acetyl-CoA carboxylase and propionyl-CoA carboxylase. The carboxylation includes CO_2 fixation to glycosylate. The pathway seems to be a single invention and has not been found elsewhere (Berg et al., 2010a).

1.4.5 Dicarboxylate/4-hydroxybutyrate cycle

The cycle was described in Crenarchaeota, in members of anaerobic Desulfurococcales and Thermoproteales (Berg et al., 2010b). This cycle can be divided into two parts. Carboxylation is performed by the oxygen-sensitive pyruvate synthase and phosphoenolpyruvate carboxylase (Berg et al., 2010b). In the first part, acetyl-CoA, one CO_2, and one bicarbonate are transformed via dicarboxylic acids to succinyl-CoA. In the second part, succinyl-CoA is converted via 4-hydroxybutyrate to two molecules of acetyl-CoA. One acetyl-CoA can be used for biosynthesis and the other serves as CO_2 acceptor for the next round of the cycle.

1.4.6 3-hydroxypropionate/4-hydroxybutyrate cycle

This cycle functions in aerobic autotrophic Crenarcheota (Berg et al., 2010b). The enzymes of the cycle are oxygen tolerant. In the cycle, one molecule of acetyl-CoA is formed from two molecules of bicarbonate. The cycle can be divided into two parts. The first part transforms acetyl-CoA and two bicarbonate molecules via 3-hydroxypropionate to succinyl-CoA and the second part converts succinyl CoA via 4-hydroxybutyrate to two acetyl-CoA molecules (Berg et al., 2007). This pathway might play an important role in ocean carbon cycling (Berg et al., 2007).

1.4.7 Comparison of autotrophic CO_2 fixation pathways

Comparison of the described CO_2 fixation pathways shows that anaerobic pathways act much more efficient than aerobic ones. Fixation of three moles of CO_2 via the reductive acetyl-CoA pathway requires only four moles of ATP, five

moles of ATP via the reductive citric acid cycle and nine moles of ATP via the Calvin Benson cycle. This is meaningful, because organisms living under anaerobic restrictions do not have a respiratory chain and have therefore less energy available for CO_2 fixation.

1.4.8 Heterotrophic CO_2 fixation

Additionally to its important role as respiratory pathway, the citric acid cycle serves as a provider for obligatory precursors of macromolecular constituents of the cell. For example, oxaloacetate serves as a precursor for the amino acid asparate, an essential building block of proteins and nucleic acids. The growth of microorganisms is therefore accompanied by a continuous removal of oxaloacetate and other intermediates from the citric acid cycle, which have to be replenished. This can be done by anaplerotic reactions, where CO_2 is added to pyruvate or phosphoenopyruvate to form oxaloacetate. The two responsible carboxylases are pyruvate carboxylase and phosphoenolpyruvate carboxylase (Feisthauer et al., 2008). All heterotrophic prokaryotic and eukaryotic organisms are able to fix CO_2 and three to eight percentage of their biomass may originate from carboxylation reactions (Feisthauer et al., 2008).

1.5 Microbial CO_2 fixation in soils

Ehleringer et al. (2000) hypothesised that an increasing contribution of microbial carbon accompanied with heterotrophic CO_2 fixation is responsible for changes in $\delta\,^{13}C$ values of soil organic matter with depth. Diffusion processes into the cell and subsequent ^{13}C enrichment within the microbial cell were used to explain isotope shifts in soil organic matter towards more positive $\delta\,^{13}C$ values. Santruckova et al. (2005) proved dark incorporation of CO_2 in aerobic soils at different pH under elevated and ambient CO_2 concentrations using $^{14}CO_2$ and referred it to heterotrophic CO_2 fixation. Most of the label was incorporated into extracellular metabolites, whereas only 1% was found within the cell. Miltner et al. (2004) and Miltner et al. (2005) tracked labelled CO_2 into bacterial and fungal amino and fatty acids in dark soil incubation experiments of

agricultural and organic rich soils under aerobic conditions. CO_2 fixation was positively correlated with soil respiration. After 81 days of incubation 3 to 5 % of respired CO_2 was re-fixed in the incubated soils and carbon derived from CO_2 accounted for 0.05 % of total carbon in the soil.

Beside heterotrophic CO_2 fixation also photoautotrophic and chemolithoautotrophic CO_2 fixation has been shown to be an abundant process in soils.

Selesi et al. (2005) showed that in differently managed agricultural soils diverse bacteria exhibited cbbL genes that encode for RubisCO, the key enzyme of the Calvin Benson cycle. Further, Selesi et al. (2007) quantified by real time PCR the abundance of cbbL genes and highlighted their high abundance in agricultural soils. cbbL genes were mainly quantified in the clay fraction, whereas almost no genes could be detected in the sand fraction.

Tolli and King (2005) investigated obligate and facultative autotrophs in forest and agricultural soils and found that chemolithoautotrophic populations respond differentially to plant type and land use.

Direct incorporation of $^{14}CO_2$ into microbial biomass has been demonstrated for paddy and upland soils in illuminated incubations (Yuan et al., 2012). Measured rates were positively correlated with cbbL gene abundance and RubisCO activity. Significant CO_2 uptake was only measured when incubated under light, leading to the conclusion that CO_2 fixation was predominantly a phototrophic process conducted by autotrophs rather than heterotrophs (Yuan et al., 2012). Further, facultative rather than obligate autotrophic bacteria have been identified to be mainly responsible for CO_2 uptake. Measured uptake rates were extrapolated to a global uptake of 0.68 to 4.9 Pg y^{-1}, which would account for a substantial CO_2 sink. Mainly phototrophic CO_2 uptake was found by Wu et al. (2014), who investigated differences of CO_2 uptake with soil depth in paddy and upland soils. Significant CO_2 fixation was measured only in illuminated incubations in the top cm of the soil. Uptake into soil organic matter, microbial biomass and dissolved organic carbon was higher in paddy soils compared to upland soils. The correlation between RubisCO activity, fixed carbon and the abundance of functional genes encoding for RubisCO highlighted the importance of phototrophs for CO_2 fixation in surface soils (Wu et al., 2014). Below 1 cm depth,

CO_2 fixation could only be detected in trace amounts and chemolithoautotrophy was regarded to be of minor importance. Further investigations on CO_2 fixation were conducted by Wu et al. (2015b), who showed variations of CO_2 fixation by autotrophic bacteria in response to different cropping systems. These led to differences in soil parameters and influenced in turn cbbL gene abundance, activity and bacterial community structure, and thus resulted in differences in $^{14}CO_2$ incorporation (Wu et al., 2015b). Similar to their previous study, substantial CO_2 uptake could only be measured in the uppermost centimetres of the soil, leading to the conclusion that mainly photoautotrophs contributed to measured uptake rates. However, Liu and Conrad (2011) showed the potential of chemolithoautotrophic acetogenesis in an Italian rice field soil. This study proved incorporation of $^{13}CO_2$ into different groups of chemolithoautotrophic organisms by stable isotope probing of ribosomal RNA. Pratscher et al. (2011) showed by RNA and DNA stable isotope probing that ammonia oxidizing archaea were responsible for chemolithoautotrophic growth in an agricultural soil. Furthermore, Beulig et al. (2014) proved high CO_2 uptake rates in soils influenced by high CO_2 concentrations and an adapted chemolithoautotrophic community.

1.6 CO_2 fixation in aquifers

Chemolithoautotrophic microorganisms have been hypothesised to be key organisms in groundwater systems, because groundwater is generally depleted in organic carbon or carbon sources might not be readily available (Alfreider et al., 2003). Furthermore, groundwater systems can provide suitable conditions for surface independent chemolithoautotrophic growth, because reduced compounds like NH_4^+, NO_2^-, $S_2O_3^{2-}$ or Fe^{2+} as well as CO_2 are abundant. Alfreider et al. (2003) investigated the diversity of cbbL genes in two groundwater systems and found that most sequences were affiliated to type IA RubisCO sequences, representing various obligate and facultative chemolithoautotrophic Proteobacteria, whereas type II RubisCO was affiliated mainly to *thiobacilli* species. The physiological significance of autotrophy was further proven by determining the potential of chemolithoautotrophic CO_2 fixation with analyses of

cbbL and cbbM genes (Alfreider et al., 2012). The distribution and diversity of RubisCO genes and transcripts in that study revealed that different kinds of RubisCO are regulated and linked to environmental conditions like nitrate concentration or oxygen availability. The research was expanded by Alfreider et al. (2009), who determined the abundance and diversity of different forms of RubisCO in several unpolluted and polluted aquifers. Kellermann et al. (2012) determined the potential for microbial CO_2 fixation in a tar oil contaminated aquifer by detection of the functional marker genes cbbL and cbbM. The study showed that chemolithoautotrophy was mainly pronounced where a fluctuating water table caused regular oxidation of reduced iron and sulphur species. Functional gene sequences retrieved from this area were most closely related to sequences of different *thiobacilli*.

A high potential for CO_2 fixation via the Calvin Benson cycle in a pristine aquifer was also suggested by Herrmann et al. (2015), who found that up to 17 % of the microbial community had the capability to fix CO_2, whereas energy was provided by reduced sulphur and nitrogen compounds. However, several studies proved evidence that also other metabolic cycles than the Calvin Benson cycle are used in groundwater systems. Alfreider and Vogt (2012) proved the utilization of the reductive citric acid cycle as a pathway for chemolithoautotrophs in different contaminated anoxic aquifers. Jewell et al. (2016) showed by a metatranscriptomic approach high activity of chemolithoautotrophs that were relevant for carbon as well as sulphur, nitrogen and iron cycling. After injection of nitrate as a favourable electron acceptor, a strong response in gene expression of chemolithoautotrophs was detected in the metatranscriptomic data. The relative changes in gene expression were coupled to the reduction of nitrate, oxidation of reduced iron and sulphur compounds as well as CO_2 fixation. These results of gene expression, which can be used as a proxy for microbial activity, lead to the conclusion that the activity of chemolithoautotrophs mediated carbon, sulphur, nitrogen and iron cycling in these aquifers (Jewell et al., 2016).

A significant role of chemolithoautotrophs for aquifer food webs has been shown by Hutchins et al. (2016). The authors showed based on stable isotope investigations of aquifer food webs that stable carbon isotope values of subsurface communities got increasingly more negative along a gradient of

decreasing photosynthetic organic matter sources, indicating chemolithoautotrophic organic matter sources more distant from the recharge area and close to the oxic/anoxic interface of the groundwater.

1.7 Influence of microbial CO_2 fixation on carbon isotope signatures of soil organic matter

Analyses of carbon isotope ratios in soil organic matter provide insights into dynamics of the carbon cycle. Stable carbon isotopes ($\delta^{13}C$) in soils can be used to distinguish between autotrophic and heterotrophic components of soil respiration (Hanson et al., 2000; Risk et al., 2012; Trumbore, 2006), to separate terrestrial and oceanic CO_2 flux components (Ogee et al., 2004; Yakir and Sternberg, 2000), long term reconstructions of ecosystem dynamics, like C3/C4 vegetation changes (Guillaume et al., 2015; Martinelli et al., 1996) and determination of turnover rates of soil organic matter after C3/C4 vegetation change (Balesdent et al., 1987; Bernoux et al., 1998; Kramer and Gleixner, 2008). A common feature of $\delta^{13}C$ in soil organic matter in aerated, well drained soils is a progressive enrichment with depth (Ehleringer et al., 2000). An enrichment of 1-3 ‰ can be observed below C3 ecosystems. This enrichment is associated with a decrease of soil organic matter concentration and increase in decomposition state (Ehleringer et al., 2000). Although there is a lack in the mechanistic understanding of this phenomenon, several hypotheses are used to explain this observation, which are summarised in Ehleringer et al. (2000).

Ehleringer et al. (2000) suggested that an increasing proportion of microbially derived carbon, which is enriched in $\delta^{13}C$ compared to soil organic matter due to heterotrophic CO_2 fixation can be the reason for the observed enrichment.

Other patterns in $\delta^{13}C$ can be observed in anoxic soils. Soils, which are constantly waterlogged and characterized by a low redox potential, exhibit a shift towards more depleted values (Alewell et al., 2011). This is explained by decomposition under anaerobic conditions, which is accompanied with an accumulation of hardly decomposable ^{13}C depleted substances like lignin (Krüger et al., 2014; Krull and Retallack, 2000). However, also addition of ^{13}C depleted microbial carbon to soil organic matter can cause depletion in $\delta^{13}C$

values (Kracht and Gleixner, 2000). Possible sources are respired CO_2, CO_2 derived from methane oxidation or acetate (Pancost et al., 2000; Schulten and Gleixner, 1999).

Radiocarbon (^{14}C) signatures reflect the time elapsed since C being measured was fixed from the atmosphere. It is constantly created in the atmosphere by interactions with high energy cosmic rays and decays with a half-life of 5730 years (Trumbore et al., 2016). Radiocarbon is a useful tool for investigating soil carbon dynamics (Trumbore, 2009). Thermonuclear weapon testing, which peaked in 1963, nearly doubled the amount of ^{14}C in the atmosphere. The ^{14}C concentration declined subsequently due to mixing within the atmosphere, incorporation into terrestrial and oceanic carbon reservoirs and dilution due to fossil fuel burning (Trumbore et al., 2016). Since atmospheric ^{14}C concentrations are decreasing every year, the signal can be used as a tracer for studying carbon dynamics. Application of radiocarbon in soils led to the finding that soil organic matter can be divided into different pools with different turnover times ranging form annual to millennial timescales (Trumbore, 2009). The radiocarbon signature of CO_2 in soil pore space can be depleted or enriched in ^{14}C compared to organic matter found at the same depth, depending on the age of C being mineralized (Trumbore, 2006). In most forest ecosystems soil CO_2 has radiocarbon values close to the atmospheric signature because of root respiration and mineralization of fast cycling carbon pools (Trumbore et al., 2006). Microbial fixation of CO_2 can provide therefore a pathway of modern ^{14}C into deeper soil layers, where particulate or dissolved CO_2 has no access (figure 1.2).

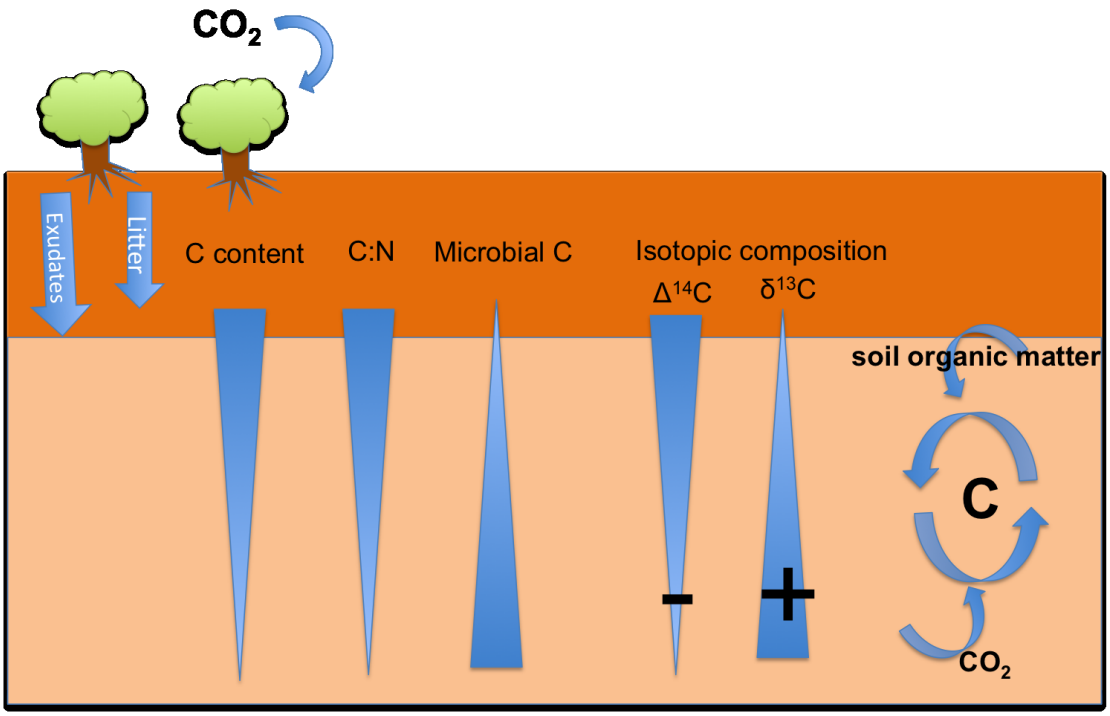

Figure 1-2: CO_2 fixation is a process that might contribute to carbon recycling in the subsurface, which is accompanied with an increasing contribution of microbial carbon with depth. It might also be a process that contributes to the shape of isotope signatures in soil depth profiles by providing carbon of a different isotopic signature to microbial biomass and soil organic matter.

1.8 Carbon isotope signatures of DIC

DIC is an integrative signal for carbon cycling in aquifer systems. There is a huge range in $\delta\,^{13}C$ of DIC in various carbon reservoirs. These variations are caused by inorganic carbonate reactions as well as by microbial mediation and isotope fractionation (Marfia et al., 2004; Mook et al., 1974). Therefore, $\delta\,^{13}C_{DIC}$ is of high usefulness in studying the influence of microbial processes as well as inorganic controls on carbon cycling (Barth and Veizer, 1999; Chasar et al., 2000). Another useful isotopic approach is radiocarbon dating of DIC (Bethke and Johnson, 2008; Han and Plummer, 2016). ^{14}C concentrations of DIC provide the possibility for estimating chronologies in regional groundwater systems on the ten thousand year timescale (Han and Plummer, 2016). In order to determine initial ^{14}C concentrations of DIC, traditional correction models have been applied to account for the different processes that affect DIC and bias ^{14}C ages (Han and Plummer, 2016). However, new approaches emerged, where groundwater age dating is not following a rigorous definition, but rather sees a sample as a mixture of waters that have resided in the subsurface for varying lengths of time

(Bethke and Johnson, 2008). Combination of $\delta^{13}C$ and ^{14}C measurements can be therefore a suitable tool to study cycling of carbon in groundwater and might help to elucidate differential carbon source utilization, e.g. chemolithoautotrophy vs. heterotrophy, or recycling of carbon within groundwater systems (figure 1.3).

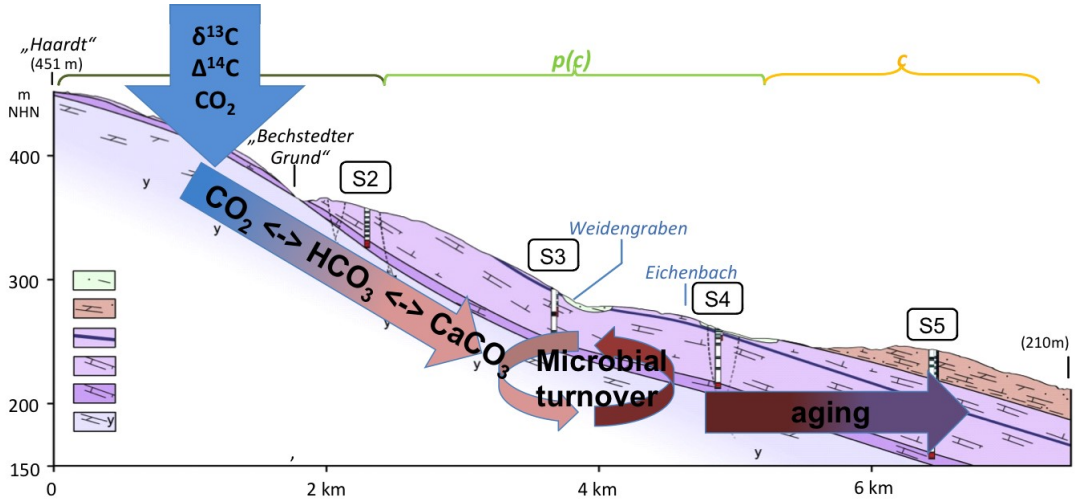

Figure 1-3: DIC isotopes can be used to trace the movement of water through the subsurface and elucidate carbon turnover within aquifers. Carbon recycling, e.g. by chemolithoautotrophic microorganisms, can be reflected in DIC isotopes.

1.9 Aim and outline of this thesis

Given the above mentioned research state the present thesis aims at improving our understanding of the role of microbial CO_2 fixation for carbon cycling within the subsurface and how CO_2 fixation contributes to carbon recycling. Special emphasis is put on the question, how carbon isotopic signatures of different carbon pools like soil organic matter or dissolved inorganic carbon are influenced by microbial CO_2 fixation due to enzymatic fractionation processes and utilization of isotopically different carbon sources. The shifts in $\delta^{13}C$ values are used in turn to quantify the amount of carbon derived from CO_2 fixation. Following objectives are addressed in this thesis:

I) To prove the activity of CO_2 fixation along soil depth profiles.
II) To assess the potential of CO_2 fixation to contribute to soil organic matter formation.
III) To prove, if CO_2 fixation can alter isotope signatures of soil organic matter.

IV) To determine, if chemolithoautotrophic microorganisms contribute to carbon cycling in groundwater systems and influence carbon isotopes of dissolved inorganic carbon.

Chapter two is a study conducted at the mofette field in Hartoušov in NW Bohemia, Czech Republic. Mofettes are organic rich soils, which are influenced by extremely high CO_2 concentrations due to cold volcanic exhalations from the subsurface. They exhibit a specialized microbial community, which is adapted to anoxic conditions and high CO_2 concentrations. We used the unique isotopic composition of the exhaling CO_2 as a naturally occurring tracer to distinguish plant from microbial derived carbon in these soils. Natural abundance isotopic measurements of soil organic matter, plants and soil gas were combined with measurements of CO_2 uptake rates and the abundance of functional genes and compared to reference soils which were not influenced by exhaling CO_2.

Chapter three deals with soils from the Amazon. Experiments were conducted with soils from the Amazonian Tall Tower Observatory (ATTO) in Brazil, which represent the most common soil type in the Amazon region. CO_2 uptake rate measurements were conducted along soil depth profiles and were used to infer, weather microbial CO_2 fixation might contribute to soil organic matter and microbial biomass carbon. The rates were further used to evaluate if CO_2 fixation might influence isotopic ratios of soil organic matter and microbial biomass. Complementary to isotopic and rate measurements, the microbial community structure was determined in order to prove the presence or absence of autotrophic microorganisms.

In chapter 4 the habitat is changed from soil to groundwater ecosystems. Groundwater samples for the experiments were derived from the Critical Zone Observatory AquaDiva, located in Thuringia, Germany. In this chapter, isotopic data from dissolved inorganic carbon, dissolved organic carbon and particulate organic carbon is combined with geochemical modelling to elucidate the internal carbon cycling of the aquifer along a redox gradient. Different sets of geochemical, molecular and modelling data are used to investigate different carbon utilization by the microbial community.

Chapter 5 discussed the main findings and chapter 6 provides an outlook for future research possibilities.

1.10 Overview of manuscripts

1.10.1 Manuscript 1 (Chapter 2)

Autotrophic fixation of geogenic CO_2 by microorganisms contributes to soil organic matter formation and alters isotope signatures in a wetland mofette

Nowak M.E., Beulig, F., von Fischer, J., Muhr, J., Küsel, K., Trumbore S.E.

Biogeosciences 12, 7169-7183, 2015

In manuscript 1, we investigated the potential of microbial CO_2 fixation to contribute to soil organic matter formation in soils, which were influenced by high CO_2 concentrations, so called mofettes. The origin of the CO_2 was geogenic and its natural isotopic signature was used to distinguish organic matter derived from CO_2 fixation from plant derived soil organic matter. Deviations of the isotopic signature in the first 10 cm coincided with high CO_2 uptake rates , a high abundance of functional genes encoding for RubisCO and low C/N ratios. This allowed us to determine the amount of carbon derived from autotrophic microorganisms, which ranged between 8 and 27 %.

M. Nowak designed the experiment, conducted sampling and experiments and wrote the manuscript. He performed all isotopic measurement, analysed and discussed the data.
F. Beulig helped with sampling, helped to extract DNA and perform qPCR measurements.
J. von Fischer, J. Muhr, K. Küsel and S. Trumbore helped with the experiment design, discussed the data, reviewed and edited the manuscript draft.

1.10.2 Manuscript 2 (Chapter 3)

The activity of CO_2 fixing microorganisms in tropical rainforest soils and their impact on carbon isotopic signatures of microbial biomass and soil organic matter

Nowak, M.E., Catao E.C.P., Santana, R.H., Behrendt, T., Krüger, R.H., Quesada, B., Trumbore, S.E.

Manuscript in preparation, to be submitted to *Soil Biology and Biochemistry*

In manuscript 2 we investigated tropical rainforest soils and the potential of CO_2 fixation in these soils. We put emphasis on determining the influence of CO_2 fixation on carbon isotopic signatures of soil organic matter. Carbon isotopes of soil organic matter showed a clear depth trend in the investigated soils. The concordant depth trend of isotopic signatures of soil organic matter and microbial biomass indicated a strong interrelationship between both pools. CO_2 fixation could be measured throughout the soil profile down to one metre depth. The amount of CO_2 fixation was not enough to cause a shift in $\delta^{13}C$ of soil organic matter, but is big enough to influence radiocarbon signatures at deeper depths of the soil profile.

M. Nowak designed the experiment, conducted the sampling experiment and wrote the manuscript. He performed all isotopic measurements, extracted DNA and analysed and discussed the data.
C. Catao evaluated the sequencing data and reviewed and edited the manuscript.
R. Santana helped with DNA extractions and PCR amplifications.
T. Behrendt, S. Trumbore and R. Krüger and B. Quesada helped with the experimental design, reviewed and edited the manuscript draft.

1.10.3 Manuscript 3 (Chapter 4)

Carbon isotopes of dissolved inorganic carbon reflect utilization of different carbon sources by microbial communities in two limestone aquifer assemblages

Nowak, M.E., Schwab, V.F., Lazar, C.S., Behrendt T., Kohlhepp, B., Totsche, K.U., Küsel, K., Trumbore, S.E.

Manuscript submitted on 10th October 2016 to *Hydrology and Earth System Sciences*

In manuscript 3 we studied the influence of biotic and abiotic factors on carbon isotopes of dissolved inorganic carbon in two differing limestone aquifer assemblages. We evaluated carbon isotopic measurements with a novel graphical method. We complemented the results with hydrochemical modelling using NETPATH and the determination of the microbial community structure based on 16S rRNA analyses. The results showed that in anoxic aquifers, microbes are able to utilize different carbon sources including recycled carbon derived from chemolithoautotrophs and rock derived sedimentary organic carbon, which is reflected in DIC isotopes. Microbial communities are therefore to a certain degree surface independent in these shallow aquifers.

M. Nowak designed the experiment, conducted isotopic measurements of DIC and DOC, sampled for DNA analyses and wrote the manuscript.
V. Schwab helped with experiment design, measured ^{13}C and ^{14}C of POC, reviewed and edited the manuscript.
C. Lazar extracted DNA and analysed the sequencing data, reviewed and edited the manuscript draft.
T. Behrendt discussed the data and edited and reviewed the manuscript draft
B. Kohlhepp, K. U. Totsche, K. Küsel and S. Trumbore reviewed and edited the manuscript draft.

2 Autotrophic fixation of geogenic CO_2 by microorganisms contributes to soil organic matter formation and alters isotope signatures in a wetland mofette

Chapter source:

Nowak, M.E., Beulig, F., von Fischer, J., Muhr, J., Küsel, K., Trumbore, S.E., 2015. Autotrophic fixation of geogenic CO2 by microorganisms contributes to soil organic matter formation and alters isotope signatures in a wetland mofette. Biogeosciences 12, 7169-7183.

Abstract

To quantify the contribution of autotrophic microorganisms to organic matter formation (OM) in soils, we investigated natural CO_2 vents (mofettes) situated in a wetland in NW Bohemia (Czech Republic). Mofette soils had higher SOM concentrations than reference soils due to restricted decomposition under high CO_2 levels. We used radiocarbon ($\Delta^{14}C$) and stable carbon isotope ratios ($\delta^{13}C$) to characterize SOM and its sources in two moffetes and compared it with respective reference soils, which were not influenced by geogenic CO_2.

The geogenic CO_2 emitted at these sites is free of radiocarbon and enriched in ^{13}C compared to atmospheric CO_2. Together, these isotopic signals allow us to distinguish C fixed by plants from C fixed by autotrophic microorganisms using their differences in ^{13}C discrimination. We can then estimate that up to 27 % of soil organic matter in the 0-10 cm layer of these soils was derived from microbially assimilated CO_2.

Isotope values of bulk SOM were shifted towards more positive $\delta^{13}C$ and more negative $\Delta^{14}C$ values in mofettes compared to reference soils, suggesting that geogenic CO_2 emitted from the soil atmosphere is incorporated into SOM. To distinguish whether geogenic CO_2 was fixed by plants or by CO_2 assimilating microorganisms, we first used the proportional differences in radiocarbon and $\delta^{13}C$ values to indicate the magnitude of discrimination of the stable isotopes in living plants. Deviation from this relationship was taken to indicate the presence of microbial CO_2 fixation, as microbial discrimination should differ from that of plants. $^{13}CO_2$-labelling experiments confirmed high activity of CO_2 assimilating microbes in the top 10 cm, where $\delta^{13}C$ values of SOM were shifted up to 2 ‰

towards more negative values. Uptake rates of microbial CO_2 fixation ranged up to 1.59 ± 0.16 µg gdw^{-1} d^{-1}. We inferred that the negative $\delta^{13}C$ shift was caused by the activity autotrophic microorganisms using the Calvin Benson Basham Cycle, as indicated from quantification of cbbL/cbbM marker genes encoding for RubisCO by quantitative polymerase chain reaction (qPCR) and by acetogenic and methanogenic microorganisms, shown present in the moffettes by previous studies. Combined $\Delta^{14}C$ and $\delta^{13}C$ isotope mass balances indicated that microbially derived carbon accounted for 8 to 27 % of bulk SOM in this soil layer.

The findings imply that autotrophic microorganisms can recycle significant amounts of carbon in wetland soils and might contribute to observed radiocarbon reservoir effects influencing $\Delta^{14}C$ signatures in peat deposits.

2.1 Introduction

Microbial assimilation of CO_2 is a ubiquitous process in soils, and can be accomplished by a wide variety of microorganisms using different metabolic pathways (Berg, 2011; Wood et al., 1941). RubisCO, the most important carboxylating enzyme for obligate and facultative chemo- or photoautotrophic microorganisms that fix CO_2 using the Calvin Benson Bassham Cylce (CBB) has been shown to be highly abundant in agricultural, forest and volcanic soils (Nanba et al., 2004; Selesi et al., 2007; Tolli and King, 2005). Direct uptake of CO_2 into microbial biomass (MB) and soil organic matter (SOM) by photoautotrophic and chemoautotrophic organisms has been measured in paddy rice and agricultural upland soils (Liu and Conrad, 2011; Wu et al., 2015a; Wu et al., 2014), as well as under manipulating experimental conditions, like H_2 amendment (Stein et al., 2005) or addition of reduced sulphur compounds (Hart et al., 2013). Autotrophic acetogenic organisms, using the Wood-Ljungdahl Pathway for CO_2 fixation, are important groups in wetland and forest soils (Küsel and Drake, 1995; Ye et al., 2014). In addition, many heterotrophic soil microorganisms fix CO_2 in order to maintain their metabolic cycle by anaplerotic reactions, either to form new sugars for cell wall synthesis or to excrete organic acids for nutrient mobilization (Feisthauer et al., 2008; Miltner et al., 2005; Santruckova et al., 2005). Global estimates of microbial CO_2 fixation in soils range

between 0.9 and 5.4 PgC per year (Yuan et al., 2012). However, it still remains unclear how much of assimilated CO_2 is stored and contributes to the formation of soil organic matter (SOM). In this study we aim at evaluating the impact of autotrophic microorganisms on carbon isotope signatures of SOM. We further aim at quantifying the contribution of autotrophs to SOM by means of natural abundance ^{14}C and ^{13}C isotope signatures in a unique environment.

Microbial utilization of CO_2 and its incorporation into SOM is also potentially an important mechanism influencing the isotope signatures of SOM (Ehleringer et al., 2000; Kramer and Gleixner, 2006). Stable carbon ($\delta^{13}C$) and radiocarbon (^{14}C) isotope signatures are important tools for determining turnover of soil organic matter and dating ancient sediments (Balesdent et al., 1987; Hughen et al., 2004; Trumbore, 2000).

Stable isotope variations in soil reflect mass-dependent fractionation processes (Werth and Kuzyakov, 2010). In many well-drained soils, there is a well-documented increase in $\delta^{13}C$ with depth that has been variously attributed to selective preservation/decomposition of different components of organic matter, recent declines in atmospheric $\delta^{13}C$ due to the Suess effect, or microbial fractionation (summarized in Ehleringer et al. 2000). Enzymatic fractionation during assimilation of CO_2 can also lead to changes in $\delta^{13}C$ values of synthesized organic matter (Hayes, 2001; Robinson et al., 2003; Whiticar, 1999). Carboxylation processes by heterotrophic microorganisms have been hypothesized to be responsible for the increase in $\delta^{13}C$ values with depth in aerated upland soils (Ehleringer et al., 2000).

Radiocarbon signatures reflect the time elapsed since the C being measured was fixed from the atmosphere, and are corrected (using measured $\delta^{13}C$ values) to remove mass dependent fractionation effects. The radiocarbon signature of CO_2 in soil pore space can be depleted or enriched in ^{14}C compared to organic matter found at the same depth, depending on the age of C being mineralized (Trumbore et al., 2006). Because soil pore space CO_2 can have quite different isotopic signatures compared to SOM at the same depth, microbial assimilation of CO_2 may influence SOM ^{14}C signatures and therefore bias estimates of carbon turnover and radiocarbon age by generating reservoir effects (Pancost et al., 2000).

In turn, comparing both, radiocarbon and stable isotope values of SOM, MB and their sources might allow quantifying the potential contribution of autotrophic microorganisms to SOM, because a mismatch of both isotopes in quantifying SOM sources indicates either fractionation of ^{13}C by carboxylation processes of different enzymes or depletion or enrichment of ^{14}C by the use of soil CO_2 (Kramer and Gleixner, 2006).

In order to test the hypothesis that microbial CO_2 fixation contributes to SOM formation and alters isotope signatures in soil depth profiles, we investigated wetland mofettes in NW Bohemia. Mofettes are cold exhalations of geogenic CO_2 from wetland soils with high CO_2 concentrations. The exhaling volcanic-derived CO_2 has a distinct isotopic signature, is enriched in $\delta^{13}C$ by about 5 ‰ and free of radiocarbon compared to atmospheric CO_2. This unique feature allows us to use geogenic CO_2 as a natural isotopic tracer, because CO_2 assimilating microorganisms take up an isotopically different CO_2 source compared to plants growing in the area, which use a mixture of geogenic and atmospheric CO_2. We used three approaches to evaluate the importance of CO_2 fixation for SOM generation in mofettes and its impact on carbon isotope values:

1) We measured natural abundance ^{13}C and radiocarbon signatures of SOM, CO_2 and plant material in mofette and reference soils, in order to identify areas where C derived from microbial CO_2 fixation altered isotope signatures of bulk SOM from expected plant signals and quantified C derived from microbial CO_2 fixation by isotope mass balances.

2) We conducted isotope-labelling experiments with $^{13}CO_2$ in order to quantify the rate of CO_2 fixation by microorganisms in soil profiles of two CO_2 vents and compared these to reference soils away from the vents.

3) We complemented existing data about microbial community and activity in wetland mofettes (Beulig et al., 2014), by assessing the importance of microorganisms using the Calvin Benson Basham Cycle for CO_2 fixation. This was especially important to infer whether differences in kinetic isotope effects compared to plants were feasible given the pathways of microbial C fixation. Therefore, we quantified cbbL and cbbM marker genes encoding for Form I and II RubisCO, respectively. Form I RubisCO

consists of eight small and eight large subunits. It can be subdivided into two groups, the “red” and “green” like groups, which can be further subdivided into Form 1A, 1B and 1C and 1D, respectively (Yuan et al., 2012; Tolli and King, 2005). Form II RubisCO consists only of large subunits. Because of its low CO_2 affinity and high O_2 sensitivity, it represents an early form, evolved under anaerobic conditions and high CO_2 concentrations (Alfreider et al., 2003). Form II RubisCO might be favourable under conditions prevailing in mofettes. cbbL 1A was identified mainly in obligate autotrophic bacteria and cbbL 1C in facultative autotrophic bacteria (Tolli and King, 2005). cbbM encodes for autotrophic organisms living under anaerobic conditions (Selesi et al., 2005).

Using this information, we aimed to quantify the amount of C derived from microbial assimilation of CO_2 into soil organic matter within soil profiles, and assess its potential to alter isotope signatures of SOM.

2.2 Materials and methods

2.2.1 Site description

The study site (50°08′48′′ N, 12°27′03′′E) is located in the northwestern part of the Czech Republic (Bohemia). The area is part of a continental rift system, where deep tectonic faults provide pathways for ascending gases and fluids from the upper earth`s mantle (Kämpf et al., 2013). Mofettes are surficial, low temperature exhalations of mantle derived CO_2. Macroscopically, they form a complex of landscape features. At centre is a spot of typically 0.5 to 1 meter bare soil. From this central spot, almost pure CO_2 emanates to the atmosphere. The mofette centre is surrounded by a raised hummock that extends 1 to 20 m away from the spot. The investigated mofettes are situated on the floodplain of the river Plesna and are part of a wetland. Geogenic CO_2 emanates with an average discharge of up to 0.62 tons CO_2 d^{-1} per spot (Kämpf et al., 2013). The surrounding hummock is built up by different vascular plant communities. *Eriophorum vaginatum* and *Deschampsia cespitosa* are dominating plant species

in the immediate proximity of the central vent and hummock structure, respectively. *Filipendula ulmaria* represents typical floodplain vegetation.

We investigated two mofettes that differed in size. Mofette 1 had a spot-diameter of 0.6 m, whereas the diameter of Mofette 2 was 1.5 m. We also sampled soils away from the influence of the mofette-exhaled CO_2 (deemed reference soils). These soils are vegetated and experience periodic anoxic conditions due to waterlogging, as evidenced by gleyed soil features and porewater geochemistry (Mehlhorn et al., 2014). In Mofettes 1 and 2, the local water table is elevated by ascending CO_2 and O_2 is mainly displaced by the CO_2 stream, leading to anoxic (but not necessarily water-logged) conditions (Bräuer et al., 2011). According to the World Reference Base for soil resources (WRB, 2007), mofette soils are characterized as Histosols with pronounced reductomorphic features (reduced Y horizons) due to the influence of up-streaming CO_2. Reference soils are classified as 'gleyic' Fluvisols (Beulig et al., 2014).

2.2.2 Sampling of soils, plants and gases for bulk geochemical and isotope measurements

For bulk $\delta^{13}C$ and radiocarbon analyses soil cores were taken from the central, un-vegetated part of the mofette structure and reference soils. Reference soils lacking CO_2 emissions were identified with a portable landfill gas analyser (Visalla GM70 portable CO_2 sensor) in close proximity to each vent structure. Reference soils 1 and 2 were defined 5 and 18 meters distant from the central vent structures, respectively. Samples for bulk stable isotope and radiocarbon analyses were taken in November 2013. In order to account for soil heterogeneity, three soil cores (I.D. 5 cm) were taken from a plot of 50 x 50 cm from mofette and reference soils. Because mofette and reference soils were characterised by very different soil features, soil cores were not divided according to horizons, but depth intervals. Based on visual inspection, soil cores were divided into depth intervals from 0-10 cm, 10-25 cm and 25-40 cm. Replicates of the respective depth intervals were mixed and sieved to 2 mm. Roots and plant debris were removed by handpicking. The sieved soil was

subsequently dried at 40° and prepared for stable isotope, radiocarbon and C/N analysis.

In April 2014, vegetation samples were taken from the same plot as soil cores, in order to characterize the isotopic composition of the plant material contributing to mofette SOM. Vegetation samples in the direct proximity of both mofettes were represented by *Eriophorum vaginatum*. Vegetation samples were also taken by clipping plants at 2cm height at 2 meter intervals along a transect that crossed moffett 2, allowing us to test how the isotope signatures ($\delta^{13}C$ and $\Delta^{14}C$) of plants changed with different mixtures of ambient and geogenic CO_2. Mofette 2 is an exposed hummock, dominated by an un-vegetated central region of CO_2 exhalation. One to two meters distant from the central exhalation, the dominant plant species was *Deschampsia cespitosa,* and at greater distances the dominant plant was *Filipendula ulmaria*. The collected samples were dried at 40° C, ground and prepared for stable isotope, radiocarbon and C/N analysis.

CO_2 was sampled from the centre of each mofette by filling 250 ml evacuated stainless steel cylinders through a perforated lance from four different soil depths (5, 15, 25, 40 cm), in order to determine its radiocarbon and stable isotope signature.

2.2.3 Soil sampling for $^{13}CO_2$ labelling experiments

Mofette soils were sampled for two labelling experiments in November 2013 and September 2014, respectively. For the first experiment, 10 x 10 cm soil monoliths, extending to 10 cm depth were sampled from each soil in November 2013. After removing the top of the Oh horizon (about 1 cm thickness), the remaining material was divided into three subsamples. Each replicate was homogenized within a sterilized plastic bag, put under an anoxic N_2 atmosphere and cooled at 4° until further processing in the lab within the same day.

For a second experiment, three soil cores (I.D. = 5 cm) were taken from 0 to 40 cm of each mofette and reference soil and subsampled from 0-5, 5-10 10-20, 20-30 and 30-40cm. 5g subsamples from each core were transferred immediately after core recovery to a sterilized 12 ml Labco® Exetainer, flushed with N_2 to preserve anoxia, sealed and brought to the laboratory at 4°C for

further processing. To obtain background (i.e. with no influence of added label) values for isotopic composition, one set of subsamples was dried and prepared for TOC, C/N, pH and $\delta^{13}C$ analyses as described above.

2.2.4 Sampling for DNA extraction

Samples for DNA extraction were taken in May 2014 from Mofette 1 and Reference 1. Samples were taken from 0-5, 5-10, 10-20, 20-30 and 30-40 cm. Three replicates of 30 g were sampled from each depth, and homogenized under anoxic conditions. Subsequently, subsamples of 5 g were transferred to 50 ml tubes, cooled with dry ice and transported under an Ar atmosphere to the laboratory for molecular analyses.

2.2.5 Analyses of geochemical parameters and natural abundance isotope signatures of vegetation and soil samples

Soil pH was determined in a 0.01 M $CaCl_2$ solution with a soil:solution ratio of 1:2.5 using a WTW pH meter. The precision of pH measurements was better than 0.1 (n=3). Total C and N concentration of soil and plant samples were determined on a "Vario EL" (Elementar Analysesysteme GmbH, Germany). Gravimetric water content was determined after drying soils for 48h at 105° and C and N content are reported per g dry soil weight.

Stable C isotope signatures of bulk soil and plant samples were determined on an isotope ratio mass spectrometer (DELTA+XL, Finnigan MAT, Bremen, Germany) coupled to an elemental analyser (NA 1110, CE Instruments, Milan, Italy) via a modified ConFloII™ interface (EA-IRMS). Stable carbon isotope ratios are reported in the delta notation that expresses $^{13}C/^{12}C$ ratios as $\delta^{13}C$-values in per mil (‰) relative to the international reference material Vienna Pee Dee Belemnite (V-PDB, Coplen et al., 2006):

$$\delta^{13}C = \left(\frac{\frac{^{13}C}{^{12}C}_{sample}}{\frac{^{13}C}{^{12}C}_{reference}} - 1 \right) \times 1000 \qquad (1)$$

Analytical precision of all samples was better than 0.1 ‰.

For discussing microbially mediated isotope effects the isotope discrimination value Δ is used, which expresses the isotopic difference between two compounds in ‰:

$$\Delta_{x\text{-}y} = \delta_x - \delta_y \qquad (2)$$

Where δ_x and δ_y refer to $\delta\,^{13}C$ values of the product and reactant, respectively.

The radiocarbon content of soil and plant samples was determined by accelerator mass spectrometry at the Jena ^{14}C facilities (Steinhof et al., 2004). Subsamples of soil containing 1 mg of carbon were combusted quantitatively and the developed CO_2 was catalytically reduced to graphite at 625°C by H_2 reduction. To simplify comparison with stable isotope ratios, radiocarbon activities are reported in $\Delta^{14}C$, which is the ‰ deviation of the $^{12}C/^{14}C$ ratio from the international oxalic acid universal standard. The $\Delta^{14}C$ value of the sample is corrected for mass dependent isotope fractionation to a common value of -25 ‰ (Mook and van der Plicht, 1999). The standard is corrected for radioactive decay between 1950 and the year (y) of the measurement (2014).

$$\Delta^{14}C = \left[\frac{\frac{^{14}C}{^{12}C_{sample,-25}}}{0.95\frac{^{14}C}{^{12}C_{Ox1,-19}} \times \exp^{\left(y-\frac{1950}{8267}\right)}} \right] \times 1000 \times d \qquad (3)$$

Errors reported for radiocarbon measurements represent the analytical error of homogenized mixed samples in ‰. Analytical precision of all radiocarbon measurements was better than 3 ‰.

2.2.6 Labelling experiments

The first labelling experiment traced the flow of fixed CO_2 directly into microbial biomass (MB), evaluated rates of CO_2 uptake associated with biological activity and compared the proportion of labelled MB in mofettes with reference soils. From each field replicate sample, 20 g aliquots were taken and put into sterilized 120 mL boro-silicate bottles with butyl rubber stoppers inside a glove box containing an N_2 atmosphere. From these subsamples, three replicates were prepared for incubation with $^{13}CO_2$. In order to obtain control samples without

biological activity, an additional aliquot of each sample was prepared and autoclaved for 2 hours at 160° and 60 bar.

Soil samples were incubated under anoxic conditions with $^{13}CO_2$ at N_2:CO_2 ratios equivalent to those experienced by the soils in the field: mofette soils were incubated with a 100 vol. % $^{13}CO_2$ atmosphere using sterile techniques and reference soils were incubated with a 10 vol. % $^{13}CO_2$ and 90 vol. % N_2 atmosphere. In order to account for soil respiration and to maintain a constant label, the headspace of every sample was removed and renewed every 3 days. The samples were incubated for 14 days in the dark at 12°C. Living and autoclaved control samples were treated identically.

After 14 days, the jars were flushed with N_2 and the soil samples were homogenized and split. One part was air dried for bulk ^{13}C analysis and the other part was prepared for extraction of the microbial biomass C by chloroform fumigation extraction (CFE) (Vance et al., 1987). CFE extracts microbial biomass C by lysing the cells with chloroform and releasing the products of cell lysis into a salt solution as dissolved organic carbon (DOC). In order to enhance extraction efficiency and to minimize the losses for extracted C by microbial degradation, the protocol from Vance et al. (1987) was slightly modified (Malik and Gleixner, 2013). The concentration of dissolved microbial biomass C (MB-DOC) and its stable carbon isotope ratio were determined by a high performance liquid chromatography system coupled to an IRMS (HPLC/IRMS) system (Scheibe et al., 2012). This method allows direct determination of concentration and carbon isotopic value of DOC in the liquid phase by coupling a LC-IsoLink system (Thermo Electron, Bremen, Germany) to a Delta+ XP IRMS (Thermo Fisher Scientific, Germany). A detailed description of the apparatus and measurement procedure is given in Scheibe et al. (2012).

The amount of microbial biomass was determined by subtracting the amount of MB-DOC of un-fumigated samples from MB-DOC of fumigated samples and dividing with a proportionality factor K_c that accounts for the extraction efficiency:

$$C_{mic} = \frac{DOC_{fum} - DOC_{unfum}}{K_C} \quad (4)$$

A value of 0.45 was used for *Kc* according to (Amha et al., 2012). The isotope ratio of microbial biomass C can be derived by applying an isotope mass balance:

$$\delta^{13}C_{MB} = \frac{\delta^{13}C_{fum} \times C_{fum} - \delta^{13}C_{unfum} \times C_{unfum}}{C_{fum} - C_{unfum}} \quad (5)$$

The net CO_2 fixation rate was calculated by determining the increase in ^{13}C from the label compared to the unlabelled control, and is normalized for C content (either total soil or microbial-C). The excess ^{13}C can be derived from the $^{13}C/^{12}C$ ratio of the sample before and after the labelling:

$$ExcessC[mg] = \frac{^{13}C_{labeled}}{^{12}C_{labeled}} \times C_{sample}[mg] - \frac{^{13}C_{unlabeled}}{^{12}C_{unlabeled}} \times C_{sample}[mg] \quad (6)$$

The $^{13}C/^{12}C$ ratio can be obtained from the measured $\delta\,^{13}C$ as follows:

$$\frac{^{13}C}{^{12}C}_{sample} = \left(\frac{\delta^{13}C_{measured}}{1000} + 1\right) \times 0.011237 \quad (7)$$

where 0.01123 is the $^{13}C/^{12}C$ ratio of the international V-PDB standard (Craig, 1957).

A second labelling experiment was performed in order to obtain uptake rates as a function of depth for mofette and reference soils. After sampling 5 g of soil into 12 ml Labco® Exetainers as described above, mofette samples were flushed with 100 vol. % $^{13}CO_2$, and reference soils with 10 vol. % $^{13}CO_2$ and 90 vol. % N_2. Soils were incubated for 7 days in the dark at 12°C. The headspace of all samples was exchanged after 3 days of incubation. After 7 days, vials were opened and flushed with N_2 for 2 min and evacuated to remove any sorbed or dissolved $^{13}CO_2$. Soil samples were subsequently air dried at 60°C and prepared for bulk ^{13}C analysis as described above. The measured enrichment in ^{13}C was used to measure uptake rates according Eq. (6).

2.2.7 DNA extraction and quantitative PCR

Total nucleic acid extractions of 0.7 g homogenised soil from mofette 1 and reference 1 were performed in triplicates according to the protocol of Lueders et al. (2004). Co-extracted organic soil compounds were removed by sequential purification with gel columns (S-400 HR; Zymo Research, Irvine USA) and silica columns (Powersoil Total RNA Kit in combination with the DNA Elution Accessory kit; MO BIO Laboratories, Carlsbad CA). Nucleic acid extraction efficiency was checked by agarose gel electrophoresis.

Copy numbers of 16S rRNA, cbbL 1A, cbbL 1C and cbbM genes in extracted DNA were determined using quantitative PCR (qPCR). qPCR was performed on a Mx3000P instrument (Agilent, Santa Clara, CA, USA) using Maxima SYBR Green Mastermix (Thermo Scientific) and the primer combinations Uni-338 F-RC and Uni-907 R (16S rRNA, (Weisburg et al., 1991), F-cbbM and R-cbbM (cbbM, (Alfreider et al., 2003)), F-cbbL and R-cbbL (cbbL IA, (Alfreider et al., 2003)) as well as F-cbbL IC and R-cbbL IC (cbbL 1C, (Alfreider et al., 2003)) as described by Herrmann et al. (2012). Cycling conditions for 16S rRNA genes as well as cbbL and cbbM genes consisted of denaturation for 10 min at 95°C, followed by 50 cycles with 4 temperature steps (1. 95°C at 30 s; 2. 55 and 57°C at 30 s for cbbL and cbbM/16S rRNA genes, respectively; 3. 72°C at 45 s; 4. data acquisition at 78°C and 15 s). Standard curves were constructed using plasmid CB54 for 16S rRNA and standard curves for cbbL and cbbM marker genes were constructed from ten times dilution series of mixtures of plasmids containing cbbL and cbbM inserts as described in Herrmann et al. (2015). PCR inhibitors were tested by ten times dilution series of representative samples. For the investigated samples 5 µl of DNA was taken as template for gene copy quantification of 16S rRNA, cbbL and cbbM.

2.2.8 Mass balance calculations

The unique isotopic composition of geogenic CO_2 and combined measurements of radiocarbon and stable isotopes allows identification of plant and microbial end-members for quantifying the importance of these two sources of SOM. Geogenic CO_2 ($\Delta^{14}C$ = -1000‰, $\delta^{13}C$ = -2 ‰) is quite different from

atmospheric CO_2 ($\Delta^{14}C$ ~+20‰, $\delta^{13}C$ = -7 ‰) in both isotopes. Therefore, $\Delta^{14}C$ values can be used to determine the overall fraction of geogenic CO_2 that is assimilated by plants or microorganisms in the mofette by using the end-members $\Delta^{14}C_{geogenic\ CO2}$ and $\Delta^{14}C_{air}$. A conventional mixing model for determining the fraction of geogenic CO_2 in SOM can be calculated according to:

$$SOM_{geogenic}[\%] = \frac{\Delta^{14}C_{SOM} - \Delta^{14}C_{air}}{\Delta^{14}C_{geogenicCO2} - \Delta^{14}C_{air}} \times 100 \quad (8)$$

This mass balance assumes that changes in $\Delta^{14}C_{SOM}$ caused by radioactive decay of ^{14}C are small compared to contributions from geogenic CO_2.

The same mass balance can be applied for calculating the fraction of geogenic CO_2 with stable isotope values. The end-members for this calculation are $\delta^{13}C$ values of plants, which grew solely on geogenic CO_2 or solely on ambient air CO_2. Plant $\delta^{13}C$ values are expected to be around 20 ‰ depleted in ^{13}C compared to the respective CO_2 source due to enzymatic fractionation, which has to be considered in determining the $\delta^{13}C$ end-member value.

We used the correlations between $\delta^{13}C$ and $\Delta^{14}C$ of plant material to prove that enzymatic discrimination of plants is constant in the vicinity of the mofette, despite potentially fluctuating CO_2 concentrations. If $\Delta^{14}C$ and $\delta^{13}C$ values of plants show a linear correlation, $\Delta^{14}C$ values of SOM can be used to derive $\delta^{13}C$ values that should be expected, if the organic matter is solely derived from plants according the mixing model:

$$\delta^{13}C_{model} = \delta^{13}C_{plantgeo} * (\Delta^{14}C_{SOMmofette} * m + t) + \delta^{13}C_{plantair} * \left(1 - (\Delta^{14}C_{SOMmofette} * m + t)\right) \quad (9)$$

where $\delta^{13}C_{plant\_geo}$ and $\delta^{13}C_{plantair}$ $\delta^{13}C_{plant\_air}$ are the measured plant input end-members exhibiting the most depleted (i.e. highest exposure to geogenic CO_2) and most enriched (exposure to atmospheric CO_2) $\Delta^{14}C$ values, respectively. $\Delta^{14}C_{SOMmofette}$ are measured radiocarbon values at a certain depth within the mofette soil. m and t are the slope and intercept of the regression between measured $\delta^{13}C$ and $\Delta^{14}C$ plant values. The model calculates the $\delta^{13}C_{SOM}$ that corresponds to measured $\Delta^{14}C_{SOM}$ values, if all SOM would be derived from plant

material. Deviation from the model indicates input of C sources other than plants with distinct isotopic compositions.

2.2.9 Statistical analyses

Reported results (e.g. $\delta^{13}C$ values, microbial biomass), represent the mean of three independent replicates. Uncertainties reported for radiocarbon data represent analytical precision of a homogenised sample comprised of three independent soil cores. Differences of $\delta^{13}C$ in mofette and reference soils as well as between soil depth intervals were analysed using Student`s t-test. Significant differences are reported at $p < 0.05$.

2.3 Results

2.3.1 pH, bulk TOC and C/N

Soil pH ranges from 3.0 to 3.5 in mofette soils and is higher in reference soils (averaging 4.4), without significant trends with depth (Table 2-1). Total organic carbon (TOC) contents are high (~12 - 20% C) in the surface 5 cm of both mofette and reference soils. In the reference soil, TOC decreases with depth to concentrations of 3 % C below 20 cm. In contrast, TOC concentrations in both mofettes decrease below 5 cm (~6 to 16 %) and increase subsequently to more than 30 % below 20 cm.

Organic matter quality as indicated by C/N ratio also highlights differences between mofette and reference soils. High C/N ratios ranging from 25 to 30 are found below 20 cm depth in both mofettes, whereas C/N ratios decrease rapidly as low as 16.5 to 9 (for mofette 1 and 2, respectively) in the upper 10 cm (Table 2-1). In both reference soils, C/N ratios remain constant throughout the profile at 10 to 14 (Table 2-1).

	pH	TOC [w-%]	C/N	Water content [%]	$\delta^{13}C$	$\Delta^{14}C$
Mofette 1						
0-5	3.68	19.64 ± 1.20	15.95	53	-26.90 ± 0.15	- 554.3 ± 2.0
5-10	3.59	26.54 ± 0.08	16.52	52	-27.55 ± 0.21	
10-20	3.68	11.53 ± 0.18	15.12	57	-26.71 ± 0.18	- 559.7 ± 2.1
20-30	3.43	16.33 ± 0.59	21.65	51	-26.79 ± 0.12	
30-40	3.40	34.00 ± 1.25	31.40	56	-27.01 ± 0.23	- 640.2 ± 1.9
Reference 1						
0-5	4.13	25.85 ± 1.72	14.37	69	-27.98 ± 0.32	- 117.5 ± 2.8
5-10	4.07	12.40 ± 0.60	14.18	49	-28.10 ± 0.24	
10-20	4.00	3.16 ± 0.26	14.52	42	-27.80 ± 0.13	- 236.3 ± 2.7
20-30	3.91	3.14 ± 0.13	12.93	31	-27.79 ± 0.16	
30-40	3.69	2.81 ± 0.50	15.88	30	-28.23 ± 0.09	- 280.2 ± 2.5
Mofette 2						
0-5	3.80	8.66 ± 0.69	8.95	52	-26.01 ± 0.14	- 648.1 ± 1.2
5-10	3.76	5.87 ± 1.11	8.97	53	-26.26 ± 0.24	
10-20	3.79	11.41 ± 0.95	9.72	50	-26.76 ± 0.19	- 618.7 + 1.3
20-30	3.52	28.72 ± 1.42	19.74	56	-27.10 ± 0.59	
30-40	-	-	-	-	-	-
Reference 2						
0-5	4.50	12.48 ± 0.31	12.16	45	-27.91 ± 0.12	-34.1 ± 2.2
5-10	4.51	7.59 ± 0.21	11.52	42	-28.85 ± 0.21	
10-20	4.48	2.94 ± 0.15	10.30	46	-28.11 ± 0.05	-114.7 ± 1.9
20-30	4.46	1.91 ± 0.10	11.85	40	-27.82 ± 0.30	
30-40	4.43	1.80 ± 0.04	10.19	35	-28.23 ± 0.06	-162.9 ± 1.9

Table 2-1: Geochemical soil properties of mofette and reference soils. $\delta^{13}C$ and geochemical data represent background (i.e. without addition of label) data obtained from sampling in September 2014. Radiocarbon data was obtained in November 2013. Uncertainties in geochemical and $\delta^{13}C$ data represent ±1σ standard deviation (n=3). Uncertainties in radiocarbon values represent analytical precision of a homogenized mixed sample.

2.3.2 Radiocarbon and stable isotope ratios of bulk SOM, plants and CO_2

Consistent with our expectation, we found that geogenic CO_2 is free of radiocarbon (-1000 ‰) and has an average $\delta^{13}C$ value of -2.36 ± 0.6 ‰.

Radiocarbon concentrations of SOM in both mofettes are generally more depleted by several hundred ‰ compared to reference soils (table 2-1). In reference soils, $\Delta^{14}C$ values decrease uniformly with depth from -60 ‰ and -34 ‰ in the top 10 cm to values of -280 ‰ and -163 ‰ at 40 cm depth in reference soil 1 and 2, respectively, reflecting radioactive decay (table 2-1).

$\delta^{13}C_{SOM}$ in mofettes has average values of -26.99 ± 0.33 ‰ and -26.38 ± 0.54 ‰ in mofette 1 and 2, respectively. In both mofettes $\delta^{13}C_{SOM}$ decreases

slightly (but not significantly) below 20 cm depth (p = 0.39 and 0.49 in mofette 1 and 2, respectively) (table 2-1). Both reference soils have $\delta^{13}C_{SOM}$ of -28.08 ± 0.4 ‰ with no distinct depth trend in reference 1 (p = 0.96) and a slight but not significant decrease in reference 2 (p = 0.35) below 20 cm. At every depth, reference soils are 1 to 2 ‰ depleted in ^{13}C compared to mofette $\delta^{13}C_{SOM}$ throughout the soil profile ($p < 0.05$) (table 2-1).

Carbon isotope signatures in vegetation samples surrounding the mofette range from -29.95 ± 0.16 ‰ to -23.81 ± 0.30 ‰ in $\delta^{13}C$ and from -10.3 ‰ to -807.7 ‰ in $\Delta^{14}C$. Variations in the two isotopes are highly correlated, and plants with most positive $\delta^{13}C$ and most negative $\Delta^{14}C$ were found closest to the mofette and vice versa (figure 2-1). The linear fit to the strong (R^2= 0.86) relationship between ^{13}C and ^{14}C found in vegetation material (figure 2-1) is used to determine parameters for the mixing model (Eq. 9). The intercept of the line with the y-axis yields a value of -22.79 ‰ and represents the $\delta^{13}C$ end-member value of plant material, which is fully labelled with geogenic CO_2 ($\delta^{13}C_{plant\_geo}$($\delta^{13}C_{plantgeo}$, or t in Eq. (9)). For the other endmember, $\delta^{13}C_{plant\_air}$, we used the $\delta^{13}C$ value of plants from the reference site that exhibited the most positive $\Delta^{14}C$ value, which yields $\delta^{13}C_{plantair}$ of -29.15 ‰. The corresponding $\Delta^{14}C$ value, i.e. the value closest to atmospheric radiocarbon concentrations, was -10.3 ‰ (= $\Delta^{14}C_{plantair}$). This is less than $\Delta^{14}C$ measured in CO_2 in clean background air in the year of sampling (~+20‰) and indicates either that the reference site experiences some influence of geogenic CO_2 or the influence of local fossil fuel release in the region.

The slope of the relationship fit to plant samples (m in Eq. (9)) is what would be expected for a linear mixture of plant material of the two end-member atmospheres (pure geogenic and pure air). Plant derived SOM would be expected to fall with this mixing line. The majority (71 %) of reference soil values are within the 95 % confidence interval of this expected slope (figure 2-1). In reference soils, ^{14}C declines with soil depth, while ^{13}C remains nearly constant. Mofette SOM generally has lower ^{13}C values than would be expected if they had the same linear relationship as plant material, and ^{14}C signatures are all much

lower than those of the reference soil (figure 2-1). Only 5 % of mofette SOM values fall within the 95 % confidence interval of the regression line.

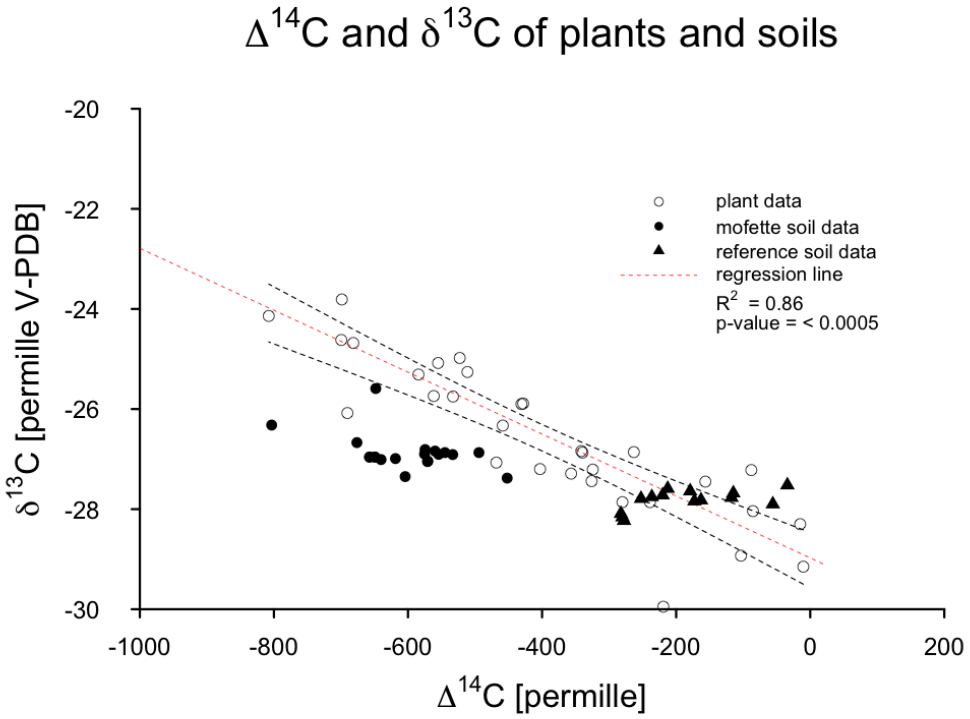

Figure 2-1: Correlation between $\delta^{13}C$ and $\Delta^{14}C$ of plants growing around the mofette structure. Dependent on the exposure to geogenic CO_2, plants incorporate different amounts of geogenic CO_2, which complicates isotope mass balance calculations for mofette SOM. However, both isotopes are highly correlated in sampled plant material, which allows prediction of $\delta^{13}C$ SOM isotope values from plant $\Delta^{14}C$. Most data points measured from mofette SOM fall outside 95% confidence levels of the regression, which suggests a deviation of mofette SOM $\delta^{13}C$ values from a pure vegetation signal. Reference SOM $\delta^{13}C$ values fall mainly within the observed plant $\delta^{13}C$ values, and do not increase with depth, as is often observed in soil depth profiles. Parameters of the regression are used to predict the $\delta^{13}C_{SOM}$ values expected in mofette soils that correspond to measured radiocarbon values, assuming that all carbon would be plant derived (Eq. 9).

2.3.3 Mass balance calculations

Radiocarbon signatures of SOM indicate that, on average, 55 to 65 % of carbon accumulated in the mofette is derived from geogenic CO_2 (assuming end-members of -10 ‰ for $\Delta^{14}C$ air and -1000‰ for $\Delta^{14}C$ geogenic CO_2). The calculated proportion increases with depth. By doing the same mass-balance calculation with $\delta^{13}C$ values, (with - 22.47 ‰ as geogenic CO_2 end-member and - 29.15 ‰ as reference end-member), one obtains lower proportions of 34 - 44

% geogenic C compared to the radiocarbon mass balance. This mismatch in quantifying the proportion of geogenic C suggests that $\delta^{13}C_{SOM}$ values differ from what we would expect if they were completely derived from plant inputs.

Equation (9) can be used to predict $\delta^{13}C$ SOM values corresponding to measured radiocarbon values, assuming that all carbon would be derived from unaltered plant material. Calculated $\delta^{13}C_{SOM}$ values are 1-2 ‰ more positive at all depths ($p < 0.05$) compared to observations (figure 2-2 B), i.e. measured $\delta^{13}C_{SOM}$ values are depleted in ^{13}C compared to a signal that would be expected, if SOM would have preserved its original plant $\delta^{13}C$ signature.

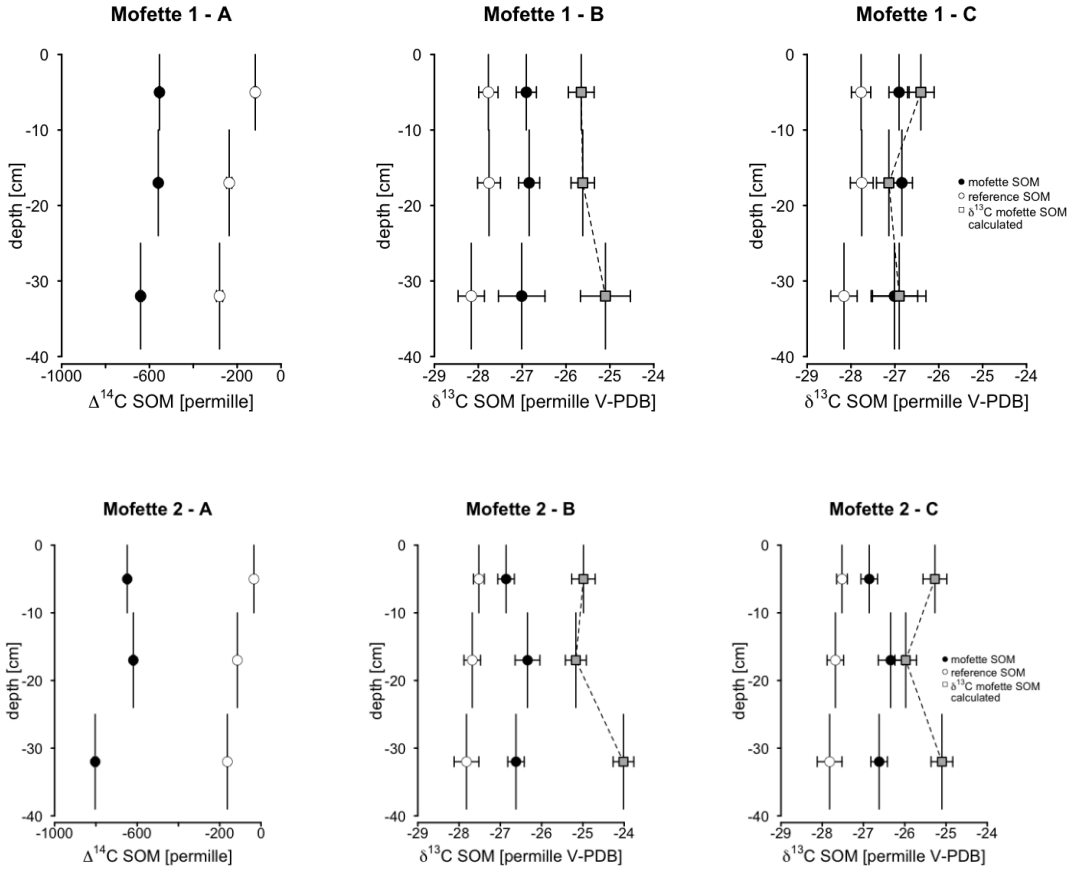

Figure 2-2: Depth profile of ^{14}C and ^{13}C signatures of SOM in mofette and reference soils. A) Radiocarbon values in mofette soils are more depleted than reference soils, reflecting incorporation of geogenic CO_2 either by plants or by microorganisms. Error bars reflect analytical precision because only one homogenized sample was analyzed. B) $\delta^{13}C$ values in both mofettes are also shifted towards geogenic CO_2, but to a smaller extent than radiocarbon values. Gray squares in $\delta^{13}C$ depth profiles show values of $\delta^{13}C$ in mofette SOM estimated using Eq (9). Measured $\delta^{13}C$ values are more depleted than estimated values at all depths. C) Estimated $\delta^{13}C$

values, assuming eq (9) but with ^{14}C values that have been corrected for radioactive decay assuming that SOM ages with depth in the same way as the reference soil These estimated $\delta^{13}C$ values agree with measured values below 20 cm depth but remain depleted compared to what is expected from a pure plant SOM source in the top 10 cm. This suggests that the observed depletion in the top 10 cm of both mofette soils is caused by addition of ^{13}C depleted microbial carbon, derived from fixed CO_2. In contrast, the mismatch between estimated and measured values below 20 cm depth in (B) can be explained by radioactive decay

2.3.4 Quantification of microbial CO_2 fixation activity

The analysis of bulk SOM and plant material revealed that mofette and reference soils are distinct in their radiocarbon as well as stable isotope values, indicating incorporation of geogenic CO_2 into mofette SOM either by plants or by microorganisms. Both isotopes show a bias in quantifying the amount of SOM derived from geogenic CO_2 by the same isotope mass balance, which suggests the presence of another source of carbon than plants, presumably microorganisms, that depletes $\delta^{13}C$ values. CO_2 fixing microorganisms might be a potential source with a distinct $\delta^{13}C$ value. In order to assess the activity of CO_2 fixing microorganisms as well as their spatial distribution along the soil profile, we conducted two isotope-labelling experiments.

In the first experiment we traced $^{13}CO_2$ directly into microbial biomass (MB) within the first 10 cm of the soil profile. After incubating the soils with $^{13}CO_2$, MB within all soils showed high enrichment in ^{13}C, except in autoclaved control soils. Microbial biomass extracts of autoclaved controls had $\delta^{13}C$ values ranging between -24.10 ± 0.38 to -27.55 ± 0.14 ‰, in both, fumigated and unfumigated samples, which is close $\delta^{13}C$ values obtained from bulk soil measurements (table 2-2). This confirms that mainly biological processes mediated CO_2 incorporation. In un-sterilized samples, unfumigated extracts showed enrichment in ^{13}C in all mofette and reference soils. The $\delta^{13}C$ of unfumigated samples ranged from -14.29 ± 0.8 ‰ to +80.47 ± 9.46 ‰ and are therefore enriched in ^{13}C compared to controls ($p < 0.05$). However, in all cases ^{13}C enrichment was higher after fumigation ($p < 0.05$). $\delta^{13}C$ values of fumigated samples ranged between 143.76 ± 3.93 ‰ and 227.04 ± 2.63 ‰.

The calculated rate of CO_2 uptake expressed per gram microbial biomass in the top 10 cm of soil (table 2-2) was higher in mofettes compared to reference soils ($p < 0.05$) ranging between 287 ± 85 and 271 ± 58 ug^{-1} gMB^{-1} d^{-1} in mofettes compared to 139 ± 32 and 99 ± 36 ug^{-1} gMB^{-1} d^{-1} in reference soils (table 2-2).

	δ ^{13}C extract (after fumigation) [‰]	δ ^{13}C control [‰]	Uptake rate/g soil [ug gdw^{-1} d^{-1}]	Uptake rate/g MB [ug gMB^{-1} d^{-1}]	% labelled MB
Mofette 1					
CFE 0 - 10 cm	233.24 ± 11.19	-25.94 ± 0.36	0.17 ± 0.03	287 ± 85	0.88 + 0.33
Bulk 0 -10 cm	-21.19 ± 0.62	-26.28 ± 0.10	0.77 ± 0.23	-	-
Reference 1					
CFE 0 - 10 cm	182 ± 5.44	-23.65 ± 0.54	0.59 ± 0.05	139 ± 32	0.40 ± 0.13
Bulk 0 -10 cm	-12.82 ± 0.95	-27.55 ± 0.14	2.65 ± 0.36	-	-
Mofette 2					
CFE 0 - 10 cm	124.51 ± 10.66	-24.10 ± 0.38	0.06 ± 0.02	271 ± 58	0.8 ± 0.16
Bulk 0 -10 cm	-21.37 ± 0.99	-26.49 ± 0.08	0.66 ± 0.15	-	-
Reference 2					
CFE 0 - 10 cm	158.05 ± 4.01	-26.46 ± 0.21	0.25 ± 0.09	99 ± 36	0.20 ± 0.10
Bulk 0 -10 cm	-17.44 ± 0.81	-27.21 ± 0.22	0.71 ± 0.16	-	-

Table 2-2: Microbial biomass C and comparison of uptake rates determined during experiment 1 with CFE and bulk measurements. Uncertainties represent ±1σ standard deviation (n=3).

The second labelling experiment measured CO_2 fixation activity along the whole soil profile with samples taken from depth intervals between 1 to 40 cm. Tracer uptake was measured only in bulk SOM. In both soils, uptake rates decrease with depth (figure 2-3). In the top 5 cm, uptake rates were higher in mofette soils compared to reference soils. Below 20 cm, rates decrease to values of 0.14 ± 0.03 ug gdw^{-1} d^{-1} in both mofettes and 0.09 ± 0.02 ug gdw^{-1} d^{-1} in reference soils. Normalizing the uptake rates to soil carbon content (ug gC^{-1} d^{-1}) instead of soil mass, removes the depth-dependence of uptake rates in reference soils ($p < 0.05$), but not in mofette soils (figure 2-3).

2.3.5 Quantification of 16s rRNA and marker genes for RubisCO

Results of 16S rRNA and RubisCO encoding marker genes are listed in table 2-3. The abundance of 16S rRNA genes per gram soil is a measure of the total abundance of microorganisms in the soil (Fierer et al., 2005). Gene copy numbers per gram soil of 16S rRNA genes were more abundant in the top 5 cm

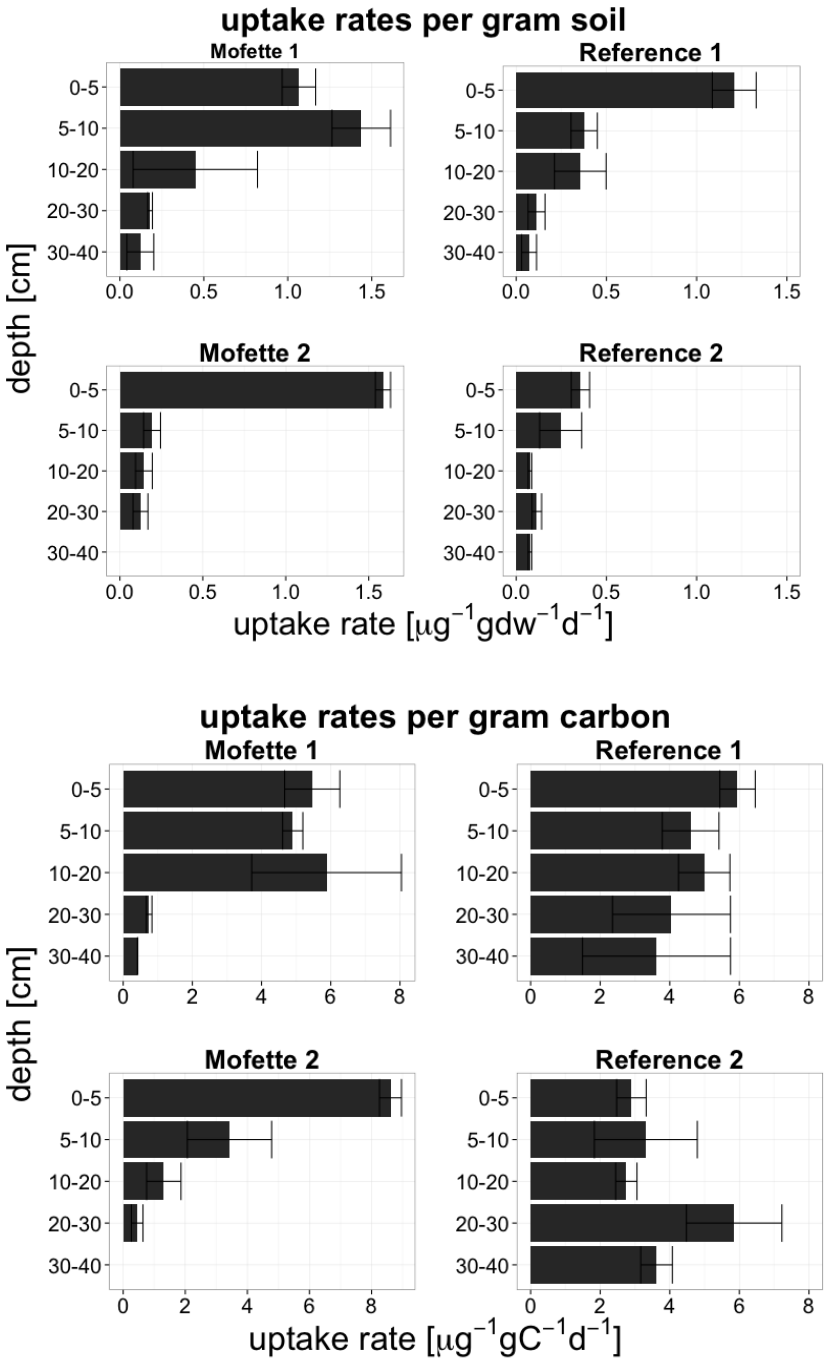

Figure 2-3: CO_2 uptake rates along depth profiles of mofette and reference soils as determined by bulk measurements from experiment 2. In both mofettes, uptake rates are highest in the top 10 cm and show a trend towards decreasing values at lower depths, especially below 20 cm. Uptake rates in reference soils also decrease with depth, but are nearly constant if normalized to organic carbon content. In contrast, uptake rates per organic carbon decline with depth in the mofette soils. This suggests increasing importance of autotrophic organisms with soil depth in the reference soil.

of the mofette soil. They decrease with depth, in both, mofette and reference soil ($p < 0.05$), but the decrease is more rapid in the mofette. The same holds true for

marker genes encoding for RubisCO. CbbL IC is the most abundant marker gene in both soils, whereas it is more abundant in the reference soil compared to the mofette. CbbL 1C is one order of magnitude more abundant than cbbL 1A and cbbM in both, reference and mofette soils. cbbL:16S rRNA ratios range between 0.07 ± 0.03 and 0.19 ± 0.04 in the mofette soil and stays fairly constant with depth ($p = 0.61$). In the reference soil the ratio decreases slightly with depth from 0.37 ± 0.16 to 0.17 ± 0.04, but values are consistently greater than in the mofette soil.

	Depth [cm]	16S rRNA	cbbM	cbbL 1A	cbbL 1C	cbbL 1C/ 16sRNA
Mofette 1	0 - 5	7.50E+10 ± 1.42E+07	5.70E+08 ± 3.21E+08	9.45E+08 ± 4.86E+08	9.23E+09 ± 4.55E+09	0.12 ± 0.06
	5 - 10	1.65E+10 ± 5.35E+06	2.21E+08 ± 1.28E+08	1.40E+08 ± 1.69E+08	1.46E+09 ± 1.20E+09	0.11 ± 0.04
	10 - 20	3.35E+09 ± 0.51E+06	1.49E+07 ± 8.45E+06	1.83E+07 ± 1.22E+07	6.02E+08 ± 1.25E+08	0.17 ± 0.03
	20 - 30	5.94E+09 ± 9.02E+05	1.62E+07 ± 1.23E+07	1.12E+07 ± 4.07E+06	3.98E+08 ± 1.53E+08	0.07 ± 0.03
	30 - 40	7.62E+08 ± 9.39E+04	8.53E+05 ± 3.02E+05	1.71E+06 ± 5.23E+05	7.91E+07 ± 2.18E+07	0.10 ± 0.03
Reference 1	0 - 5	4.63E+10 ± 3.01E+07	3.43E+08 ± 3.18E+08	1.14E+09 ± 4.74E+08	1.58E+10 ± 7.20E+09	0.37 ± 0.23
	5 - 10	2.98E+10 ± 2.02E+07	2.01E+08 ± 5.98E+07	2.69E+08 ± 1.52E+08	7.78E+09 ± 8.12E+08	0.28 ± 0.08
	10 - 20	2.81E+10 ± 4.83E+07	1.31E+08 ± 4.73E+07	3.06E+08 ± 1.59E+08	5.95E+09 ± 1.50E+09	0.21 ± 0.06
	20 - 30	1.24E+10 ± 4.37E+07	9.75E+07 ± 3.99E+07	9.11E+07 ± 3.90E+07	2.25E+09 ± 6.84E+08	0.18 ± 0.03
	30 - 40	4.65E+09 ± 9.61E+07	1.57E+08 ± 9.26E+07	3.47E+07 ± 2.20E+07	5.95E+08 ± 1.78E+08	0.10 ± 0.06

Table 2-3: Quantification of 16S RNA, cbbL and cbbM marker genes. Uncertainties represent ±1σ standard deviation (n=3).

2.4 Discussion

2.4.1 Carbon sources in mofette soils

Low C/N ratios, as found in the top 10 cm of both mofettes, reflect microbially degraded OM (Rumpel and Kogel-Knabner, 2011) and C/N ratios as low as 9 (top 10 cm of mofette 2) suggest a high contribution of microbial biomass to bulk SOM (Wallander et al., 2003). A significant contribution of microbial biomass carbon at these depths is also supported by very high 16S rRNA copy numbers, extracted from mofette 1, which are one order of magnitude higher than known from other soils (Fierer et al., 2005). Also numbers of RubisCO encoding genes are two orders of magnitude more abundant than in agricultural soils (Selesi et al., 2007) and twice as high as in organic rich paddy rice fields (Wu et al., 2015), suggesting microbial carbon derived from CO_2 assimilation as an important carbon source. Further evidence is given by the isotope data, as mofette SOM at 0 to 10 cm differs from a pure plant signal. The deviation of $\delta^{13}C_{SOM}$ towards more negative values compared to plant signatures suggests that microbialy derived carbon in shallower depths is fractionated against ^{13}C, which provides further evidence that autotrophic microorganisms contribute significantly to mofette SOM.

Below 20 cm, inceasing C contents in both mofettes are accompined with a steep increase in C/N, which is attributed to lower proportions of microbial carbon and accumulation of undecomposed plant organic matter, as suggested from studies at other mofette sites (Rennert et al., 2011).

2.4.2 Quantification of SOM isotope shifts by combined $\Delta^{14}C$ and $\delta^{13}C$ mass-balances

TOC, C/N ratios and the abundance of 16S rRNA genes in mofette soils all suggest that microbial carbon might constitute a significant part of bulk SOM. The isotope mass balance model can be used to assess the contribution of plant vs. microbial derived carbon. The approach assumes that microbially derived carbon is distinct either in its ^{14}C or its ^{13}C isotope ratio compared to plant carbon. The isotope mass balance model derived from equation 9 shows that microbial carbon that is added to SOM has to be depleted in $\delta^{13}C$ compared to

plant inputs, leading to an overall negative $\delta^{13}C$ shift in bulk SOM of 1-2 ‰ compared to a pure plant signal at all depths (figure 2-2 B).

However, the model assumes that the radiocarbon content of mofette SOM solely depends on the amount of fixed geogenic CO_2 and does not consider radioactive decay. ^{14}C depletion by radioactive decay, especially with soil depth, can lead to an overestimation of fixed geogenic CO_2 and consequently to an overestimation of the shift in $\delta^{13}C$ values. In order to account for ^{14}C depletion by radioactive decay, $\Delta^{14}C$ values of reference soil SOM can be subtracted from $\Delta^{14}C_{SOMmofette}$ in Eq (9).

After correcting the model for radioactive decay, the calculated $\delta^{13}C_{SOM}$ depletion still matches the data for the first 10 cm of both mofettes, where measured $\delta^{13}C$ values are more negative than calculated ones (figure 2-2 C). Below 10 cm, the calculated $\delta^{13}C_{SOM}$ coincides with measured values in both mofettes, suggesting that SOM $\delta^{13}C$ preserved the signal of the plant source and only radioactive decay lead to the initial $\delta^{13}C$ shift in the model (figure 2-2 C). This supports findings from previous studies, where carbon accumulation accompanied with high C/N ratios was attributed to accumulation of poorly decomposed plant material (Rennert et al., 2011). The only exception from this pattern is at 30 - 40 cm in mofette 2, where measured $\delta^{13}C$ values are still more negative than calculated ones, even after correction for radioactive decay (figure 2-2 C). This might be caused by extremely low carbon dynamics, e.g. due to permanently waterlogged conditions, which would lead to an overestimation of the $\delta^{13}C$ isotope shift in the model. Although water levels fluctuate in the floodplain, permanently waterlogged conditions are likely to occur deeper in moffete 2, where high CO_2 discharge rates might lead to an elevation of the water table. Waterlogged conditions lead to low carbon turnover, and correction of radioactive decay with reference soil values might not be sufficient, because reference soils at these depths are only temporally waterlogged. This might explain the mismatch of measured and calculated $\delta^{13}C$ values at the deepest sampling point in mofette 2 and would indicate a potential bias of modelled C-isotope signatures towards too positive $\delta^{13}C$ values.

Another source of error in the model is accumulation of recalcitrant compounds within the SOM pool, like lignin or lipids, which might also lead to a shift in $\delta^{13}C$ values compared to the original bulk plant material (Benner et al., 1987; Werth and Kuzyakov, 2010). The accumulation of phenolic compounds is usually accompanied with an increase in C/N ratios (Hornibrook et al., 2000; Werth and Kuzyakov, 2010), which is not the case in the top 10 cm of the mofette soil. Therefore, lignin accumuation is not likely to have caused the depletion in the top 10 cm of both mofettes. Nevertheless, increased lignin accumulation might also be the reason for the observed depletion in $\delta^{13}C$ below 20 cm depth in mofette 2.

Therefore, the model shows that $\delta^{13}C$ values in the top 10 cm of both mofettes are significantly lower than expected for SOM derived from plants alone, indicating significant addition of $\delta^{13}C$ depleted carbon. Below 10 cm depth, the calculated and measured $\delta^{13}C$ values agree after correcting for possible sources of error, like radioactive decay and alteration of $\delta^{13}C$ due to decomposition processes.

Microbial carbon that is added to mofette SOM by several CO_2 fixation pathways is likely to be depleted in $\delta^{13}C$ because of enzymatic fractionation processes (Fuchs, 2011). The deviation in $\delta^{13}C$ in the top 10 cm of both mofettes also is in accord with high CO_2 fixation rates and the abundance of functional marker genes for CO_2 fixation at this depth (figure 2-4). This implies that microbial carbon derived from CO_2 assimilating organisms is a major driver of the observed $\delta^{13}C_{SOM}$ depletion.

2.4.3 Quantification of microbial carbon C derived from CO_2 fixation

In order to quantify the proportion of CO_2-derived microbial carbon from the observed isotope shift, it is important to know the metabolic pathway that was used for CO_2 fixation and its corresponding isotope fractionation factor. Beulig et al. (2016) investigated by metatranscriptomic and metagenomic approaches microbial key processes in mofette soil 1. Consistent with our quantification of cbbL/cbbM marker genes, Beulig et al. (2016) detected high frequencies of transcripts encoding key enzymes for the Calvin Benson Cycle as

well as the Reductive Acetyl CoA Cycle. The Acetyl CoA Cycle is used by acetogens, methanogens and sulphate reducers for catabolism and anabolism (Drake et al., 2006). According to Beulig et al. (2016), transcripts of key enzymes for the Acetyl CoA pathway in the mofette soil are also related to these groups. Most transcripts encoding for the Calvin Benson Cycle were related to chemoautotrophic bacteria and algae, living under anaerobic restrictions. The activity of autotrophic bacteria using the Calvin Benson Cylce is also supported by our data, as shown by the good correlation of cbbL/cbbM marker genes and uptake rates (figure 2-4).

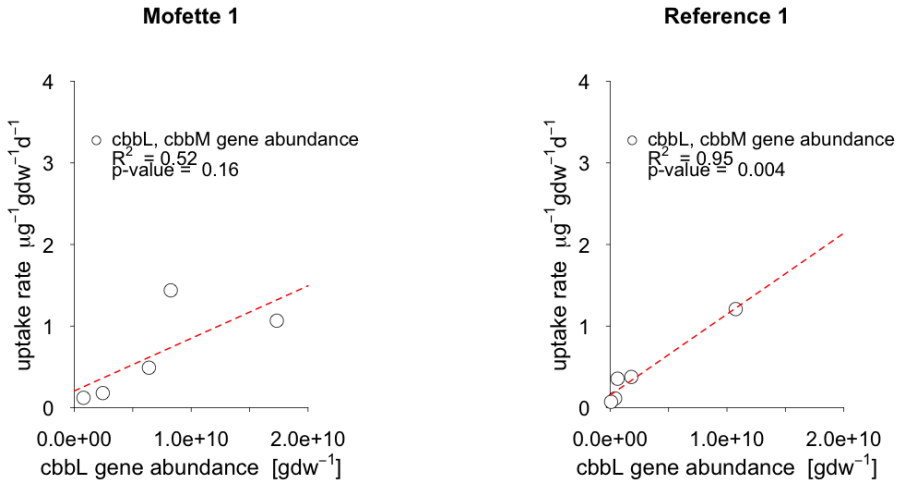

Figure 2-4: Correlation of marker genes encoding for RubisCO and measured uptake rates in mofette soil 1 and reference soil 1 in the soil depth profile from 0 to 40 cm depth. The good correlation in the reference soil indicates high contribution of chemolithoautotrophic microorganisms to measured uptake rates. In the mofette soil R^2 is considerable lower, most probably, because also other CO_2 fixation cycles that the CBB cycle, like the Acetyl-CoA cycle, are important pathways in these soils.

Carbon that is fixed by autotrophs or algae using Form I RubisCO, the dominant form in the mofette, is depleted by -27 to -30 ‰ compared to the source CO_2 ($\Delta \approx$ -27 to -30 ‰) (Hayes, 2001; Pancost and Damste, 2003). A similar value can be expected for acetate formed from geogenic CO_2 during acetogenesis. In systems where acetate is not limiting, depletion is less pronounced ($\Delta \approx$ -32 ‰) than in acetate-limited systems ($\Delta \approx$ -58.6 ‰) (Conrad, 2005; Gelwicks et al., 1989). A value of -32 ‰ is in accordance with acetate $\delta\,^{13}C$

values measured by Beulig et al. (2014) in a mofette study from the same area. Therefore, given a $\delta^{13}C$ value of geogenic CO_2 of around -2 ‰, the C end-member derived from microbial CO_2 fixation adds carbon with an average $\delta^{13}C$ value of -30 to -34 ‰ to bacterial biomass and SOM in mofettes. Taking the differences between measured and calculated $\delta^{13}C$ (with and without correction for radioactive decay, respectively) for mass balance calculation according to equation 8, microbially fixed geogenic CO_2 carbon in the top 10 cm of the mofette soil can make up between 8 ± 2 % and 15 ± 4 % in mofette 1 and between 23 ± 4 % and 27 ± 5 % in mofette 2.

2.4.4 Importance of microbial CO_2 fixation for isotope ratios in peat soils

Our data provide evidence that assimilation of CO_2 by several groups of autotrophic microorganisms contributes to SOM formation derived from CO_2. Recycling of CO_2 in peat deposits has been proposed to cause 'reservoir' effects in radiocarbon, biasing dating of peat (Kilian et al., 1995). As an explanation, Pancost et al. (2000) proposed recycling of $\Delta^{14}C$ depleted methane that diffuses from the catotelm layer up the peat profile, where it is oxidized by methanotrophic organisms and subsequently assimilated by mycorrhizal fungi living in association with *Ericaceae* rootlets. However, the authors could not find evidence from biomarker analyses of methanotrophic or fungal organisms and attributed recycling of ^{14}C depleted CO_2 to plants. Our findings suggest that other groups besides fungi are involved in CO_2 recycling, namely CO_2 utilizing autotrophic microorganisms. Pancost et al. (2000) estimated that 20 % of C in the investigated peat is derived from this recycling process. This proportion is very similar to our estimates for autotrophic fixation of CO_2 in the 0-10 cm of mofette soil. Hence we would propose that direct fixation of CO_2 could be a major process influencing peat radiocarbon signatures.

2.4.5 Importance of CO_2 fixation for soil carbon in reference soils

When normalized for the mass of carbon (as opposed to mass of soil), rates of CO_2 fixation in the reference soil at depth remain similar to values at the surface (figure 2-3). We cannot use the isotope-mixing model to estimate the

amount of C derived from CO_2 fixation in the reference soil, because the soil atmosphere as well as plants at the reference soil are not directly influenced by geogenic CO_2. However the rate measurements suggest increasing importance of CO_2 assimilating microorganisms for carbon stocks with depth. In addition, the high relative abundance of RubisCO marker genes relative to 16S rRNA genes suggest that autotrophic organisms constitute a substantial part of the microbial community throughout the soil profile. Their activity is also indicated by the strong correlation between RubisCO marker genes and uptake rates ($R^2 = 0.94$, $p < 0.05$) (figure 2-4). Higher CO_2 concentrations, which are usually observed with depth, might also lead to an increase of CO_2 assimilation, because of higher substrate availability for RubisCO or other carboxylases with depth.

In contrast to the mofette soil, which is characterized as an organic rich histosol, reference soils are classified as gleysols, with high organic carbon contents only in the A horizon. They are characterized by frequently changing redox conditions due to groundwater fluctuations, which might provide sufficient electron donors and acceptors for chemolithoautotrophic microorganisms (Akob and Küsel, 2011).

Beulig et al. (2014) characterized the microbial community of a reference soil at the same study site. The authors found that Proteobacteria constituted a substantial part of the microbial community. Many Proteobacteria are facultative autotrophs using the CBB cycle and have a facultative anaerobe metabolism (Badger and Bek, 2008). They would be therefore able to assimilate CO_2 also under the experimental conditions.

A contribution of phototrophic and chemoautotrophic microorganisms to SOM has been demonstrated already by other studies (Hart et al., 2013; Yuan et al., 2012), but solely for top soils. Wu et al. (2014) and Wu et al. (2015) investigated soil depth profiles up to 15 cm depth , but found no significant incorporation below 5 cm depth in upland and paddy soils under not manipulating experimental conditions, like illumination .

Our data suggest that autotrophic microorganisms are active even in the reference-subsoil. Microorganisms using the CBB cycle would add ^{13}C-depleted carbon to SOM. Indeed, $\delta\,^{13}C$ profiles of both reference soils do not show shifts

towards more positive values with depth, as is usually observed from other Gleysols, although radiocarbon data indicates that SOM becomes older with depth (Alewell et al., 2011; Bol et al., 1999). Further, both reference soils have C/N ratios close to 10 throughout the soil profile, which normally indicates a higher contribution of microbial C to SOM (Rumpel and Kogel-Knabner, 2011). This strongly suggests a contribution of autotrophic microorganisms to carbon stocks in the subsoil, though ultimately its influence on the C isotopic signature of SOM at depth must be further evaluated.

2.5 Conclusions

$\delta^{13}C$ and $\Delta^{14}C$ values of SOM in wetland mofettes are influenced by incorporation of geogenic CO_2 fixed not only by plants, but also by microbes, as indicated by deviation of $\delta^{13}C$ values from those expected if plant C inputs were the sole source of SOM-C. The unique isotopic composition of geogenic CO_2 and the different enzymatic fractionation of plants and microorganisms allows us to quantify microbially derived C using combined ^{14}C and ^{13}C mass balances, because microbial carbon is more depleted than plant C. Other parameters, like C/N ratio, 16S rRNA and cbbL gene abundance also indicate addition of C fixed from geogenic CO_2 by microbes. According to the isotope mass balances, microbial carbon derived from CO_2 fixation accounts for 8 - 27 % of bulk SOM in mofette soils. The significant contribution of autotrophic microorganisms to SOM also implies that they might be able to cause reservoir effects in radiocarbon by recycling of old CO_2, as has been already suggested for peat soils.

Further, high CO_2 fixation rates, especially in mineral horizons of the reference soil, as well as the high of RubisCO marker genes indicate a significant contribution of autotrophic microorganisms to subsoil carbon.

2.6 Acknowledgements

We thank Heike Geilmann and Steffen Rühlow for assistance with $\delta^{13}C$ analysis of bulk soil and CFE extracts. We thank Heike Machts and Axel Steinhof for

radiocarbon analysis of soil and plant samples. Further we thank Iris Kuhlmann for assistance in CFE extractions, as well as Julia Kuhr for helping in DNA extraction and soil sampling. We kindly acknowledge Gerd Gleixner for helpful discussions and comments on the manuscript. We would also like to acknowledge two anonymous reviewers, whose comments improved the manuscript. This project was supported by the graduate research training group "Alteration and element mobility at the microbe- mineral interface" (GRK 1257), which is part of the Jena School for Microbial Communication (JSMC) and funded by the Deutsche Forschungsgemeinschaft (DFG).

3 The activity of CO_2 fixing microorganisms in tropical rainforest soils and their impact on carbon isotopic signatures of microbial biomass and soil organic matter

Chapter source:

Nowak, M.E., Catao E.C.P., Santana, R.H., Behrendt, T., Krüger, R.H., Quesada, B., Trumbore, S.E. The activity of CO_2 fixing microorganisms in tropical rainforest soil and their impact on carbon isotopic signatures of microbial biomass and soil organic matter

This manuscript is in preparation for *Soil Biology and Biochemistry*

Abstract

Recent research suggests that microorganisms are an important source of organic carbon, especially deeper in soil profiles. An abundant but poorly constraint belowground process is microbial CO_2-fixation, i.e the microbial assimilation of CO_2 for cell growth or maintenance. Microbial CO_2 fixation is a process that occurs in soils, but its potential importance as a mechanisms recycling C is not very well known. CO_2 fixation can be performed by heterotrophic as well as autotrophic microorganisms. Chemolithoauotrophs have been shown to be very abundant and active in different types of soil. Because their enzymes fractionate carbon isotopes by carboxylation reactions, they might be responsible for carbon isotope shifts observed in soil depth profiles. In turn, heterotrophic CO_2 fixation has been hypothesised to cause enrichment of stable carbon isotope values of soil organic matter with depth.

We investigated how rates of CO_2 fixation varied with depth in tropical rainforest soils collected along a gradient in elevation at the ATTO (Amazon Tall Tower Observatory) site in Manaus, Brazil. The soils represent two soil orders (Ferralsols and Alisols) and have profiles of total C, microbial biomass and radiocarbon of soil organic matter (SOM) that drop steeply from the surface to 1 meter depth. The investigated soils have high amounts of microbial biomass of more than 3000 ug gdw^{-1} in the first 5 cm, which decreases rapidly with depth. Stable carbon isotopes of SOM increase with soil depth from -29.59 ± 0.11 ‰ at the surface to -26.04 ± 0.19 ‰ at 1 meter depth. Stable carbon isotopes of microbial biomass also increase with depth from -30.44 ± 1.40 ‰ at the surface

to -26.63 ± 1.71 ‰ at 1 meter depth. This suggests a very strong interrelationship between SOM and microbial biomass.

We estimated rates of CO_2 fixation from the uptake of ^{13}C labelled CO_2 into microbial biomass using chloroform fumigation extraction (CFE). The measured rates were highest at the surface in all soils and decreased with depth. However, normalized to uptake per gC, highest uptake rates were measured between 5 and 10 cm. It accounted for 0.26 % and 0.12 % of soil respiration in ferralsols and alisols, respectively.

16S rRNA targeted pyrosequencing indicates that heterotrophic microorganisms specialised to degrade complex plant compounds dominate the microbial community in the top soil. Therefore, heterotrophic CO_2 fixation is likely to be the responsible process for the highest uptake rates, since rates were highest in the uppermost soil layer. CO_2 fixation is also a possible factor that might influence carbon isotopic values of microbial biomass and soil organic matter. Although CO_2 fixation rates were smaller than would be necessary to cause a shift towards more enriched stable carbon isotope values, CO_2 fixation is a significant process that might provide a pathway of recent ^{14}C from root respiration into subsoil organic matter.

3.1 Introduction

Although roots and plant litter play an important role in the formation of soil carbon (Ekschmitt et al., 2008; Nepstad et al., 1994), microbial carbon has recently been identified as an important source for soil organic matter (Ludwig et al., 2015; Miltner et al., 2012; Rumpel and Kogel-Knabner, 2011). In addition, studies have highlighted the importance of soil microbial activity and diversity for SOM formation and stabilization (Gleixner, 2013; Lange et al., 2015). Microbial residues can account for more than 50 % of extractable organic matter and more than 80 % of nitrogen in soils (Simpson et al., 2007). Dead microbial biomass can persist in soils or be re-utilized by living soil microorganisms (Miltner et al., 2012), and microbial biomolecules like carbohydrates or proteins are the main contributor to stabilized organic matter (Ludwig et al., 2015).

Microbial CO_2 fixation is a process that might contribute to carbon recycling in soils (Miltner et al., 2005) and has been demonstrated in certain CO_2 rich soils to be an important source of SOM (Nowak et al, 2015).

Miltner et al. (2005) estimated that 1-2 % of respired CO_2 can be recycled by CO_2 fixation and the contribution of CO_2 fixation to soil organic matter is estimated between 0.05 % to 0.59 % (Miltner et al., 2005; Yuan et al., 2012). Autotrophic microorganisms can use six different metabolic pathways to assimilate CO_2 (Berg, 2011). RubisCO, the most important carboxylating enzyme for obligate and facultative chemo- or photoautotrophic microorganisms that fix CO_2 using the Calvin Benson Bassham Cycle (CBB) is highly abundant in agricultural, paddy, forest and volcanic soils (Ge et al., 2013; Nanba et al., 2004; Selesi et al., 2005; Tolli and King, 2005; Wu et al., 2014). Uptake of CO_2 into microbial biomass (MB) and soil organic matter by photoautotrophic and chemolithoautotrophic organisms has been proven in wetland and agricultural soils (Liu and Conrad, 2011), as well as in other soil types under different experimental conditions (Hart et al., 2013; Stein et al., 2005).

Further, many heterotrophic microorganisms fix CO_2 in order to execute anaplerotic reactions by either forming new sugars for cell wall synthesis, synthesis of amino acids or to excrete organic acids for nutrient mobilization (Feisthauer et al., 2008; Miltner et al., 2004; Santruckova et al., 2005).

Heterotrophic CO_2 fixation has been hypothesised to influence isotope signatures of soil organic matter by adding ^{13}C enriched organic carbon to the soil organic matter pool (Ehleringer et al., 2000). In turn, chemolithoautotrophic CO_2 fixation generates microbial carbon that is depleted in ^{13}C due to enzymatic fractionation processes (Nowak et al., 2015).

The degree to which CO_2 fixation can possibly influence isotope profiles in soils depends on the rate of CO_2 fixation (compared to the amount of OM) and the isotope effect associated with each process (autotrophic or heterotrophic fixation). Though as yet not explored, CO_2 fixation can also possibly influence the ^{14}C signature, especially in deep soils, where CO_2 in pore space is often far higher in ^{14}C than the organic matter.

In order to study the process of CO_2 fixation in tropical rainforest soils and its potential influence on soil organic matter isotopic signatures, we conducted

several experiments with soils obtained from the Amazon Tall Tower Observatory (ATTO) in Central Amazonia, Brazil. Tropical rainforest soils are important globally as a store for organic C and to date there is little information on microbe – SOM links compared to other soil types. We sampled soils from 5 different pits up to 1 m depth and conducted isotopic measurements of bulk soil organic matter, microbial biomass and soil CO_2. We conducted additionally rate measurements using $^{13}CO_2$ label, in order to assess the activity of CO_2 fixing microorganisms along soil depth profiles. We complemented this study with the determination of the bacterial community structure by 16S rRNA pyrosequenzing. With this we aimed at determining the influence of CO_2 fixation on carbon isotopes of soil organic matter in tropical rain forest soils.

3.2 Materials and Methods

3.2.1 Site description

Soils were collected from the ATTO site, located in Central Amazonia, 150 km north-east from Manaus, in the Uatumã Sustainable Development Reserve. The sites are located near the base of a 325 m tall tower, which was build for atmospheric gas measurements, located 13 km NE from the river Uatumã (Andreae et al., 2015).

Soils were collected along an elevational gradient, from floodplain soils near the Uatumã river to the highest point on a local plateau with closed forest vegetation, representative of regional *terra firme* forest. Black water floodplain vegetation (igapo) dominates along the main river channel with intercalated non-flooded alluvial terraces (paleoigapo) and open forest vegetation on white sands (campina) between the river and the slope of the plateaus. Five soil pits surround the tall tower and allow access to soils of the *terra firme*, floodplains and white sands down to 2 meter depth. According to the World Reference Base for soil resources, plateau soils are represented predominantly by yellow clayey ferralsols (latosols and oxisols), whereas alisols and sandy podzols predominate in the valleys. Soil carbon stocks are estimated as 129 ± 7 Mg ha^{-1} on terrace to 164 ± 7 Mg ha^{-1} on the plateau (Andreae et al., 2015). Terrace soils are generally less weathered than plateau soils. Soils from the terrace have a greater capacity

to supply nutrients with higher total P and higher total reserve bases, perhaps due to more rapid access to regolith (Chadwick and Asner, 2016). River terrace soils have higher bulk density, indicating higher soil compaction, and exhibit often signs of anoxia in deeper soil layers (mottling).

3.2.2 Sampling

Soils were sampled in 2014 in November, which represents the transition time between dry and rainy season. We sampled soils using three soil pits in the plateau and two pits in the terrace area. To access fresh material, ~1 m of soil was excavated from the pit faces. Soils were sampled in triplicate at 0, 5, 10, 20, 50 and 100 cm depth. One part of the soil was dried at 105°C for 24 hours in order to prepare samples for determination of water content, bulk carbon and nitrogen, elemental composition as well as the $\delta^{13}C$ radiocarbon concentration. The other part was used for isotope labelling experiments and determination of microbial biomass.

Another set of samples was taken from one pit in the plateau at 0-5 cm for long-term incubations and DNA extractions.

3.2.3 Geochemical parameters

Roots >2mm were removed from soils and they were dried and ground. Bulk soil C and N concentrations were determined using a Vario EL elemental analyser (Elementar Analysesysteme GmbH, Germany). Bulk analyses of elements Al, Fe, Mn and, P were measured with ICP-OES (Optima 3300DV, Perkin Elmer).

3.2.4 Stable isotope and radiocarbon measurements

Stable C isotope signatures of bulk soil were determined on an isotope ratio mass spectrometer (IRMS; DELTA Plus XL, Finnigan MAT, Bremen, Germany) coupled to an elemental analyser (NA, 1110, CE Instruments, Milan, Italy) via a modified ConFloII interface. Stable carbon isotope ratios are reported in the delta notation that expresses $^{13}C/^{12}C$ ratios as $\delta^{13}C$-values in per mil (‰) relative to the international reference material Vienna Pee Dee Belemnite (V-PDB):

$$\delta^{13}C = \left(\frac{\frac{^{13}C}{^{12}C}_{sample}}{\frac{^{13}C}{^{12}C}_{reference}} - 1 \right) \times 1000 \quad (1)$$

Three replicates of each sample were measured and error bars represent the standard error of the mean.

Microbial biomass C of both, labelled and unlabelled samples and its stable carbon isotope composition were determined using chloroform fumigation extraction (CFE) (Vance et al., 1987). The C concentration and ^{13}C of the extracted liquid phase was measured directly by coupling a high performance liquid chromatography (HPLC) system via a LC-IsoLink device (Thermo Electron, Bremen, Germany) to a Delta+ XP IRMS (Thermo Fisher Scientific, Germany). A detailed description of the apparatus and the measurement procedure is provided in Scheibe et al. (2012).

The isotope ratio of microbial biomass can be derived according to:

$$\delta^{13}C_{MB} = \frac{\delta^{13}C_{fum} \times C_{fum} - \delta^{13}C_{unfum} \times C_{unfum}}{C_{fum} - C_{unfum}} \quad (2)$$

where MB stands for microbial biomass, fum for fumigated and unfum for unfumigates soil, respectively. Errors reported for microbial biomass C and $\delta^{13}C$ are the standard errors of the mean of three replicated samples.

The radiocarbon content of soil samples was determined by accelerator mass spectrometry at the Jena ^{14}C facilities (Steinhof et al., 2004). Subsamples of soil containing 1 mg of carbon were combusted under vacuum with CuO at 900° C and the developed CO_2 was cryogenically purified and catalytically reduced to graphite at 625°C by H_2 reduction.

All radiocarbon values are reported in pmC, which is defined as the fractionation corrected ratio between the ^{14}C activity of the sample compared to the new oxalic acid standard (NBS SRM 4990C) according:

$$pmC = R * \frac{1}{0.7459} * \left(\frac{1+\delta^{13}C_{NOX}}{1+\delta^{13}C} \right)^{\theta} \quad (3)$$

Errors reported for ^{14}C analyses are the standard errors of the mean of three replicated samples.

3.2.5 Labelling experiments

CO_2 uptake rates were determined using labelling experiments that differed in duration of incubation with tracer $^{13}CO_2$. The first experiment traced CO_2 directly into microbial biomass. 10 g of fresh soil were transferred into 20 mL glass vials then closed with butyl rubber stoppers and crimp caps. The headspace was flushed with CO_2 free air, after which 1 ml of pure $^{13}CO_2$ was added with a gas tight syringe, giving a final concentration of $^{13}CO_2$ in the vial of roughly 5 %. Vials were incubated for one week in the dark at room temperature. Microbial biomass was extracted from the soil by CFE (Vance et al., 1987). CFE extracts microbial biomass by lysing bacterial cells. The released microbial carbon is subsequently extracted with a salt solution (0.05M K_2SO_4). The amount of microbial biomass is determined as the difference in the amount of C extracted from fumigated samples, minus that from un-fumigated samples. This is converted to microbial biomass-C using a proportionality factor K_c that accounts for the extraction efficiency.

$$C_{mic} = \frac{Extract_{fum} - Extract_{unfum}}{K_c} \quad (4)$$

A value of 0.45 was used for K_c (Vance et al., 1987).

A second experiment was performed to evaluate the influence of different moisture regimes on CO_2 fixation and the microbial community in surface soils. Two different sets of soils were incubated in a similar set-up, this time with soils adjusted to 20 % and 60 % water holding capacity. Samples from 0-5 cm were prepared in triplicates as described above, but were incubated for a total of 90 days. After 90 days, two replicates were extracted by CFE and the third was used for DNA extraction.

3.2.6 DNA extraction

DNA was extracted immediately after the incubation was stopped by opening the vial. DNA was extracted from 2 g of soil using the PowerSoil DNA Isolation Kit (MO BIO, Carslbad, CA, USA) following the manufacturer's protocol.

After DNA extraction Polymerase Chain Reaction (PCR) was performed. PCR was performed in 20-µL reactions using 1x buffer, 0.25 mM dNTP mix, 3 mM $MgCl_2$, 0.175 pmol of forward and reverse primer, 1.5 U Taq polymerase (Phoneutria, Brazil), 5-10ng DNA and deionized ultrapure water. PCR conditions consisted of an initial denaturing step of 95°C for 7 min, followed by 25-33 amplification cycles at 95°C for 30 s, 57°C for 30 s and 72°C for 1.7 min and a final extension step for 7 min at 72°C.

For 16S rRNA gene amplification primers 787 F (5´-ATTAGATACCCNGGTAG-3´) and 1492R (5´-GNTACCTTGTTACGACTT-3´) were used. Primers were designed with the appropriate 454 pyrosequencing adaptors sequences and multiplex identifiers (MID´s). Pyrosequencing of the amplicons was carried out in two 1/8 picotiter plates using 454 GS-FLX Titanium (454 Life Sciences; Roche, Basel, Switzerland) by Macrogen Inc. (Seoul, Korea).

3.2.7 Sequence Analysis

Analysis of sequences was performed with QUIME 1.8.0 software following the protocol described in Santana et al. (2015).

3.3 Results

3.3.1 Carbon content

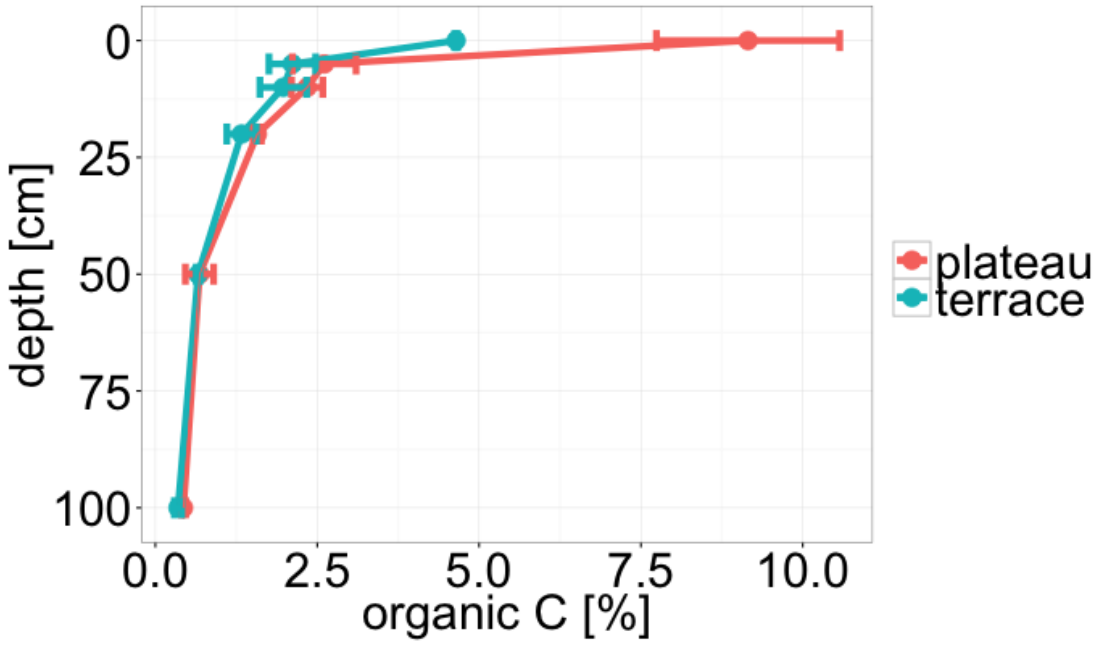

Figure 3-1: Soil organic carbon content for plateau and terrace soils.

Carbon contents of plateau and terrace soils differ at 0 cm depth and are similar at lower depths (table 3-1 and 3-2). Concentrations decrease uniformly in both soils (figure 3-1).

Depth	C-bulk [%]	Micr. Biom. [ugC gdw^{-1}]	C/N	Al [g kg^{-1}]	Fe [g kg^{-1}]	P [mg kg^{-1}]
0	9.15 ±1.41	9013 ± 1737	15.86 ± 0.93	132 ± 8	50 ± 3	235 ± 4
5	2.61 ± 0.49	7194 ± 2628	12.38 ± 0.58	141 ± 22	55 ± 5	181 ± 12
10	2.35 ± 0.24	4220 ± 796	11.93 ± 0.47	136 ± 12	53 ± 2	170 ± 13
20	1.58 ± 0.06	292 ± 51	11.65 ± 0.45	138 ± 31	57 ± 4	139 ± 6
50	0.68 ± 0.22	354 ± 209	10.51 ± 0.46	170 ± 10	66 ± 6	154 ± 16
100	0.43 ± 0.03	111 ± 82	9.31 ± 0.33	141 ± 15	58 ± 1	140 ± 11

Table 3-1: Measured geochemical parameters in plateau soils

Depth	C-bulk [%]	Micr. Biom. [ugC gdw-1]	C/N	Al [g kg-1]	Fe [g kg-1]	P [mg kg-1]
0	4.65 ± 0.02	6216 ± 71	13.09 ± 0.08	72 ± 37	11 ± 5	269 ± 4
5	2.12 ± 0.36	3104 ± 599	11.42 ± 0.45	77 ± 23	11 ± 3	228 ± 24
10	1.98 ± 0.36	2143 ± 1052	11.36 ± 0.53	93 ± 4	13 ± 0.5	233 ± 9
20	1.33 ± 0.23	1034 ± 961	10.76 ± 0.74	92 ± 11	13 ± 0.5	208 ± 40
50	0.66 ± 0.03	519 ± 442	9.56 ± 0.52	117 ± 43	16 ± 5	197 ± 27
100	0.35 ± 0.06	338 ± 231	6.91 ± 0.74	134 ± 22	19 ± 2	207 ± 16

Table 3-2: Measured geochemical parameters in terrace soils.

3.3.2 C/N ratio

Plateau and terrace soils show differences in their C to N ratio throughout the soil profile but in both soils C/N declines with depth (table 3-1 and 3-2). Plateau soils have higher C/N ratios than terrace soils. C/N ratios decline rapidly in the first 5 cm and decrease less rapidly and linearly below 5 cm in both soils (tables 3-1 and 3-2.

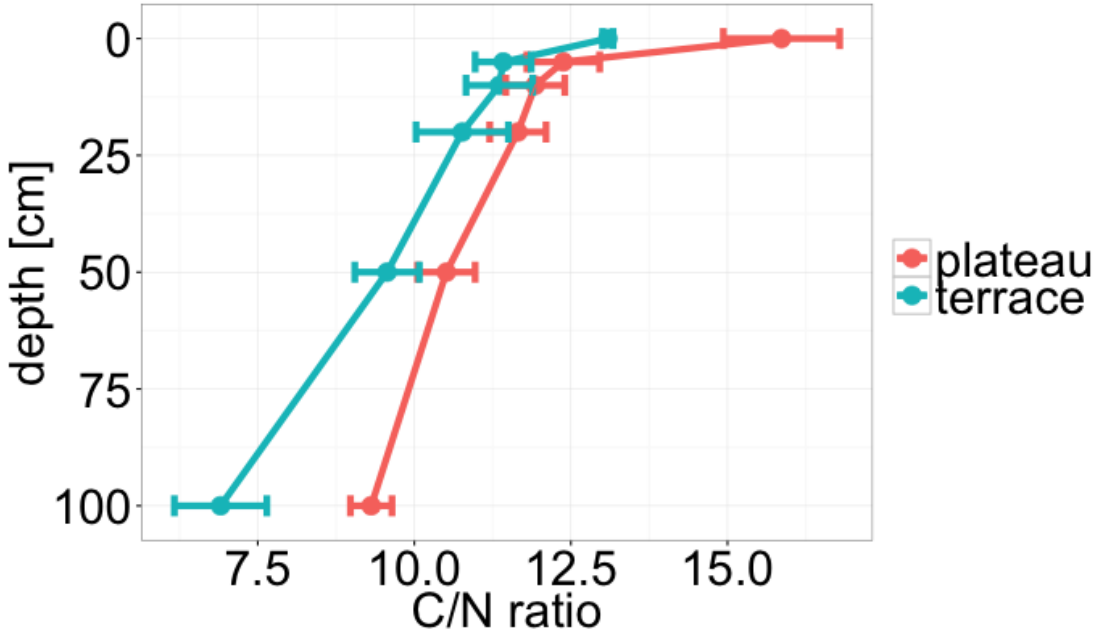

Figure 3-2: C/N ratios with depth in terrace and plateau soils.

3.3.3 Microbial biomass

Microbial C is higher in plateau soils with values up to 9013.86 ± 1737.68 ug gdw^{-1} of soil at 0 cm depth (Figure 3). In the terrace soil, microbial

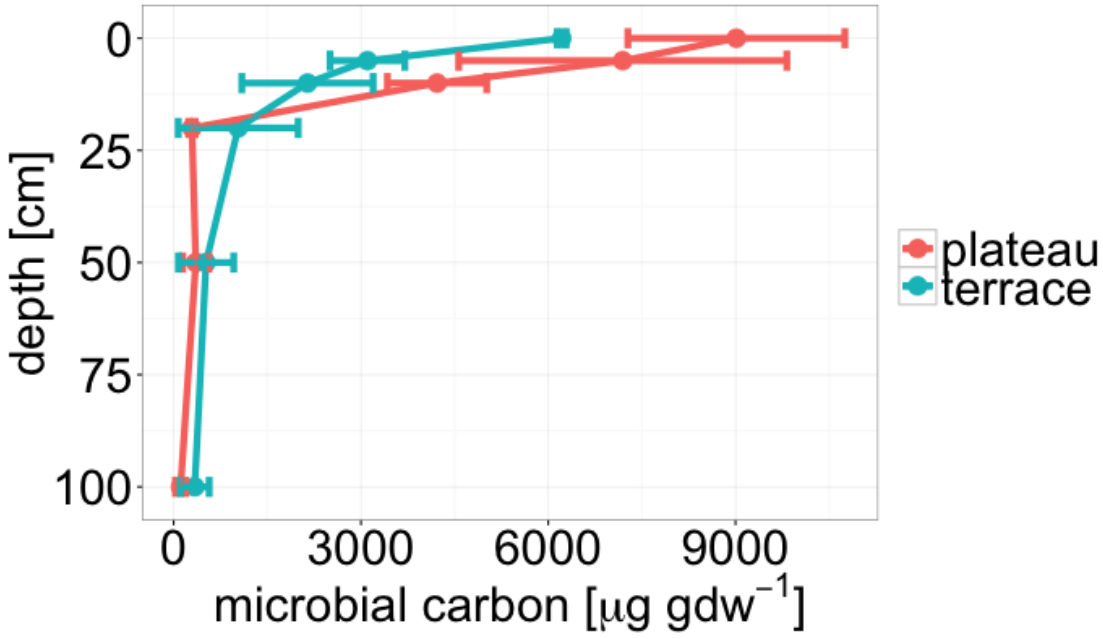

Figure 3-3: Distribution of microbial biomass carbon with depth in plateau and terrace soils.

biomass carbon amounts up to 6216.24 ± 71.18 ug gdw^{-1} at the same depth. Values decrease rapidly in both soils (table 3-1 and 3-2). Differences in microbial C disappear below 10 cm depth.

3.3.4 Elemental composition

Plateau soils are characterised by higher Aluminium contents than terrace soils. Aluminium concentrations in plateau soils show no distinct trend with depth (figure 3-4). Terrace soils exhibit lower Al concentrations but concentrations increase continuously with depth (table 3-2).

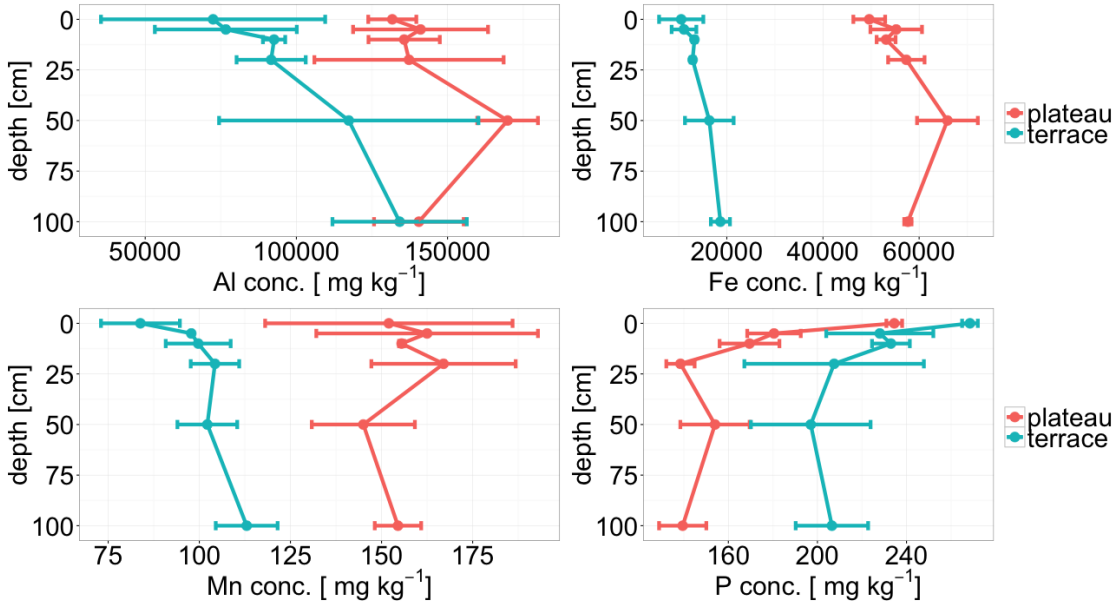

Figure 3-4: Elemental composition of plateau and terrace soils

Iron concentrations do also differ in profiles of terrace and plateau soils (figure 3-4), whereas plateau soils have higher Fe concentrations than terrace soils (table 3-1 and 3.2). Plateau soils have therefore a far higher iron content than terrace soils.

Phosphorous concentrations are higher in terrace soils compared to plateau soils. They decrease with depth in both soils (figure 3-4) (table 3-1 and 3-2).

3.3.5 Stable carbon isotopes of bulk carbon and microbial biomass

In contrast to carbon concentrations, there is no difference in the carbon isotopic composition of bulk carbon between terrace and plateau soils. $\delta\,^{13}C$ values range at an average value of -29.59 ± 0.11 ‰ in the uppermost layer in both soil types. Carbon isotopic values increase in both soil types until a depth of 20 cm and increase less steep below 20 cm (table 3-3).

depth	$\delta\,^{13}C$ bulk (mean) [‰ V-PDB]	$\delta\,^{13}C$ MB (mean) [‰ V-PDB]	14C bulk [pmC]
0	-29.60 ± 0.10	-30.43 ± 1.40	106.87 ± 0.72
5	-28.49 ± 0.39	-30.53 ± 0.96	107.07 ± 0.94
10	-28.13 ± 0.40	-29.94 ± 0.51	105.09 ± 1.33
20	-27.51 ± 0.08	-29.25 ± 0.79	99.61 ± 5.21
50	-26.49 ± 0.54	-28.22 ± 0.25	85.62 ± 7.10
100	-26.19 ± 0.36	-26.62 ± 1.71	57.88 ± 1.29

Table 3-3: Isotopic data of $\delta^{13}C$ of microbial biomass and bulk SOM and ^{14}C of bulk SOM

A similar enrichment can be observed for carbon isotopic values of microbial biomass. There is no significant difference in $\delta^{13}C$ of microbial biomass between terrace and plateau soils. $\delta^{13}C$ of microbial biomass has values of -30.44 ± 1.40 ‰ at 0 cm depth, decreases slightly to a value of -30.53 ± 0.96 ‰ at 5 cm depth and increases subsequently to a value of -26.63 ± 1.71 ‰ at 100 cm depth (table 3-3).

Comparing bulk $\delta^{13}C$ values with $\delta^{13}C$ of microbial biomass shows that microbial biomass has more depleted $\delta^{13}C$ values throughout the soil profile (figure 3-5).

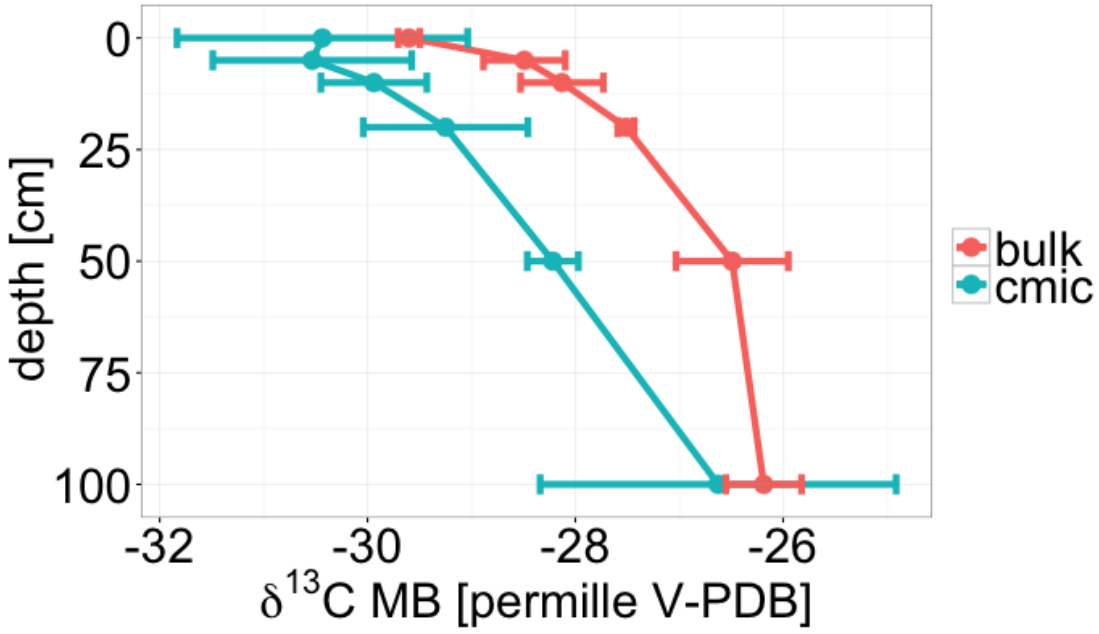

Figure 3-5: Comparison of $\delta^{13}C$ values of microbial biomass and bulk organic matter. The two lines represent the mean of all five soil pits in both, plateau and terrace soils.

3.3.6 Radiocarbon

Similar to $\delta^{13}C$ values of bulk carbon, there is no difference in bulk radiocarbon values between terrace and plateau soils. Highest radiocarbon concentrations appear at 0 cm depth. There, radiocarbon signatures are slightly higher in plateau soils with radiocarbon concentrations of 107.51 ± 0.30 pmC compared to 106.23 ± 0.65 pmC in terrace soils (figure 3-6). Below 5 cm depth, radiocarbon concentrations in both soil types equal each other and values decline linearly to values of 57.88 ± 1.29 at 100 cm depth (table 3-3).

Radiocarbon signatures of soil CO_2 range at 105 pmC at 0 cm depth and decrease to value of 102 pmC at 10 cm depth and increase subsequently to values of 106 pmC and 103 pmC at 20 cm and 60 cm, respectively (figure 3-6)

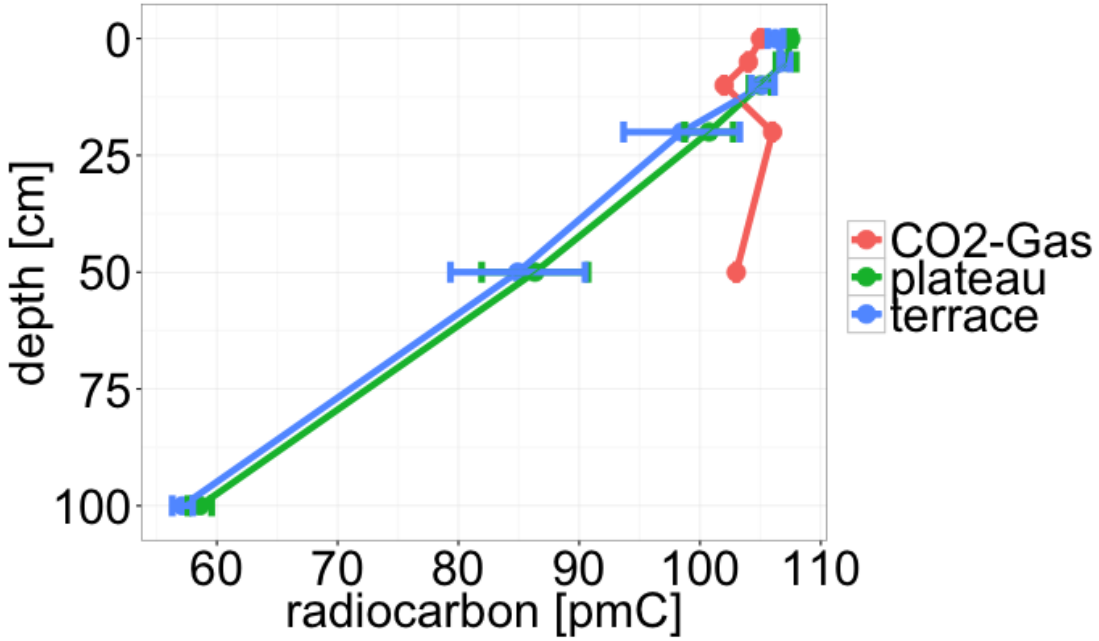

Figure 3-6: Radiocarbon signature of bulk soil organic carbon and soil CO_2 for plateau and terrace soils.

3.3.7 CO_2 uptake rates

CO_2 labelling experiments revealed that CO_2 fixation took place throughout the whole soil profile during the experiment (Figure 3-7). Extracts of incubated soils show no enrichment in $\delta^{13}C$ before fumigation and values were within the range of measured natural abundance values of microbial biomass (figure 3-7). However, after fumigation, extracts showed a considerable enrichment of up to several

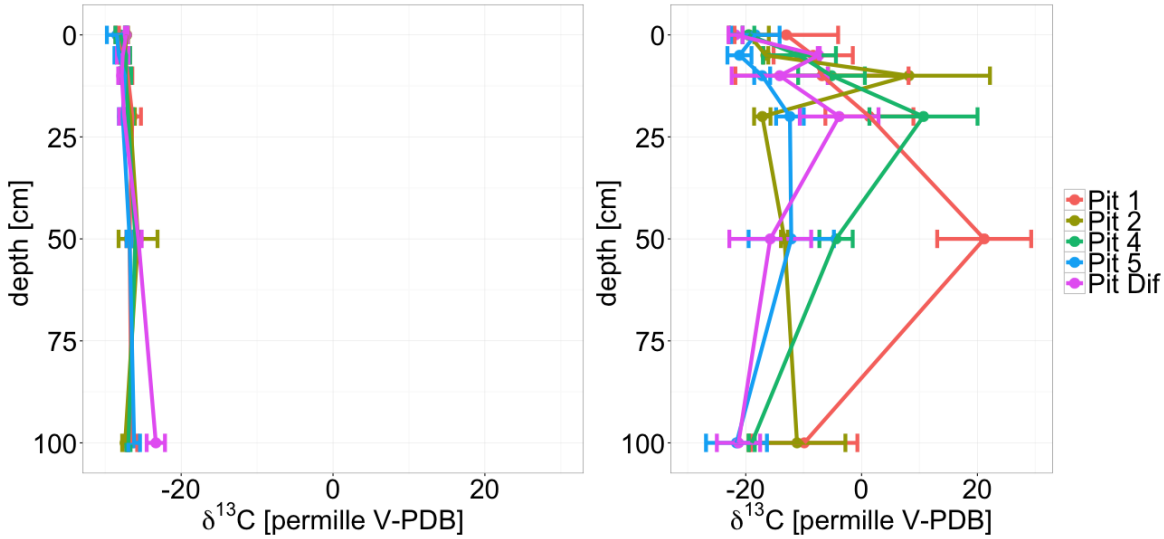

Figure 3-7: Enrichment of CFE extracts in ^{13}C before (left) and after (right) fumigation. Extracts show considerable enrichment only after microbial cells were lysed by chloroform fumigation, indicating incorporation of label by CO_2 fixation.

tens of permille. Thus, ^{13}C from labelled CO_2 was incorporated into soil microbial biomass and released after cell lysis. The measured enrichment can be recalculated to microbial uptake rates of CO_2 (figure 3-8). Uptakes rates where highest within the first 10 cm of soil and decreased with depth. Highest uptake rates were measured in plateau soils. Rates ranged between 0.45 ± 0.13 ug gdw^{-1} d^{-1} and 0.38 ± 0.21 ug gdw^{-1} d^{-1} within the first ten centimetres in plateau soils and between 0.22 ± 0.05 ug gdw^{-1} d^{-1} and 0.10 ± 0.03 ug gdw^{-1} d^{-1} in terrace soils. Uptake rates decreased to values of 0.04 ± 0.03 ug gdw^{-1} d^{-1} and 0.01 ± 0.01 ug gdw^{-1} d^{-1} at 100 cm depth in plateau and terrace soils, respectively.

After normalizing rates to uptake per gC, highest uptake rates can be measured between 5 and 10 cm depth in both, plateau and terrace soils. They range between 17.06 ± 4.97 ug gC^{-1} d^{-1} and 4.16 ± 2.25 ug gC^{-1} d^{-1} in plateau and between 11.29 ± 2.70 ug gC^{-1} d^{-1} and 3.13 ± 0.43 ug gC^{-1} d^{-1} in terrace soils. Below 10 cm specific uptake rates decrease but are in the same range than in the top soil (figure 3-8).

Rates of the long-term incubation experiment are within a similar range. After 90 days of incubation, rates for CO_2 uptake were 0.21 ug gdw^{-1} d^{-1} for soils adjusted to 20 % whc and 0.12 ug gdw^{-1} d^{-1} for soils adjusted for to 60 % whc.

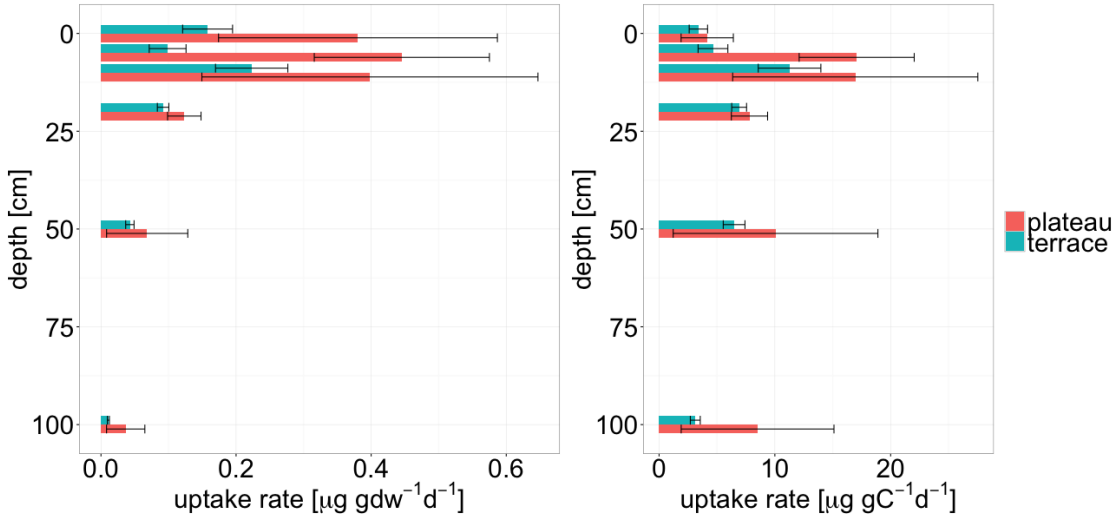

Figure 3-8: CO_2 uptake rates for plateau and terrace soils. On the left side are uptake rates per g soil and on the right side are specific uptake rates per g carbon.

3.3.8 DNA Extractions

The two moisture treatments led to minor changes in microbial community structure of the 0-5 cm samples after the 90 day incubation. In the following, the term low moisture soil is used for soils adjusted to 20 % whc and high moisture for soils adjusted to 60 % whc. The most abundant bacterial phylum in low moisture soils was Firmicutes with 32.97 % to 32.47 %, followed by Acidobacteria with 30.16 % to 32.13 %. In high moisture soils Acidobacteria constituted the majority of all reads with 32.02 % to 36.84 % followed by Firmicutes with 27.18 % to 27.25 %. Further abundant groups were Verrucomicrobia, with 11.63 % to 12.87 % in low moisture soils and 9.34 % to 16.05 % in high moisture soils, Proteobacteria, with 12.77 % to 12.95 % in low moisture soils and 13.21 % to 15.94 % in high moisture soils as well as Planctomycetes with 2.68 % to 3.61 % in low moisture soils and 1.60 % to 2.65 % in high moisture soils. Unassigned bacteria constituted between 1.05 % to 1.76 % in both soils. Bacterial phyla with lower abundance below 1 % in both, low and high moisture soils were Chlamydiae, Actinobacteria, Bacteroidetes, WS4, and OD1. The most abundant archaeal phylum was Euryarchaeota (0.30 % to 0.28 % and 0.25 % to 0.35 % in low and high moisture soils, respectively), followed by Crenarchaeota (0.08 % to 0.21 % and 0.10 % to 0.14 % in low and

high moisture soils, respectively). Euryarchaeota were represented by methanogenic groups like methanomicrobia, whereas ammonia oxidizing Thaumarchaeota dominated the Crenarchaeota.

3.4 Discussion

3.4.1 Soil types and elemental composition

Plateau soils at the ATTO site are classified as Ferralsols (Andreae et al., 2015), soils that are characterised by strong weathering and desilication and are common in humid, free draining environments. Ferralsols are in an extremely advanced state of pedogenesis. Kaolinite as well as iron and aluminium oxides dominate their mineral fraction (Quesada et al., 2011). This is reflected in our study by higher aluminium contents in plateau soils compared to terrace soils, which are classified as Alisols. The terrace soils are considerably younger than plateau soils and represent intermediate age soils, most probably developed on sediments from the Pleistocene (Andreae et al., 2015). They have therefore higher nutrient contents, including higher phosphorous content and lower C/N ratios. The terrace Alisols have a characteristic accumulation of clay with depth, which might explain the increase in aluminium concentrations with depth that is observed in our study.

3.4.2 Soil carbon content

Differences in carbon content between plateau and terrace soils are large at the surface and diminish with depth. The higher organic matter content in surface soils might be related to the higher clay content and to organo-mineral interactions, which are common in ferralsols (Dick et al., 2005; Quesada et al., 2011). Plateau soils have higher iron concentrations and iron oxides are known to contribute to organic matter stabilisation in ferralsols (Dick et al., 2005). Organic matter in ferralsols is preserved mainly by a surface complexation between variable charge minerals and the organic molecules, which protects it against microbial decomposition (Dick et al., 2005). Additionally, clay minerals or aggregates protect organic matter against oxidative destruction (Six et al., 2002).

Higher carbon and clay contents can also be responsible for the higher microbial biomass in plateau soils, which is higher than in terrace soils within the first 10 cm. Microbial biomass is usually positively correlated with organic carbon and clay content (Kaiser et al., 1992; Vance et al., 1987). A positive relationship between microbial carbon and the clay fraction is also supported by our data. Similar to carbon contents, differences in microbial biomass carbon diminish below 10 cm depth.

3.4.3 Carbon turnover

C/N ratios of both, plateau and terrace soils show a step decrease within the first centimetres of soil. This suggests a strong processing of organic mater already in the topsoil and rapid carbon turnover within the uppermost centimetres (Rumpel and Kogel-Knabner, 2011). Differences in C/N between terrace and plateau soils can be related to different vegetation patterns.

A fast turnover of soil organic matter within the first five centimetres of soil is also supported by the radiocarbon data, where values of the uppermost layer are close to atmospheric values at the year of measurement (~103 pmC), which indicates fast turnover times of only a few years. However, mean turnover times estimated from ^{14}C ages decrease rapidly with depth. Our results are consistent with findings from other tropical rainforest soils, which showed that turnover in the first 25 cm is rapid with more than 60 % of carbon having turnover times of 25 years or less (Telles et al., 2003).

3.4.4 Relationship between soil microbial biomass and soil organic matter

A preferred utilization of SOM by microorganisms has been shown in studies where compound specific radiocarbon measurements of bacterial biomarkers were applied (Kramer and Gleixner, 2008; Rethemeyer et al., 2005). The studies suggested an increasing contribution of SOM as a substrate for soil microorganisms with increasing depth. Further, Gleixner (2013) as well as Miltner et al. (2012) proposed that SOM is mainly derived from microbially formed compounds of several timed recycled organic carbon (microbial loop).

Such concepts can be used to explain the observed identical depth trend in soil microbial biomass and soil organic matter.

The enrichment in bulk SOM, which is observed in the studied soils, is concordant with an enrichment of microbial biomass $\delta^{13}C$ values. The concordant enrichment of both, microbial biomass and soil organic matter with depth indicates a strong relationship between both pools (Ehleringer et al., 2000).

Another indicator for an increasing contribution of microbial carbon to SOM is the C/N ratio. C/N ratios at 0 cm, just below the litter layer, range at 15.86 ± 0.93 in plateau soils and at 13.09 ± 0.08 in terrace soils. Low C/N ratios in tropical soils indicate retention of nitrogen in the soil (Sombroek et al., 1993), but can also be indicative for a high contribution of microbial carbon to soil organic matter (Nowak et al., 2015). C/N ratios as low as 8 approach ratios known for soil microorganisms and are therefore a strong indicator for contribution of microorganisms to SOM (Wallander et al., 2003). Decreasing C/N ratios with depth indicate therefore an increasing contribution of microbial carbon to bulk soil organic matter.

3.4.5 Quantification of microbial CO_2 fixation

The measured CO_2 uptake rates can help quantifying microbial CO_2 fixation and evaluate its contribution to microbial biomass and SOM.

The highest CO_2 uptake rates where measured within the first 10 cm of soil. There was also a higher uptake in plateau soils compared to terrace soils. This suggests that CO_2 uptake rates are related to soil carbon content as well as microbial carbon contents. A link between edaphic factors like soil organic carbon and CO_2 uptake rates has also been observed in studies conducted with other soils (Wu et al., 2015b). Uptake rates of the long-term incubation were within the same range as uptake rates measured during the short-term incubation, indicating a continuous activity of CO_2 fixing microorganisms during the incubation period. At the end of the 90 day incubation, 7.95 ug gdw^{-1} were fixed in low moisture soils and 4.60 ug gdw^{-1} in high moisture soils. This corresponds to 0.013 % and 0.008 % of total soil organic matter in the top soils

and is comparable with values obtained by other studies (Miltner et al., 2005). Extrapolating measured uptake rates to subsoils below 50 cm depth would yield a value of 0.08 % for plateau soils and 0.04 % for terrace soils after 90 days of incubation. When normalizing measured uptake rates to microbial biomass carbon, fixed CO_2 amount to 0.47 % of microbial carbon in the first five cm of plateau soils and 0.26 % in terrace soils. In subsoils below 50 cm depth, fixed CO_2 amount to 2.35 % of microbial biomass in plateau soils and 0.52 % in terrace soil after a 90 day incubation. Extrapolating to annual rates, it would take ~10 years to replace microbial biomass-C with CO_2-fixed-C in the deep plateau soils, and ~50 years for plateau soils.

CO_2 uptake rates can also be compared to soil respiration fluxes. Ferralsols and Alisols cover more than 30 % of the Amazon area, with Ferralsols as the most common soil type overall (Quesada et al., 2011). Total soil respiration in Ferralsols of the same region is 12.1 Mg C ha^{-1} yr^{-1} (Chambers et al., 2004). Converting soil-depth integrated uptake rates to fluxes of CO_2 yields values of around 0.03 Mg C ha^{-1} yr^{-1} for plateau soils and 0.01 Mg C ha^{-1} yr^{-1} for terrace soils. This corresponds to 0.25 % and 0.12 % of total soil respiration (which includes root respiration) for plateau and terrace soils, respectively. This fraction increases below the top 10 cm, that are responsible for ~80%-90% of total soil respiration (Trumbore et al., 1995). CO_2 fixation can therefore recycle a significant amount of soil respiration, especially in deep soils.

3.4.6 The potential influence of microbial CO_2 fixation on stable carbon isotope values of SOM

As main a driver of the observed $\delta^{13}C$ shift in soil organic matter, Ehleringer et al. (2000) hypothesised an increasing contribution of microbial carbon that is enriched in $\delta^{13}C$. Ehleringer et al. (2000) suggested heterotrophic CO_2 fixation as an explanation for the required enrichment in soil microbial biomass. Heterotrophic CO_2 fixation is an important reaction within the Krebs cycle, which describes catabolic carboxylation reactions performed mainly by the enzyme phosphoenolpyruvatecarboxylase (PEPC) (Feisthauer et al., 2008). CO_2 fixation by anaplerotic reactions during heterotrophic growth is estimated to account for

up to 10 % of cell carbon and can be performed not only by prokaryotes, but also by fungi and invertebrates (Kellermann et al., 2012). Ehleringer et al. (2000) explained enrichment of carbon derived from heterotrophic CO_2 fixation by diffusion processes of CO_2 within the microbial cell. However, equilibration of CO_2 with cell water can also result in isotopic enrichment, because PEPC utilizes bicarbonate as a substrate (Melzer and Oleary, 1987), and bicarbonate is isotopically enriched compared to dissolved CO_2 (Mook et al., 1974). Bicarbonate is transported by carbonic anhydrase into the cell by catalysing equilibration between the cell cytoplasm and the outer atmosphere (Smith et al., 1999). The fractionation factor between bicarbonate and CO_2 is about +9 ‰ (Mook et al., 1974), and can lead to an even higher enrichment than assuming solely enrichment due to diffusion. Uptake of CO_2 was measured throughout the soil profile and CO_2 fixation is therefore a potential process that might have contributed to the observed enrichment in $\delta^{13}C$ values in both, soil microbial biomass and soil organic matter.

In our soils, although there is an overall increase in ^{13}C with depth, microbial biomass is always depleted in $\delta^{13}C$ compared to bulk soil organic matter at the same depth. One possible explanation for more negative $\delta^{13}C$ values of microbial biomass compared to bulk soil organic matter is the addition of ^{13}C depleted microbial carbon. ^{13}C depleted carbon can be produced by autotrophic microorganisms. This can be the case, if chemolithautotrophic or phototrophic CO_2 fixation processes occur. Almost all autotrophic CO_2 fixation pathways discriminate against ^{13}C, especially the Calvin Benson Cycle and the Acetyl CoA cycle (Fuchs, 2011). A significant contribution of autotrophic microorganisms to soil microbial biomass might therefore add ^{13}C depleted carbon and shift $\delta^{13}C$ values of SOM towards more depleted values compared to SOM (Nowak et al., 2015). Autotrophic microorganisms have been shown to be abundant in many types of soils and can contribute to soil organic matter formation (Ge et al., 2015; Miltner et al., 2005; Nowak et al., 2015; Selesi et al., 2005; Tolli and King, 2005; Wu et al., 2015b; Wu et al., 2014; Yuan et al., 2012).

3.4.7 DNA analyses

Quantification of uptake rates and $\delta^{13}C$ values of SOM suggest that CO_2 fixation plays a significant role for belowground carbon cycling in the investigated soils. The molecular data can help to evaluate whether the measured rates were related to heterotrophic or autotrophic CO_2 uptake. However, due to the amounts of soil and DNA concentrations, we only have these data for the 0-5 cm depth interval.

In the 0-5cm depth interval where C contents are greatest in these soils, sequencing data suggest a high abundance of heterotrophic organisms, which are specialised in the degradation of complex plant material. Within both, high and low moisture soils bacteria belonging to the family of Acidobacteriaceae constitute the biggest group with more than 13 % of total reads. Acidobacteriaceae belong to the phylum Acidobacteria, which are an abundant group in many soils (Quaiser et al., 2003). Acidobacteriaceae are known from a variety of acidic environments (Barns et al., 2007). They are heterotrophs and can degrade an array of simple carbon compounds as well as plant and microbial polysaccharides, including cellulose (Eichorst et al., 2011).

Also bacteria belonging to the phylum Firmicutes, like the family Ruminococcaceae, the second most abundant family in our soils, are specialised in degrading complex plant materials (Biddle et al., 2013). Proteobacteria constitute the third large group of bacteria in the studied soils and accounted for more than 13 % of all reads in both, low moisture and high moisture soils. All bacteria belonged exclusively to Alphaproteobacteria, which are morphologically and metabolically extremely diverse. Some are phototrophic bacteria, whereas others are chemolithoautotrophs or organoheterotrophs (Kersters et al., 2006). The most abundant group in our studied soils belonged to the family Rhodospirillaceae, which is a phototrophic purple non-sulphur bacterium (Imhoff, 2006). Therefore, phototrophic bacteria seem to play a significant role in the studied soils, although their importance as a C source is minor compared to plant inputs. Other abundant groups, which are related to decomposition of organic matter are Hyphomicrobiaceae, a family that grows chemoorganotrophically and prefers to grow on one carbon compounds such a

methanol and Caulobacteraceae, a family that lives chemoorganotrophic and that occurs in oligotrophic habitats (Kersters et al., 2006). Further, bacteria of the candidate order Ellin 329 were detected, a group that was recently described from temperate peatlands. They were shown to be involved in hydrolysis of poly-, di- and monosaccarides and might therefore also play an important role in organic matter decomposition.

Obligate chemolithoautotrophic microorganisms are predominantly belonging to archaeal groups like the methanogenic archaea Methanosarcina or Thaumarchaeota like Nitrososphaerales, but these are not abundant in the surface soils.

The data suggests therefore that heterotrophic CO_2 uptake was mainly responsible for the CO_2 fixation rates measured in the soil surface layer and that chemolithoautotrophes had only a minor contribution at this depth. This is in accordance with findings from Miltner et al. (2004) and (Santruckova et al., 2005), who found that CO_2 uptake in agricultural and artificial soils was predominantly performed by heterotrophic microorganisms.

3.4.8 Impact of microbial CO_2 fixation on carbon isotopic signatures

Ehleringer et al. (2000) suggested that if only 5 % of total biomass would be derived from heterotrophic CO_2 fixation, the enrichment in $\delta^{13}C$ would be sufficient to cause a shift of 1 to 1.5 ‰ towards more positive values. The measured contribution of microbial biomass to total SOM ranged between 0.26 % and 2.35 % in our soils, and is therefore below this threshold. Turnover times of microbial biomass are in the range of months in tropical areas (Batjes and Sombroek, 1997). This suggests that the amount of CO_2 that is fixed within the three-month period of our experiment is below what is needed to cause a shift in $\delta^{13}C$ towards more enriched values in the upper soil. Heterotrophic CO_2 fixation can therefore not explain the observed enrichment with depth.

Although phototrophic CO_2 uptake did not contribute to measured uptake rates, because the soils were incubated in the dark, they may nevertheless play an important role in the investigated soil in general, because phototrophic bacteria were an abundant group. Phototrophic CO_2 fixation might contribute ^{13}C

depleted organic carbon to the microbial biomass and can cause a shift towards more depleted values, as it is observed for microbial biomass $\delta^{13}C$ in depth profiles of our soil. However, phototrophic CO_2 fixation occurs solely in the top few mm of the soil and does not influence carbon cycling below 5 cm depth (Wu et al., 2014; Yuan et al., 2012). It is therefore unlikely that phototrophs influence $\delta^{13}C$ values of microbial biomass throughout the whole soil profile.

Although chemolithoautotrophic CO_2 uptake do not seem to play a role in the top 5 cm of soil, their activity cannot be ruled out for deeper layers of the soil profile, where we do not have molecular data. The influence of chemolithoautotrophic CO_2 fixation on $\delta^{13}C$ values of microbial biomass and soil organic matter cannot be assessed with our data. However, as for heterotrophic CO_2 fixation, the amount of fixed CO_2 appears to be too small to cause a considerable change in $\delta^{13}C$ values.

The data suggest that CO_2 fixation is neither the reason for an enrichment of $\delta^{13}C$ values with depth, nor responsible for a depletion of microbial biomass compared to bulk soil organic matter. Other reasons for the gradual enrichment of the soil microbial biomass with depth can be a progressive enrichment when C compunds in microbial biomass are recycled (Gleixner, 2013). A reutilization of dead microbial biomass by living soil organisms might cause a trophic enrichment during progressive recycling (McCutchan et al., 2003). A reason for the depletion of microbial biomass compared to SOM might be fractionation during decomposition, with microbes preferentially respiring lighter CO_2 and retaining heavier C within their biomass (Werth and Kuzyakov, 2010).

Although it appears that microbial CO_2 fixation does not have an influence on stable carbon isotopic signatures of SOM in tropical rainforest soils, it might impact radiocarbon signatures. CO_2 in the soil atmosphere is partly derived from root respiration and has other, more modern radiocarbon signatures than SOM at the same depth (Trumbore et al., 1995). This is also the case in the soils of the present study, where soil CO_2 had values close to the recent atmospheric concentration up to a depth of 50 cm. Direct incorporation of soil CO_2 into microbial biomass and SOM can add therefore modern atmospheric radiocarbon to slow cycling carbon pools in deeper soil layers, where plant derived carbon

has little access, like the mineral associated fraction or clay fraction (Trumbore, 2009).

Measured CO_2 uptake rates range between 0.04 ugC gdw^{-1} d^{-1} and 0.45 ugC gdw^{-1} d^{-1} in plateau soils. Building up measured carbon stocks solely with microbial CO_2 fixation, independent of its pathway, would require 659 years in the topsoil of plateau soils and between 273 and 325 years below 50 cm depth. The same holds true for terrace soils, where formation of carbon solely by CO_2 fixation would require 806 years at 0 cm and between 423 and 876 years below 50 cm depth. Microbial CO_2 fixation can therefore add a significant amount of radiocarbon to subsoils, where turnover times are in the range of millennia. This might provide direct access of modern carbon to pools where transport of plant derived carbon, e.g. by dissolved organic carbon, is limited (Kaiser and Kalbitz, 2012; Sanderman and Amundson, 2008).

3.5 Conclusion

Carbon concentrations as well as carbon isotopes of soil organic matter and microbial biomass were measured in tropical rainforest soils. Two soil types could be distinguished, which differ slightly in nutrient, clay mineral, and carbon content. The more weathered and older Ferralsols found in the plateau regions are characterized by lower phosphorous, but higher clay and carbon contents compared to Alisols in the terrace positions. These differences are also reflected in differences in microbial biomass, whereas plateau soils exhibit higher microbial biomass carbon in the top 10 cm compared to terrace soils. The C/N ratio in both soils decreases rapidly within the first 5 cm, which indicates rapid turnover of organic matter within the first 5 cm of soils. This is also supported by the radiocarbon data, which indicates rapid turnover times within the first centimetres. Carbon isotopes of soil organic matter show a common enrichment with depth, which is accompanied by a parallel increase in $\delta^{13}C$ of microbial biomass. This suggests a strong interrelationship between soil microbial biomass and soil organic carbon within tropical rainforest soils. However, microbial biomass is consistently lower in the ^{13}C compared to bulk soil. The molecular data suggest that heterotrophic and phototrophic CO_2 fixation are the dominant used fixation pathways in the surface 0-5 cm. The observed enrichment in

microbial biomass can be caused by heterotrophic CO_2 fixation, but the measured rates suggest that the magnitude of microbial CO_2 fixation is not sufficient to cause a shift in $\delta^{13}C$ of microbial biomass. Phototrophic Proteobacteria and methanogenic Archaea are the most abundant autotrophic microorganisms. The shift of $\delta^{13}C$ values of microbial biomass compared to soil organic matter towards more negative values can be caused by fractionation during decomposition and is most probably not related to fractionation processes by chemolithoautotrophic or phototrophic organisms. However, it is likely that CO_2 fixation can influence radiocarbon signatures with depth. In timescales of centuries, CO_2 fixation adds a significant amount of carbon to the soil organic matter pool, especially in the subsoils. Therefore, despite the mechanism that is behind the CO_2 fixing process, CO_2 fixation can transfer radiocarbon to the subsurface and contribute to subsurface carbon cycling.

Acknowledgements

We would like to thank Reiner Ditz and Steffan Wolff for sampling and on site logistics. We further thank Beto Quesada for providing access to laboratories at the Institito Nacional de Pesquisas da Amazonia in Manaus. We kindly acknowledge Heike Geilmann, Axel Steinhof and Heike Machts for measuring $\delta^{13}C$ and ^{14}C samples. We further thank Michael Raessler for ICP-OES measurements and Ines Hilke and Birgit Froehlich for carbon and nitrogen measurements. MN was funded by the International Max-Planck Research School for Global Biogeochemical Cycles (IMPRS gBGC).

4 Carbon isotopes of dissolved inorganic carbon reflect utilization of different carbon sources by microbial communities in two limestone aquifer assemblages

Chapter Source:

Nowak, M.E., Schwab, V.F., Lazar, C.S., Behrendt T., Kohlhepp, B., Totsche, K.U., Küsel, K., Trumbore, S.E. Carbon isotopes of dissolved inorganic carbon reflect utilization of different carbon sources by microbial communities in two limestone aquifer assemblages.

Manuscript submitted on 10th October 2016 to *Hydrology and Earth System Sciences*

Abstract

In groundwater, isotopes of dissolved inorganic carbon (DIC) are used to indicate both transit times and biogeochemical evolution of groundwaters. These signals can be complicated in carbonate aquifers, as both abiotic (i.e. carbonate equilibria) and biotic factors influence $\delta^{13}C$ and ^{14}C of DIC. We applied a novel graphical method for tracking changes in $\delta^{13}C$ and ^{14}C of DIC in two distinct aquifer complexes identified in the Hainich Critical Zone Exploratory (CZE), a platform to study how water transport links surface and shallow groundwaters in carbonate and marlstone rocks in central Germany. For more quantitative estimates of contributions of different biotic and abiotic carbon sources to the DIC pool, we used the geochemical modelling program NETPATH, which accounts for changes in dissolved ions in addition to C isotopes.

Although water residence times in the Hainich CZE groundwaters based on hydrogeology are relatively fast (years or less), DIC isotopes in the two shallow, mostly anoxic, aquifer complexes (HTU 4 and HTU 5) were depleted in ^{14}C compared to a deeper, oxic, aquifer complex (HTL). Carbon isotopes and chemical changes in the deeper HTL wells could be explained by interaction of recharge waters equilibrated with post-bomb ^{14}C sources with carbonates. However, oxygen depletion and $\delta^{13}C$ and ^{14}C values of DIC below those expected from the processes of carbonate equilibrium alone indicate dramatically different biogeochemical evolution of waters in the upper aquifer complexes

(HTU 4 and HTU 5 wells). Depletions of ^{14}C and ^{13}C in the upper aquifer complexes result from a number of biotic and abiotic processes, including oxidation of ^{14}C depleted OM derived from recycled microbial carbon and sedimentary organic matter as well as water rock interactions. The microbial pathways inferred from DIC isotope shifts and changes in water chemistry in the HTU wells were supported by comparison with *in situ* microbial community structure based on 16S rRNA analyses.

Our findings demonstrate the large variation in the importance of biotic as well as abiotic controls on ^{13}C and ^{14}C of DIC in closely related aquifer assemblages. Further, they support the importance of subsurface derived carbon sources like DIC for chemolithoautotrophy and rock-derived organic matter for supporting heterotrophic groundwater microbial communities and indicate that even shallow aquifers have microbial communities that use a variety of subsurface derived carbon sources.

4.1 Introduction

Groundwater is the most important freshwater reserve on earth and a crucial part of the global hydrological cycle. Although the proportion of groundwater on global freshwater reserves is only 0.06 %, it represents as much as 98 % of readily available water for humans and agriculture.

According to the Intergovernmental Panel On Climate Change (IPCC), groundwater demand by humans is likely to increase in future, due to a general increase of global water use and a decline in surface water availability caused by higher precipitation variability (Parry et al., 2007). In contrast to expected higher groundwater withdrawal, groundwater recharge rates are likely to decrease on a regional scale because of climate change (Aeschbach-Hertig and Gleeson, 2012).

The Critical Zone (CZ) is defined as the space ranging from the outer extent of vegetation through soils, down to the saturated and unsaturated bedrock (NRC, 2001). It is the crucial connection between groundwater and surface conditions and is the space where fundamental physical, chemical and biological processes

act, which are of high importance for sustaining soil and groundwater quality for agricultural and groundwater use (Akob and Küsel, 2011). Assessments of groundwater vulnerability and sustainable groundwater management require a sound knowledge of water movement and carbon transport through the CZ (Küsel et al., 2016).

In this study, we measured radiocarbon and stable carbon isotopes of dissolved inorganic carbon (DIC), dissolved organic carbon (DOC) and total organic carbon (TOC) in a transect of wells located in the Hainch Critical Zone Exploratory (Hainch CZE), Thuringa, Central Germany. Our aim was to study carbon turnover and water dynamics in two superimposed limestone aquifer assemblages with different flow dynamics and physicochemical properties (figure 4-1).

Radiocarbon (^{14}C) and stable carbon isotopes ($^{13}C/^{12}C$) of dissolved constituents provide a suitable tool to trace water movement through the critical zone, as well as to identify different carbon sources contributing to the aquifers' carbon pools (Bethke and Johnson, 2008). The most common approach in applying radiocarbon in groundwater studies is measuring the ^{14}C activity of dissolved inorganic carbon (DIC), which includes dissolved CO_2, bicarbonate and carbonate ions. These C species are derived from equilibration of percolating waters with soil atmosphere CO_2, as well as equilibration of the dissolved CO_2 with carbonates in the soil matrix or aquifer rocks.

In order to determine initial ^{14}C concentrations in DIC, traditional correction models have been applied to account for the different processes that affect DIC and bias ^{14}C ages (Han and Plummer, 2016). Corrections have to be considered for dissolution of carbonates by dissolved CO_2 (Tamers et al., 1975) according to:

$$CO_2 + H_2O + CaCO_3 \rightarrow Ca^{2+} + 2HCO_3^- \quad (1)$$

, isotopic exchange between DIC and soil CO_2 (Fontes, 1992; Han and Plummer, 2013):

$$C^*O_{2(g)} + HCO_3^- \leftrightarrow CO_{2(g)} + HC^*O_3^- \quad (2)$$

, as well as isotopic exchange between DIC and carbonates in the aquifer (Eichinger, 1983; Fontes and Garnier, 1979; Han and Plummer, 2013):

$$HC^*O_3^- + CaCO_{3(s)} \leftrightarrow HCO_3^- + CaC^*O_{3(s)} \quad (3)$$

where * in equations two and three refers to carbon atoms that were exchanged between gaseous liquid and solid species. Other factors influencing ^{13}C and ^{14}C of DIC are heterotrophic respiration of organic matter (OM) (Aravena et al., 1995) and mineral precipitation and weathering (Wigley, 1976).

Han et al. (2012) developed a novel graphical method, the Han-Plummer plot, that allows recognizing systematic patterns between $^{13}C_{DIC}$ and $^{14}C_{DIC}$, which are indicative for the processes described above. For example, interactions between carbonates and DIC should follow a mixing line, as ^{13}C and ^{14}C are affected in constant proportions set by the carbonate endmember. On the other hand addition of organic matter C can vary in both, ^{13}C signature (e.g. fermentation versus oxidation by O_2) and radiocarbon signature, depending on the organic matter source.

In limestone-landscapes like the Hainich CZE, groundwater recharge rates can be high due to karstification or quite low due to thick soils developed on quarternary sediments like loess loam (Kohlhepp et al., 2016). In such regions, recharge waters containing biogenic soil CO_2 react with the aquifer rock according to equation 1. These types of waters fall in the Han-Plummer plot in a very specific region, the so-called Tamer´s point (Han et al., 2012), i.e. with 50% of the DIC derived from the soil-CO_2 and 50% from the carbonate rock according to equation 1. Values that fall off this pure calcite equilibration point reflect the influence of isotopic exchange in the aquifer or soil according to equation two and three, water rock interactions, or microbial oxidation of organic matter. The relative importance of these processes can be distinguished according to the

specific position of DIC carbon isotopic values in the Han-Plummer plot (Han et al., 2012).

Carbon isotopes of DIC can give therefore information about both, movement of water through the soil (Gillon et al., 2012), as well as sources and sinks of different carbon pools within the aquifer (Aravena et al., 1995).

While the graphical method emphasizes only C isotopes, information from other dissolved constituents can provide additional information about the biogeochemical factors influencing groundwater. For example, carbonate dissolution will not only affect DIC but also the concentrations of dissolved Ca^{+2} and Mg^{+2} and microbial processes like sulfate reduction will alter SO_4^{2-}. In order to assess quantitatively the contribution of biotic and abiotic processes to groundwater carbon biogeochemistry and their impact on DIC isotopes, we used additionally the geochemical inverse modelling program NETPATH (Plummer et al., 1992).

A special focus of our study was to evaluate the contribution of autotrophic microorganisms to carbon cycling within the aquifer. Chemolithoautotrophic microorganisms, i.e. microbes that metabolise CO_2 instead of organic carbon, have been shown to be key players and important primary producers in groundwater microbial communities (Alfreider et al., 2012; Hutchins et al., 2016; Kellermann et al., 2012). A high potential for microbial CO_2 fixation has already been demonstrated in our studied aquifers by molecular analyses (Herrmann et al., 2015; Lazar et al., 2016a; Schwab et al., 2016). We hypothesized that turnover of OM derived from chemoautotrophic microorganisms should be reflected in DIC isotopes, since OM derived from CO_2 fixation should be isotopically distinct from other sources like surface derived OM or sedimentary organic matter. Therefore, we conducted 16S rRNA gene assays, in order to determine the microbial community structure within the two limestone aquifer assemblages and relate it to measured carbon isotopes of DIC, DOC and TOC as well as water chemistry.

With this we aim at gaining a comprehensive understanding about groundwater flow and carbon turnover from different sources and sinks.

4.2 Methods

4.2.1 Study site

The Hainch CZE is located in Thuringia, Central Germany. It spreads from the Hainich low mountain range (in the SW), representing the groundwater recharge area of this study, towards the valley of the Unstrut river (in the NE). The southwestern part of the study site shares the largest deciduous beech forest in Germany, the Hainich National Park. Within the forest area, the NW-SE oriented Hainich ridge is the topographical and subsurface water divide with surface/subsurface discharge towards the east (Unstrut subcatchment) and west (Werra subcatchment). The geological succession of Mesozoic sedimentary rocks is moderately inclined towards the NE and comprises the Muschelkalk (m) group outcropping in the upper and midslope area and the Keuper (k) group at the footslope. As the strata dips steeper than the slope angle, lower stratigraphic units outcrop in higher topographic positions. The Upper Muschelkalk (mo) subgroup, which hosts the aquifer assemblages of this study, is further subdivided into the Trochitenkalk formation (moTK) with predominantly limestones and the alternated bedded limestone-marlstone succession of the Meissner formation (moM). Mesozoic rocks are partly to totally covered by Pleistocene Loess loam in the mid/footslope area. Footslope valleys are filled with unconsolidated alluvium (Küsel et al., 2016; Kohlhepp et al., 2016).Agricultural areas with different management intensities surround the largely unmanaged forest area at the eastern hillslope of the Hainich low mountain range. The Hainich CZE comprises here a variety of surface and belowground observational plots along a transect of groundwater wells of 5.4 km length in an intensively investigated area of about 29 km^2 size (Kohlhepp et al., 2016; Küsel et al., 2016). The well transect consists of five locations (H1 to H5) that span the land-use change from deciduous managed forest (H1), unmanaged woodland (H2), grassland/pasture (H3) to cropland agriculture (H4 and H5) longitudinal to the assumed ground water flow direction (figure 4-1). The wells provide access to two main aquifer assemblages HTL and HTU (Hainich transect lower/upper aquifer assemblage, respectively (Küsel et al., 2016), which consist of one (HTL) and, respectively, nine (HTU) individual

aquifer storeys (Kohlhepp et al., 2016; Küsel et al., 2016). Aquifers are sampled in depth between 0.6 m and 54 m (HTU), respectively 2 m and 89 m (figure 4-1). HTL comprises aquifer storeys in the Trochitenkalk formation (moTK) and comprises thickly bedded porous limestone packages that act as karst-fracture aquifers. HTU comprises mainly aquifer storeys of the overlying Meissner formation (moM), comprising fracture aquifers with fine fissures and a less pronounced karstification due to the finely alternating succession of limestones and low-permeable marlstone beds (figure 4-1; Küsel et al., 2016; Kohlhepp et al., 2016).
Vertical exchange is strongly inhibited by frequent and low-permeable marlstone interbeds resulting in confined flow conditions and a layer-cake architecture (Kohlhepp et al., 2016). HTL is characterised by more intense karstification and fast flow through large conduits (Küsel et al., 2016). Both aquifer assemblages and the included aquifer storeys are separated by intercalated marlstone interbeds.

Groundwater recharge in HTL takes place mainly within the forested upper to middle hillslope of the transect. By contrast, HTU outcrops cover all land use types and recharge also takes place in the lower hill slope area, with mixed land use with forests, pastures and cropland areas (Küsel et al., 2016) (figure 4-1).

Soils in the forested upper to midslope area are represented by predominantly shallow Rendzic Leptosols and Cambisols, which developed mainly on marl- and limestones. Luvisols and Planosols/Stagnosols (WRB nomenclature; WRB, 2006) developed on siliciclastic sediments like Pleistocene Loess loam or unconsolidated Holocene deposits at the foot slope position (Küsel et al., 2016).

Groundwater samples of this study were obtained from 8 groundwater wells at the well sites H3, H4 and H5 (figure 4-1). Depths of each site and nomenclature used for each sampling point are provided in table 4-1.

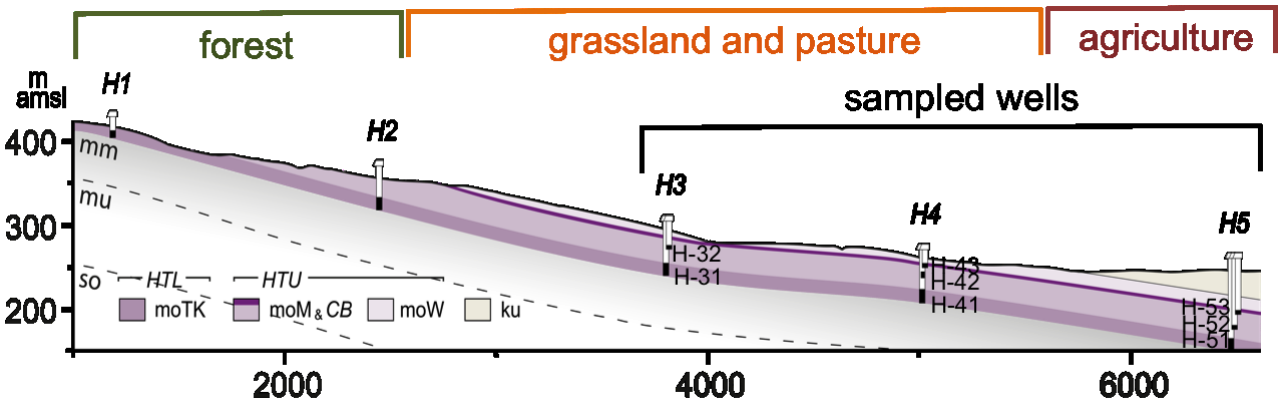

Figure 4-4-1: Cross-section of the studied Hainich transect. Stratigraphic units moTK, moM as well as moW represent Middle Triassic units of the Upper Muschelkalk Formation. ku describes Upper Triassic sediments of the Keuper Formation. Sampled wells for this study comprised locations H3, H4 and H5. The lower aquifer assemblage HTL is recharged in the forested area in the upper part of the Hainich mountain range. Aquifer assemblage HTU is recharged in the forest, grassland and agricultural areas.

4.2.2 Sampling

Regular sampling was conducted every month over the year from May 2014 until April 2015. Water samples for $\delta^{13}C$ and ^{14}C analyses were obtained with a submersible groundwater pump (MP1, Grundfos, Erkrath, Germany). Samples were taken after stationary hydraulic and geochemical conditions were reached which usually required exchanging at least three well volumes. Water samples were taken following recommendations of the International Atomic Agency (IAEA, 2009). One litre Schott bottles with gastight screw caps were filled on a bypass with low water flow from bottom to top in order to avoid degassing of CO_2 during sampling. The bottle was rinsed two times and subsequently filled full to the brim, closed quickly with a gas tight screw cap, cooled at 4°C in the dark and transported to the lab for further analyses. For collecting material for TOC and DNA, a high filtration campaign was conducted in May 2015. 1000 liters of water were pumped from well H 5.1, H 5.2 and H 4.3 through pre-combusted (500°C) glass fiber filters with 0.2 µm pore size placed on a custom filtration unit (Schwab et al., submitted). After pumping 1000 litres, filters were removed, packed into aluminium foliation and cooled on dry ice for TOC and DNA analyses.

4.2.3 Hydrochemistry

Specific electrical conductivity, pH, water temperature, dissolved oxygen concentration and saturation as well as redox potential were measured directly electrometrically in the field (WTW, Weilheim, Germany), using a flow through cell. Dissolved inorganic carbon (DIC), total organic carbon (TOC) and dissolved organic carbon (DOC) were determined by high temperature catalytic oxidation and a non-dispersive infrared sensor (multi 18 N/C 2100S, AnalytikJena, Germany). Nitrite, nitrate, orthophosphate, sulphate and chloride were determined by ion chromatography using an IC 20 system (Dionex, Sunnyvale, CA) equipped with an IonPac AS11-HC column. Major cations were measured by ICP-OES (725 ES, Varian/Agilent, USA) (Kohlhepp et al., 2016).

4.2.4 $\delta^{13}C$ DIC analyses

Stable carbon isotope ratios of DIC ($\delta\,^{13}C_{DIC}$) were measured according the method described by Assayag et al. (2006). $\delta\,^{13}C_{DIC}$ analyses were performed on an isotope ratio mass spectrometer (IRMS) coupled to a Gasbench II (Finnigan MAT Delta^{Plus} XL, Bremen, Germany) and a CTC PAL-80 autosampler. All isotope analyses were conducted within one week after sampling. In brief, 1.5 ml of water were transferred from sampled 1 litre bottles with a gastight syringe to 12 ml screw caped Labco vials with butyl rubber septa, which were pre-flushed with N_2. 0.5 mL of 85 % H_3PO_4 was added to acidify the sample to a pH below 2 and dissolved CO_2 was liberated by shaking and equilibrating water and headspace for 24 h. Three replicates were prepared from each water bottle for $\delta\,^{13}C$ analyses. Standards were prepared for linearity and drift corrections as well as normalizing measured values to the international V-PDB scale (Coplen et al., 2006).

Stable carbon isotope ratios are reported in the delta notation that expresses $^{13}C/^{12}C$ ratios as $\delta^{13}C$-values in per mil (‰) relative to the international reference material Vienna Pee Dee Belemnite (V-PDB):

$$\delta^{13}C = \left(\frac{\frac{^{13}C}{^{12}C}_{sample}}{\frac{^{13}C}{^{12}C}_{reference}} - 1 \right) \times 1000 \qquad (4)$$

Precision of $\delta^{13}C_{DIC}$ based on three repeated measurements from one sampled bottle was better than 0.3 ‰ (±1σ).

4.2.5 ^{14}C analyses of DIC

Radiocarbon concentrations of DIC were measured by accelerator mass spectrometry (AMS) at the Jena ^{14}C facilities (Steinhof et al., 2004). Groundwater DIC was extracted by a headspace-extraction method adapted from Gao et al. (2014). In brief, 25 mL of groundwater samples, corresponding to about 1 mg C, were transferred into 60 mL I-Chem septum sealed screw cap vials within a glove bag containing an N_2 atmosphere. Vials were closed with Teflon/silicone septa and additionally underlain Black Viton septa (Sigma Aldrich, St. Louis, MO, USA), in order to avoid contamination of ^{14}C depleted carbon from the septa rubber (Gao et al., 2014). After closing the vials, 0.5 ml of 85 % H_3PO_4 were added with a syringe to acidify the sample and convert all DIC into CO_2 ($CO_{2(aq)}$). The sample was shaken gently and left to equilibrate at room temperature for at least 24 hours. Three sets of standards were prepared for every batch of samples to correct for contamination either from atmosphere intrusion or from ^{14}C free septa material. For standards containing either no or modern ^{14}C concentrations, 17.5 mg of IAEA-C1 (0 pMC) and in house coral standard powder (CSTD coral, obtained from Ellen Druffel, UC Irvine, 94.45 ± 0.18 pMC) were dissolved in 25 ml acidified water, respectively. Additionally, a blank was prepared to check for the background of the acidified water. Acidified water was prepared by adding degassed 85 % H_3PO_4 to ultra pure MilliQ water until a pH of lower 2 was reached and by stripping the water with a N_2 stream for 1 hour.

After preparation, sample as well as standard CO_2 was directly extracted from the vial headspace into a high vacuum extraction line with a syringe connected to the line. Extraction efficiency was checked by measuring the pressure within the vials, after CO_2 release and equilibration with the headspace on the extraction.

The extracted CO_2 was subsequently catalytically reduced to graphite at 625 °C by H_2 reduction and measured by AMS.

All radiocarbon values are reported in percent modern carbon pmC, which is defined as the fractionation corrected ratio between the ^{14}C activity of the sample compared to the new oxalic acid standard (NBS SRM 4990C) according to (Steinhof et al., 2004):

$$pmC = R * \frac{1}{0.7459} * \left(\frac{1+\delta^{13}C_{NOX}}{1+\delta^{13}C}\right)^{\theta} \quad (5)$$

Errors reported for $^{14}C_{DIC}$ analyses are the external analytical precision based on repeated measurements of a control sample, which was better than 0.46 pMC (±1σ).

4.2.6 $\delta^{13}C$ analyses of DOC and TOC

DOC $\delta^{13}C$ values of samples from November 2014, March 2015 and May 2015 were determined on a high performance liquid chromatography system coupled to an IRMS (HPLC/IRMS) system (Scheibe et al., 2012). HPLC/IRMS allows direct determination of $\delta^{13}C$ values of DOC in the liquid phase by coupling a LC-IsoLink system (Thermo Electron, Bremen, Germany) to a Delta+ XP IRMS (Thermo Fisher Scientific, Germany). A detailed description of the apparatus and measurement procedure is given in (Scheibe et al., 2012). Errors reported for DOC analyses represent the external analytical precision based on repeated measurements of one control sample. External precision was better than 0.15 ‰. Low DOC content coupled with high salt content of DOC prevented radiocarbon measurements on the collected samples.

$\delta^{13}C$ and ^{14}C values of TOC were obtained by combustion of material trapped on the precombusted glass fiber filters. Pieces of filters were cut out and weighted into tin capsules. The $^{13}C/^{12}C$ isotope ratio was determined on an isotope ratio mass spectrometer (DELTA+XL, Finnigan MAT, Bremen, Germany) coupled to an elemental analyser (NA 1110, CE Instruments, Milan, Italy) via a modified ConFloII™ interface (EA-IRMS). Stable carbon isotope ratios are reported in the delta notation that expresses $^{13}C/^{12}C$ ratios as $\delta^{13}C$-values in per mil (‰) relative to the international reference material NBS 22. Only one sample of filter

could be run for each well. Error reported for TOC values is the analytical precision for one sample run.

4.2.7 DNA extraction and sequencing

DNA was extracted from the filtered groundwater using the RNA PowerSoil® Total Isolation kit followed by the RNA PowerSoil® DNA elution accessory kit (MO BIO, Carlsbad, CA, USA) following the manufacturer's protocol, and then stored at -20 °C

Groundwater DNA aliquots were shipped to LGC Genomics GmbH (Berlin, Germany) for Illumina MiSeq sequencing and the 341F - 785R primer pair was used. Because the DNA concentrations from the filter pieces were low, PCR products were used for sequencing, and not genomic DNA. This first round of PCR was carried out on DNA samples using the B8F – U1492R primer pair, and conditions for PCR were 30 cycles with 1 min at 94°C, 1 min at 55°C and 2 min at 72°C. The Illumina sequence datasets were denoised and analyzed using Mothur v.1.36.1 following the Schloss SOP (http://www.mothur.org/wiki/MiSeq_SOP). Sequences obtained in this study were deposited in the European Nucleotide Archive under project number.

4.2.8 ^{14}C DIC age models and hydro-chemical modelling

4.2.8.1 Han-Plummer plot

In order to use DIC isotopes as a proxy for water flow and carbon turnover in the subsurface compartments of the CZ, we applied the graphical method developed by Han et al. (2012). The method is based on plotting $^{14}C_{DIC}$ against $^{13}C_{DIC}$ as well as the reciprocal of the DIC concentration. Processes affecting DIC and its isotopic composition include calcite/dolomite dissolution (Tamers et al., 1975), isotopic exchange under open or closed conditions (Eichinger, 1983; Fontes and Garnier, 1979; Han and Plummer, 2013), heterotrophic respiration of organic matter (Aravena et al., 1995) as well as precipitation and recrystallization of calcite (Wigley, 1976). Adjustment models exist for most of the mentioned processes, which can be applied in order to determine the initial ^{14}C concentration (Han and Plummer, 2016). The Han-Plummer plot can help to

identify processes that affect the DIC isotopic signature. Key features of the Han-Plummer plot are described here briefly with the aid of figures 6a and 6b.

On figure 4-6, point A represents the isotope value of CO_2 in the recharge zone. The isotopic composition of soil CO_2 in the Hainich area was obtained from (Hahn, 2004), who measured soil CO_2 values averaging -23.00 ‰ in soils close to the recharge area. Considering a fractionation factor of -1.32 ‰ between gaseous and dissolved CO_2 (Mook et al., 1974), a $\delta^{13}C$ value of -24.32 ‰ can be derived for dissolved soil CO_2 (point A'). We initially chose 100 pmC (i.e. preindustrial atmospheric CO_2) as the initial radiocarbon concentration of soil CO_2. We do not correct for mass-dependent fractionation of radiocarbon as this is accounted for in the correction of reported radiocarbon data (Trumbore et al., 2016).

Water that is equilibrated with soil CO_2 reacts with carbonates either under open system conditions in the soil or under closed conditions within the aquifer. Equilibration with carbonates according to equation (1) shifts DIC values in the Han-Plummer plot to the so-called Tamer´s point, which represents the $\delta^{13}C$ or ^{14}C value of DIC diluted by $CaCO_3$ according to:

$$^{13/14}C_0 = \left(\frac{C_a}{C_t}\right) \times {}^{13/14}C_g + 0.5\,\frac{C_b}{C_t}\left({}^{13/14}C_g + {}^{13/14}C_s\right) \qquad (6)$$

where $^{14}C_0$ represents the ^{13}C or ^{14}C values of DIC reacted with $CaCO_3$. C_a, C_b and C_t refer to $CO_{2(aq)}$ and HCO_3^- and total DIC concentrations, respectively. $^{13/14}C_g$ and $^{13/14}C_s$ refer to $\delta^{13}C$ or radiocarbon concentrations of soil gas and solid carbonate, respectively.

In our study, Tamer´s point is located at -12.16 ‰ for $\delta^{13}C$ and 50 pmC, considering a carbonate isotopic end-member of 0.29 ‰ and 0 pmC (point C in figure 4-6). Isotopic exchange, which can occur either in the soil by reaction between soil CO_2 and DIC or in the saturated zone between DIC and solid carbonates can also be identified with the graphical method. Isotopic exchange in the soil zone, which is usually accompanied with slow water infiltration (Han

and Plummer, 2016), would shift $\delta^{13}C$ and ^{14}C from Tamer´s point towards values close to A´, whereas the endpoint of DIC fully equilibrated with respect to soil CO_2 can be derived according to (Han and Plummer, 2016):

$$\delta^{13}C_0 = \left(\frac{C_a}{C_t}\right) \times \left(\delta^{13}C_g + \varepsilon_{a/g}\right) + \left(\frac{C_b}{C_T}\right) \times \left(\delta^{13}C_g - \varepsilon_{g/b}\right) \quad (7)$$

and

$$^{14}C_0 = \left(\frac{C_a}{C_T}\right) \times \left(^{14}C_g + 0.2\varepsilon_{a/g}\right) + \left(\frac{C_b}{C_T}\right) \times \left(^{14}C_g - 0.2\varepsilon_{g/b}\right) \approx {}^{14}C_g \quad (8)$$

where $^{14}C_0$ and $\delta^{13}C_0$ represents the ^{13}C or ^{14}C values of DIC equilibrated with soil CO_2. C_a, C_b and C_t refer to $CO_{2(aq)}$ and HCO_3^- and total DIC concentrations, respectively. $\delta^{13}C_g$ and $^{14}C_g$ refer to stable isotope composition and radiocarbon concentrations of soil CO_2, respectively. $\varepsilon_{a/g}$ and $\varepsilon_{g/b}$ are the respective carbon isotope fractionation factor of gaseous CO_2 and dissolved CO_2 and gaseous CO_2 and HCO_3^-.

Isotopic exchange under closed conditions would include isotope exchange reactions between DIC and $CaCO_3$ and shift $\delta^{13}C$ and ^{14}C values in direction to the calcite end-member C. Fully equilibrated DIC isotopic signatures can be derived according to (Han and Plummer, 2016):

$$\delta^{13}C_0 = \left(\frac{C_a}{C_t}\right) \times \left(\delta^{13}C_s - \varepsilon_{s/a}\right) + \left(\frac{C_b}{C_T}\right) \times \left(\delta^{13}C_s - \varepsilon_{s/b}\right) \quad (9)$$

and

$$^{14}C_0 = \left(\frac{C_a}{C_t}\right) \times \left(^{14}C_s - 0.2\varepsilon_{s/a}\right) + \left(\frac{C_b}{C_T}\right) \times \left(^{14}C_s - 0.2\varepsilon_{s/b}\right) \quad (10)$$

where $\varepsilon_{s/a}$ and $\varepsilon_{s/b}$ refers to carbon isotope fractionation factor of $CaCO_3$ and $CO_{2(aq)}$ and $CaCO_3$ and HCO_3^-, respectively.

End-members for isotopic exchange under closed conditions are represented by point D and by point E in figure 4-6. DIC that is affected by isotopic exchange to various extents, either under closed or open conditions, would shift DIC isotope values along the dashed lines between Tamer´s point and points E and D in figure 4-6.

Other processes that might affect the isotopic composition of DIC include heterotrophic respiration of organic matter, which can be linked to a variety of microbial metabolisms (Han et al., 2012). The influence of heterotrophic respiration on DIC can be obscured, if oxidized OM in the aquifer has similar $\delta^{13}C$ or ^{14}C values to soil CO_2. However, by plotting $\delta^{13}C$ or ^{14}C against the reciprocal of the DIC concentration, heterotrophic respiration can be identified, because DIC usually increases in this case (Han et al., 2012) (figure 4-7 and 4-8). Corresponding shifts in DIC isotopes are dependent on the isotopic composition of the oxidized organic matter.

4.2.8.2 NETPATH modelling

The mass-fluxes suggested by the Han-Plummer plot, were quantified with the inverse geochemical modelling program NETPATH (Plummer et al., 1992). NETPATH calculates the chemical evolution of waters along a real or hypothetical flow path between an initial and final well (El-Kadi et al., 2011). Models include inverse geochemical calculations, equations for chemical and isotopic mass balance as well as Rayleigh equations for evolutionary paths of isotopes in aquifers. The models are adjusted to measured mineralogy, as well as chemical and isotopic composition of the groundwater (El-Kadi et al., 2011). A unique feature of NETPATH is its ability to perform radiocarbon age estimates for groundwater by applying traditional ^{14}C adjustment models and accounting additionally for water rock interactions, mixing, redox reactions and isotope exchange processes.

For determining carbon evolution within the flow path, NETPATH uses the concept of total dissolved carbon (TDC) (Plummer et al., 1992):

$$mTDC = mDIC + mCH_4 + mDOC \qquad (10)$$

NETPATH accounts also for organic matter oxidation, including its isotopic composition, which is not done by traditional ^{14}C adjustments models. Calculated ^{14}C activity of water A_{nd} in the final well is adjusted for chemical reactions but not for radioactive decay. The radiocarbon age is subsequently calculated according to:

$$t(years) = \left(\frac{5730}{\ln 2}\right) * \ln\left(\frac{A_{nd}}{A}\right) \quad (11)$$

where 5730 represents the radiocarbon half-life, A is the observed ^{14}C activity of TDC in the final well and t is travel time between initial and final well.

Fractionation factors for Rayleigh isotope effects were obtained from Mook et al. (1974). Constrains and phases for the calculations were chosen according to changes that were observed in the hydro-chemical data. Input data for the model is provided in the supplemental material.

We chose three wells, representing the three major water chemistry clusters in the two aquifer complexes at the Hainich CZE. Based on hydrogeological considerations (Kohlhepp et al., 2016), we estimated three flow paths for the evolution of water chemistry between wells for each case. Modelled flow paths for HTL were H-31 (initial well) to H-41(final well) and H-41 (initial well) to H-51 (final well). For HTU we modelled flow path H-32 (initial well) to H-42 (final well) (=HTU 1) and H-32 (initial well) to H-52 (final well) (=HTU 2). We considered therefore that no connection occurs between wells H-42/H-43 and H-52/H-53.

4.3 Results

4.3.1 Hydrochemistry

Within the time period of monitoring there was no significant change from previous reported hydro-chemical patterns (table 4-1) (Herrmann et al., 2015; Küsel et al., 2016). Water chemistry reflects the limestone environment of the

catchment. Ca^{2+}, Mg^{2+}, HCO_3^-, CO_3^{2-} and SO_4^{2-} are the main ions in the system (table 4-1). The waters are characterised as earth alkaline bicarbonatic to bicarbonatic-sulfatic waters (Küsel et al., 2016). The footslope wells of HTL (H42/43/52/53) are depleted in oxygen, whereas the upper/midslope HTL-wells (H14/23/32) contain moderate concentrations in dissolved oxygen. By contrast HTL has higher values of dissolved oxygen ranging from 1.6 mg/L in H-31 to 0.23 mg/L in H-51. A substantial decrease in Ca^{2+} is observed in HTU along the flow path. In contrast, in HTL Ca^{2+} concentrations increase, with a doubling of Ca^{2+} at location H-51 compared to H-31 or H-41. Mg^{2+} concentrations are higher in HTU compared to HTL and highest at well H-52 and H-53. K^+ concentrations triple in HTU along the presumed flow path but remain constant at a low level in HTL. Fe^{2+} concentrations are close to zero in both aquifer assemblages, but increase in well H-42 (HTU). NO_3^- concentrations decline along the flow path to near zero in HTU and to < 10 mg/L in HTL. Sulphate concentrations in the majority of wells are close to 100 mg/L but decrease in HTU at location H-42 and increase sharply in HTL in well H-51.

DIC concentrations in both aquifers are close to 70 mg/L but are higher in HTU in wells H-42 and H-43 and lower at location H-51 in HTL.

DOC concentrations are below 1 mg/L in HTU as well as HTL with temporal variations in both aquifers.

4.3.2 $\delta^{13}C$ and ^{14}C of DIC

The majority of wells have nearly constant $\delta\,^{13}C$ values, with a mean annual value of -11.66 ± 0.19 ‰ (figure 4-2). However, $\delta\,^{13}C_{DIC}$ in wells H-52 and H-53 of HTU are significantly more enriched compared to all other wells with values of -8.94 ± 0.25 ‰ and -9.54 ± 0.13 ‰, respectively.

^{14}C DIC results show a similar pattern. All wells show little temporal variation during the monitoring period. In HTL, ^{14}C concentrations decrease from well H-31 to H-41, but increase again in well H-51. Radiocarbon values of HTU decrease continuously from 62.23 ± 7.01 pmC in H-32 to 13.38 ± 0.54 pmC in H-53 (figure 4-3).

According to results from $\delta\ ^{13}C_{DIC}$ and $^{14}C_{DIC}$ measurements, the observed wells can be divided into three groups (boxplots in lower part of figure two and three). Group 1 comprises all oxic wells of HTL and well H-32 of HTU, which is also oxic. Group 2 and 3 describe the anoxic wells of HTU in location H-4 and H-5, respectively.

4.3.3 $\delta^{13}C$ DOC

Unlike DIC values, $\delta\ ^{13}C$ of DOC shows no distinct spatial patterns, with all wells in both aquifer assemblages averaging -23.45 ±1.55 ‰ without clear trends over the observation period (table 4-2).

Aquifer	Well	Depth	TIC	DOC	TOC	pH	O_2	Ca^{2+}	Mg^{2+}	$Fe_{t[umol\ L^{-1}]}$	NH_4^{+}[umol L^{-1}]	K^{+}	SO_4^{2-}	NO_3^{-}
HTL	H-31	43 m	6.16 ± 0.0	0.27 ± 0.06	0.30 ± 0.07	7.25	0.28± 0.10	2.42 ± 0.06	1.94 ± 0.06	0.38 ± 0.44	4.98 ± 3.19	0.08± 0.003	0.72 ± 0.02	0.55 ± 0.13
HTL	H-41	45 m	6.97 ± 0.36	0.18 ± 0.08	0.19 ± 0.08	7.27	0.31± 0.06	2.66 ± 0.19	1.69 ± 0.12	2.49 ± 4.00	11.95 ± 4.64	0.13± 0.03	1.00 ± 0.23	0.22 ± 0.08
HTL	H-51	84 m	6.31 ± 0.22	0.18 ± 0.08	0.20 ± 0.09	7.18	0.18± 0.24	4.56 ± 0.11	1.71 ± 0.10	0.24 ± 0.30	3.74 ± 2.86	0.05± 0.006	3.03 ± 0.19	0.15 ± 0.09
HTU	H-32	15 m	6.70 ± 0.53	0.20 ± 0.10	0.22 ± 0.10	7.32	0.12± 0.03	2.37 ± 0.06	2.01 ± 0.03	0.07 ± 0.02	1.25 ± 1.96	0.07± 0.003	0.76 ± 0.04	0.55 ± 0.08
HTU	H-42	9 m	7.84 ± 0.43	0.20 ± 0.08	0.23 ± 0.10	7.16	0	2.08 ± 0.03	2.04 ± 0.02	3.14 ± 0.45	21.17 ± 1.96	0.17± 0.005	0.37 ± 0.014	0.004± 0.002
HTU	H-43	8.5 m	7.80 ± 0.18	0.21 ± 0.09	0.23 ± 0.08	7.17	0	2.21± 0.12	2.03 ± 0.03	1.66 ± 2.24	14.23 ± 4.36	0.14± 0.004	0.40 ± 0.017	0.003 ± 0.001
HTU	H-52	65 m	6.30 ± 0.30	0.19 ± 0.10	0.23 ± 0.10	7.31	0	1.71 ± 0.02	2.19 ± 0.04	1.70 ± 2.79	52.30 ± 3.92	0.25± 0.004	0.97 ± 0.05	0.04 ± 0.06

Table 4-1: Hydrochemical data

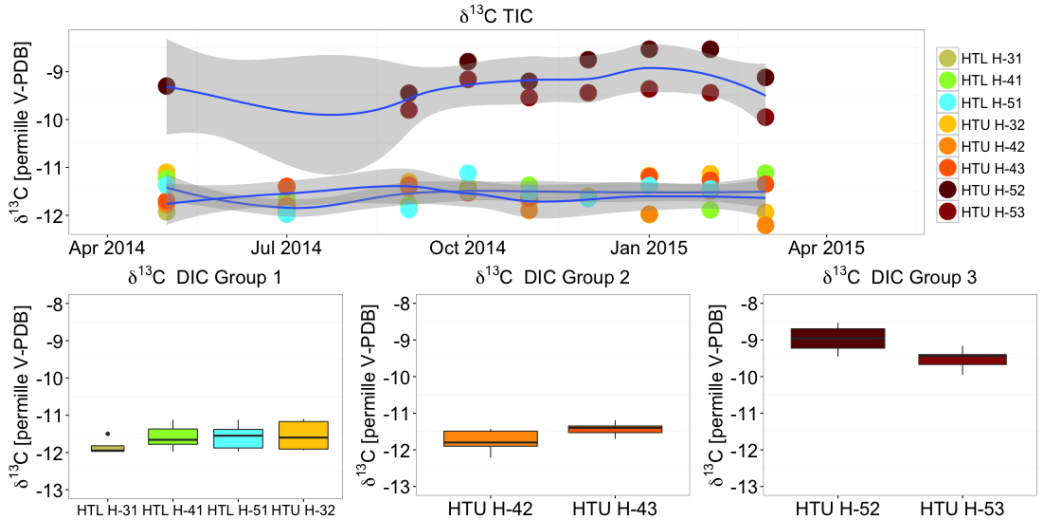

Figure 4-4-2: Stable isotope monitoring of $\delta^{13}C_{DIC}$. Upper part: $\delta^{13}C_{DIC}$ values show minor temporal but strong spatial variations. According to results from $\delta^{13}C_{DIC}$ and $^{14}C_{DIC}$, wells can be divided into three groups (boxplots in lower part). Group 1 comprises all oxic wells of HTL and well H-32 of HTU, which is also oxic. Group 2 and 3 are the anoxic wells of HTU in location H-4 and H-5, respectively. The blue line in the time series represents a fitted conditional mean through each group. Grey bands represent 99% confidence interval values. Group 3 wells exhibit very different, ^{13}C enriched $\delta^{13}C$ values compared to group 1 and 2.

4.3.4 $\delta^{13}C$ and $\Delta^{14}C$ of TOC

$\delta\,^{13}C$ and ^{14}C TOC values from filters obtained in May 2015 are given in table 4-2. $\delta\,^{13}C$ of TOC is most depleted in well H-43 with a value of -33.8 ± 0.2 ‰. TOC values in wells H-51 and H-52 are -28.7 ± 0.2 ‰ and -28.4 ± 0.2 ‰, respectively.

^{14}C values of TOC are 74.4 ± 0.3 pmC in well H-51 (HTL) and 41.2 ± 2.0 pmC in H-43 and 35.2 ± 0.2 pmC in H-52 (both HTU).

$\delta\,^{13}C$ and ^{14}C of soil organic matter (SOM) at 45 cm depth in the recharge zone of HTL and HTU are -25.80 ± 0.18 and -26.09 ± 0.12, respectively. The respective ^{14}C values are 88.50 ± 1.40 and 87.50 ± 0.31. Carbonates of both aquifer assemblages are free of radiocarbon (i.e. 0 pmC) and have an average $\delta\,^{13}C$ value of 0.29 ± 0.3 ‰.

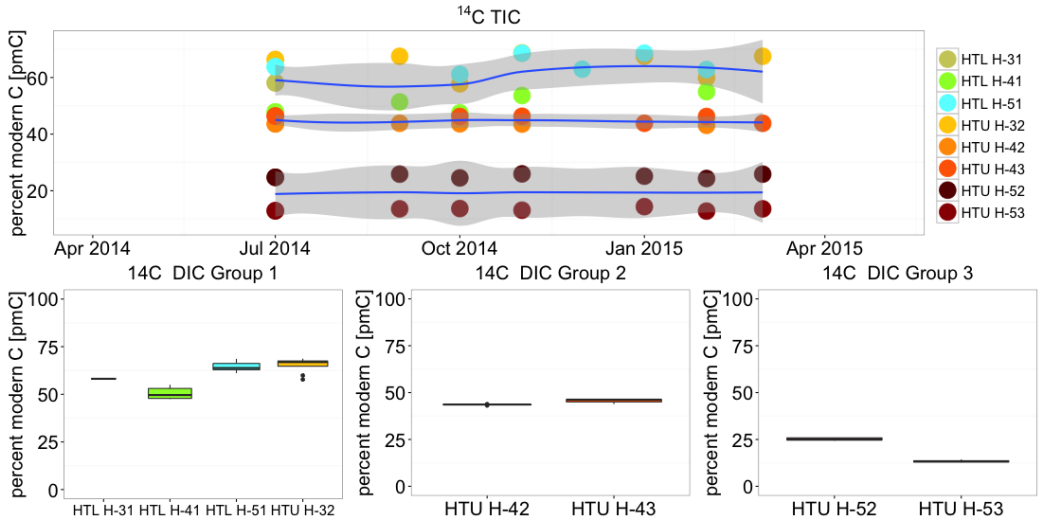

Figure 4-4-3: Results of radiocarbon monitoring of DIC in the investigated wells. Similar to $\delta^{13}C$ values, $^{14}C_{DIC}$ values show little temporal but strong spatial variations. $^{14}C_{DIC}$ concentrations decrease according to group 1 > group 2 > group 3. Wells of group 1 show more variation during the year than group 2 and 3 wells.

4.3.5 Bacterial 16S rRNA gene diversity

The bacterial community diversity in all three well samples display different patterns (figure 4-4). The sample from well H-43 (Group 2) is dominated by Proteobacteria (30.9 % of the total reads) and Candidate Division OD1 (12 %), and also composed of Firmicutes, Candidate Division OP3, Nitrospirae, Bacteroidetes and Chloroflexi. On the genus level, the most dominant groups are the sulfate-reducing *Desulfosporinus* (5.2 %) of the Firmicutes, unclassified genera of the Gallionellaceae family (2.1 %, Betaproteobacteria), and unclassified groups belonging to the Deltaproteobacteria (8.8 %).

The sample from well H-51 (Group 1) is dominated by Proteobacteria (32.4 %), and also composed of Nitrospirae and Actinobacteria. On the genus level, the most dominant groups are *Albidiferax* (8.4 %, Betaproteobacteria), *Nitrospira* (5.9 %), unclassified genera of the Caulobacteraceae family (4.1 %, Alphaproteobacteria), *Aquicella* (1.3 %) and *Acidiferrobacter* (1.2 %) of the Gammaproteobacteria, and unclassified groups belonging to the Deltaproteobacteria (5.2 %).

The sample from well H5-2 (Group 3) is dominated by Proteobacteria (28.5 %), Chlorobi (26 %) and Candidate Division TM7 (16.6 %), and is also composed of Nitrospirae and Bacteroidetes. On the genus level, the most dominant groups are

Syntrophus (5.1 %), *Desulfovibrio* (2 %) and *Desulfocapsa* (1 %) of the Deltaproteobacteria, *Sulfuritalea* (2.6 %, Betaproteobacteria), and *Sulfuricurvum* (1 %, Epsilonproteobacteria.

4.3.6 Archaeal 16S rRNA gene diversity

The archaeal community structure also shows distinct patterns for all three groups (figure 4-5). The samples from wells H-51 (Group 1) and H-52 (Group 3) were almost solely composed of the ammonia-oxidizing Marine Group I (MG-I) Thaumarchaeota. The sample from H-52 (Group 3 well) also contained sequences affiliated with the subgroup 7/17 of the Bathyarchaeota (6.3 % of the total reads).

Sample H-43 (Group 2 well) exhibits the most diverse archaeal community. The most dominant groups were unclassified genera of the hydrogenoclastic (using H_2 and CO_2) methanogenic family *Methanoregulaceae* (22 %); subgroups -6 and -11 of the Bathyarchaeota (19.9 % and 11.5 %); and subgroup 1.1c of the *Thaumarchaeota* (12.9 %). The MG-I *Thaumarchaeota* which dominated the samples from wells H-51 and H-52 represented only 1.6 % of the archaeal community in well H-43.

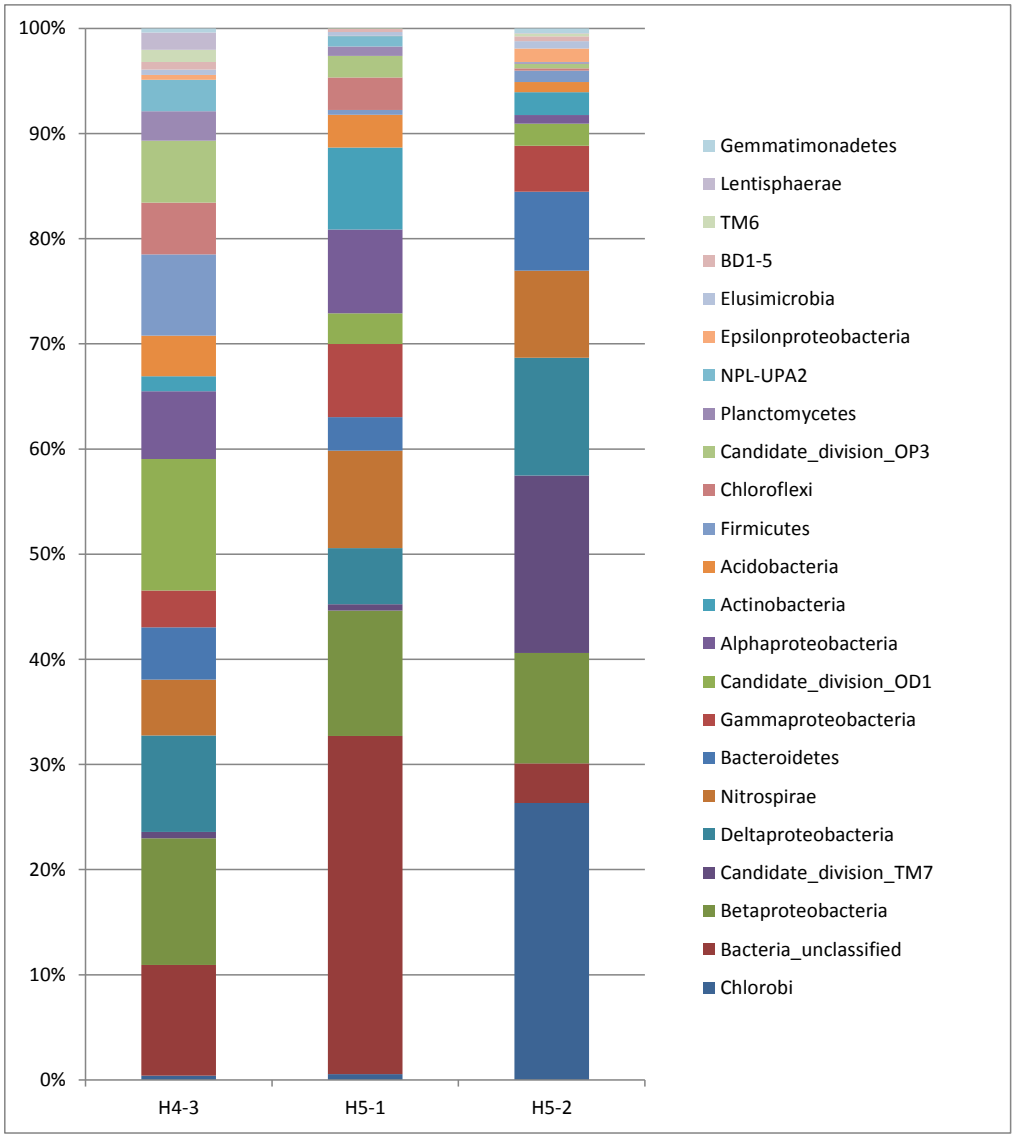

Figure 4-4-4: Phylogenetic affiliations of DNA-based bacterial 16S rRNA gene reads in percent of total reads in groundwater samples of wells H-43, H-51 and H-52 for time point May 2015.

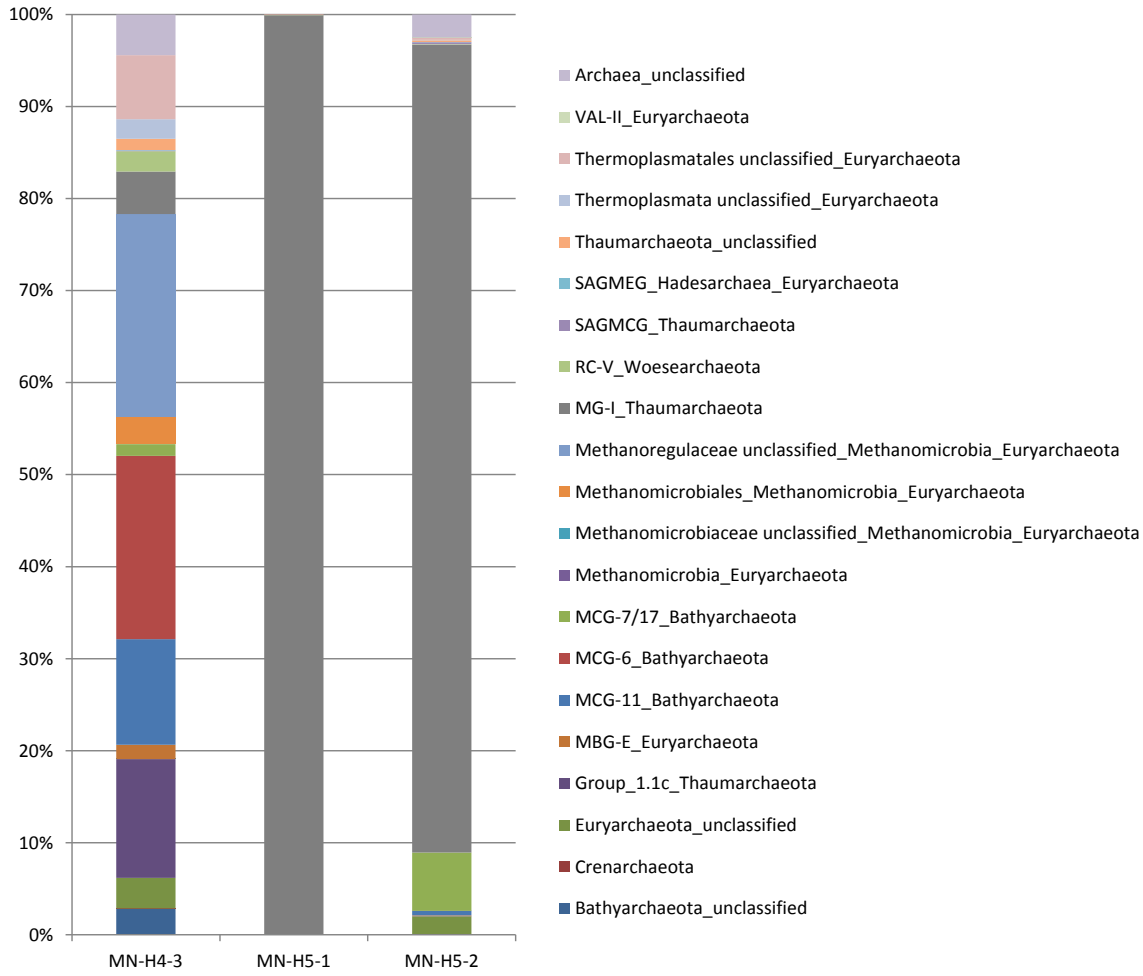

Figure 4-4-5: Phylogenetic affiliations of DNA-based archaeal 16S rRNA gene reads in percent of total reads, for groundwater samples of all wells for time point May 2015.

4.3.7 Graphical evaluation of radiocarbon data

Concordant to results of the $\delta^{13}C_{DIC}$ and $^{14}C_{DIC}$ monitoring, three clusters of points can be distinguished when DIC data are plotted in the Han-Plummer plots (Figs. 6a-c). The first group falls on Tamer´s point for $\delta^{13}C$ but is enriched in ^{14}C (arrow d in figure 4-6). This group (Group 1) comprises all wells of HTL and well H-32 of HTU.

Group 2 also falls close to Tamer´s line for $\delta^{13}C_{DIC}$, but is depleted in ^{14}C and has elevated DIC concentrations (arrow e in figure 4-6 and arrow b in 6b and 6c). This pattern is indicative for oxidation of organic matter that is depleted in ^{14}C but close to SOM $\delta^{13}C$, accompanied with calcite dissolution. Group 2 comprises wells HTU H-42 and H-43.

Wells HTU H-52 and H-53 constitute the third group (Group 3). Group 3 wells fall off Tamer´s point for $\delta^{13}C$ and ^{14}C towards more enriched $\delta^{13}C$ and depleted ^{14}C values. Enriched $\delta^{13}C$ and depleted ^{14}C values can be indicative of enhanced calcite dissolution (Han et al., 2012). However, both wells fall off the calcite dissolution line (arrow b in figure 4-6) and they are shifted towards more depleted $\delta^{13}C$ values (arrow c in figure 4-6), indicating the influence of more depleted organic C sources or dissolution-precipitation processes (line e in figure 4-6).

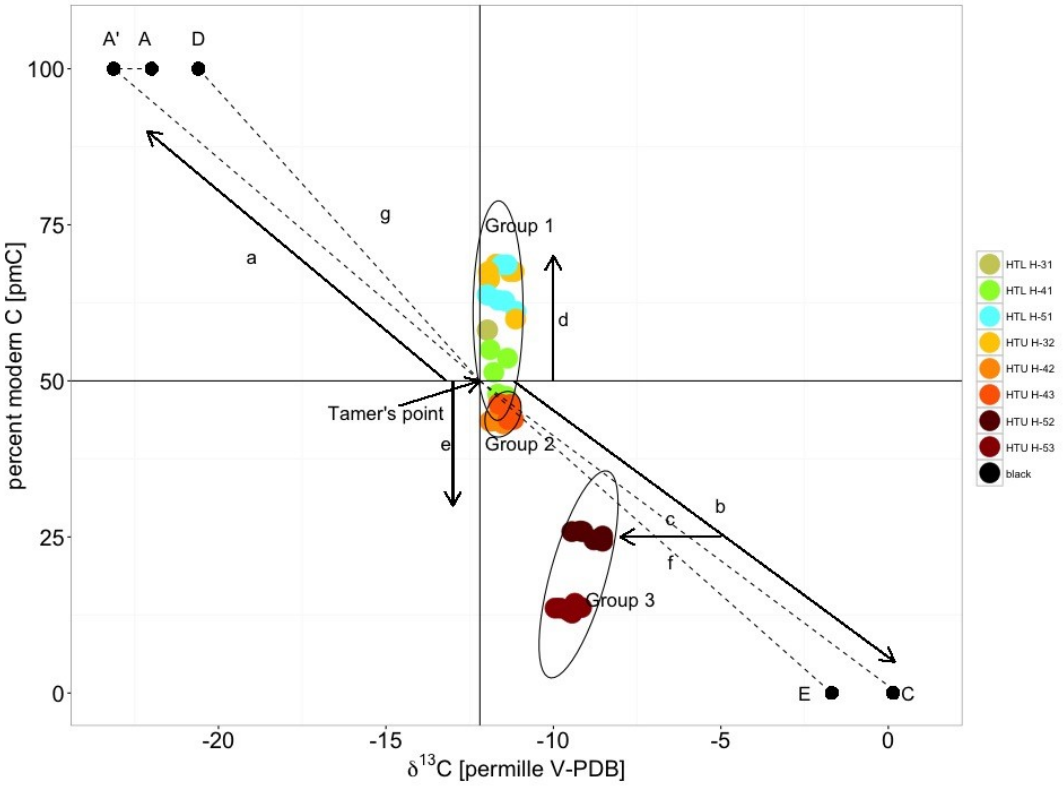

Figure 4-4-6: Han - Plummer plot with data from groundwater sampling wells. The Methods section describes in detail the theory behind these plots and identifies the various elements shown on the figure. By plotting ^{14}C vs. $\delta^{13}C$ three different groups can be distinguished. The oxic wells of HTL including well H-32 forming (Group 1), wells H-42 and H-43 (Group 2) as well as H-52 and H-53 (Group 3). The Han-Plummer plot indicates ^{14}C enrichment due to bomb carbon for group 1 wells (arrow d), oxidation of ^{14}C depleted OM accompanied with calcite dissolution in group 2 wells (arrow e) and complex water rock interactions and OM turnover in group 3 wells (arrow c). Further explanations are given in the text. Data ellipses represent the 95% confidence interval of data points assuming a multivariate t-distribution.

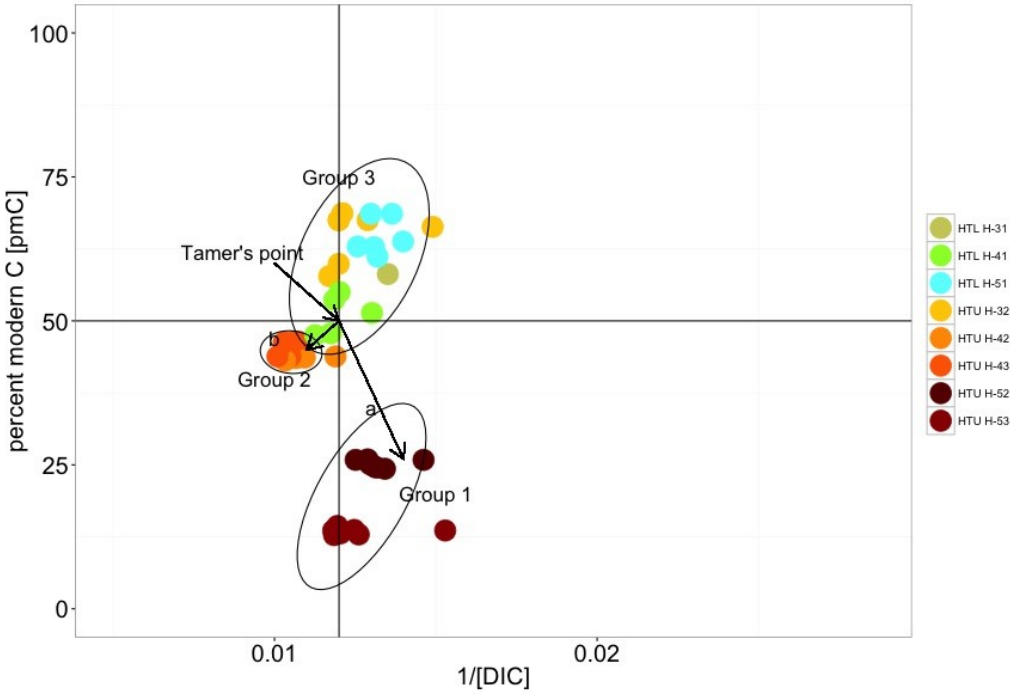

Figure 4-4-7: Plotting ^{14}C vs. 1/[DIC] also allows distinguishing the three groups. Group 2 is not distinct in ^{14}C compared to Group 1, but differs in DIC concentration. Group 2 is distinct from group 1 in $\delta^{13}C$ but does not differ in DIC concentration.

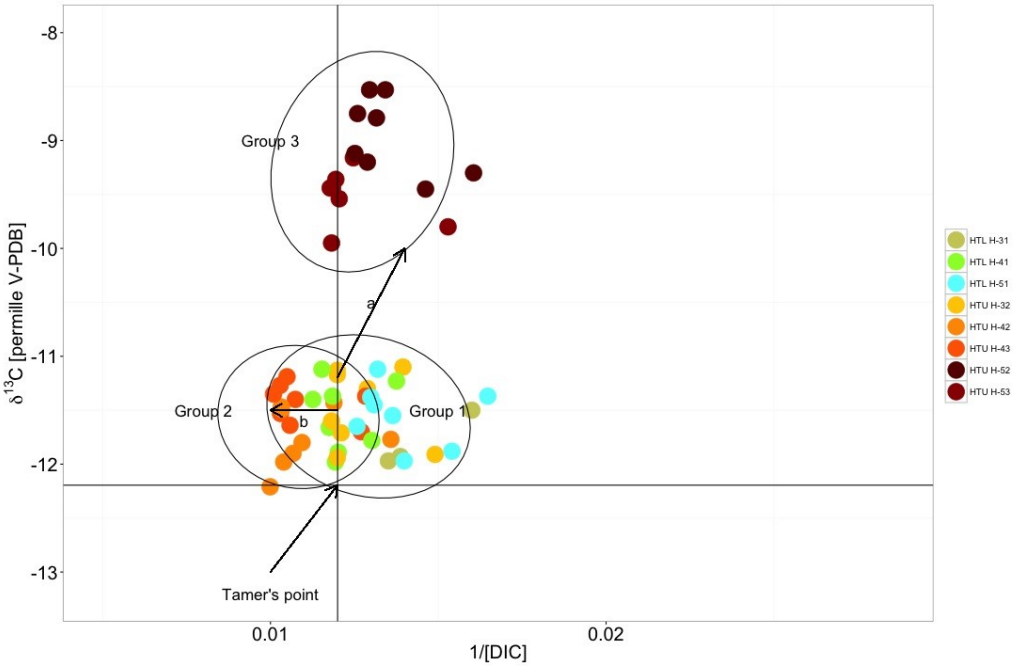

Figure 4-4-8: Plotting $\delta^{13}C$ concentrations against 1/[DIC].

4.3.8 NETPATH modelling

For flowpath H-31 to H-41 (Group 1 wells) hydrochemical composition and isotope values for DIC can be reconstructed assuming mainly reactions between

Aquifer	Well	$\delta\ ^{13}C_{DIC}$	$^{14}C_{DIC}$	$\delta\ ^{13}C_{DOC}$	$\delta\ ^{13}C_{TOC}$	$^{14}C_{TOC}$
HTL	H-31	-11.97 ± 0.20	58.13 ± 0.40	-23.45 ± 1.21	-	-
HTL	H-41	-11.63 ± 0.21	50.53 ± 3.28	-22.30 ± 1.95	-	-
HTL	H-51	-11.63 ± 0.31	62.23 ± 7.01	-22.36 ± 1.69	-28.7 ± 0.2	74.4 ± 0.3
HTU	H-32	-11.58 ± 0.37	65.19 ± 4.03	-	-	-
HTU	H-42	-11.76 ± 0.28	45.51 ± 3.62	-22.87 ± 1.62	-	-
HTU	H-43	-11.39 ± 0.15	45.59 ± 1.20	-25.36 ± 0.69	-33.8 ± 0.2	41.2 ± 2.0
HTU	H-52	-8.94 ± 0.38	25.14 ± 0.66	-22.45 ± 0.84	-28.4 ± 0.2	35.2 ± 0.2
HTU	H-53	-9.54 ± 0.29	13.38 ± 0.54	-23.23 ± 1.52	-	-

Table 4-2: Measured isotopic data of DIC, DOC and TOC

water and carbonate rock. Computed stable isotopes of DIC are off the 1σ uncertainty for $\delta\ ^{13}C_{DIC}$ (Δ=0.72 ‰, p>0.01), but reproduce measured radiocarbon values (Δ=0.11 pmC, p=0.79) (table 4-4). For calculating initial ^{14}C concentrations, Tamer´s model provides the best match, which is in accordance with the graphical method. Dissolution of 1.01 mmol L^{-1} of calcite is required to explain the evolution of water chemistry between the two wells (Table 4-3).

For flowpath H-41 to H-51 (Group 1 wells) $\delta\ ^{13}C_{DIC}$ values can be computed assuming 0.31 mmol L^{-1}calcite dissolution. Computed values are within the 1σ uncertainty of measured values (Δ=0.11 ‰, p=0.38) (table 4-4). However, there is a less good agreement for radiocarbon (Δ=5.83 pmC, p=0.07) and DIC in the final well has higher ^{14}C concentrations than in the initial well. NETPATH computes modern radiocarbon ages for both flow paths in HTL.

Two separate flow paths were assumed for the upper aquifer assemblage. The best match for flow path HTU-1 (H-32 to H-43) was found by oxidizing 0.8 mmol L^{-1} of organic matter coupled to iron reduction (dissolution of 0.18 mmol L^{-1} goethite) and sulphate reduction (precipitation of 0.18 mmol L^{-1} of pyrite) (table 4-3). The best match for calculating isotope values was obtained using the values measured in TOC as the source of oxidized C (table 4-4). Calculated isotope values of the model match well for $\delta\ ^{13}C_{DIC}$ (Δ=0.01 ‰, p=0.91) but less well for $^{14}C_{DIC}$ (Δ=2.92 pmC, p=0.07) (table 4-4). Water age is computed as 403 years.

Table 4-3: Mass fluxes derived from the NETPATH model. The unit of all displayed mass transfers is mmol L^{-1}. Negative leading signs indicate that the respective phase is removed from the water phase. "Exchange" refers to cation exchange and numbers in brackets in the "calcite" column refer to isotopic exchange between DIC and calcite minerals.

	Reaction [mmol L^{-1}]									
Flowpath	Calcite [iso-ex]	Dolomite	CH_2O	CH_4	CO_2	Gyspum	Pyrite	Goethite	NH_3 Gas	Exchange
H-31 - H-41	1.01	-	-	-	-	-	-	-	-1.46	-
H-41 - H-51	0.31	-	-	-	-	-	-	-	-1.78	-
H-32 - H-43	1.53	-	0.77	-	-	-	-0.18	0.18	-	1.70
H-32 - H-52 a	1.57 [2.00]	0.18	-	1.33	-3.78	-3.53	1.87	-	-	4.62
H-32 - H-52 b	1.26 [2.00]	1.18	1.82	-	-3.96	-	0.10	-	-3.22 (N_2)	4.10

Isotope values	Measured $\delta\,^{13}C_{DIC}$ (± 1σ)	Computed $\delta\,^{13}C_{DIC}$	Measured $^{14}C_{DIC}$ (±1σ)	Computed $^{14}C_{DIC}$	Used model for A_0	Input TOC $\delta\,^{13}C$	Input TOC ^{14}C	Age (years)
H-41	-11.63 ± 0.21	-10.91	50.53 ± 3.28	50.88	Tamers	-28.70 ± 0.2	74.40 ± 0.3	modern
H-51	-11.63 ± 0.31	-11.74	62.23 ± 7.01	56.40	Tamers	-28.70 ± 0.2	74.40 ± 0.3	modern
H-42	-11.76 ± 0.28	-11.75	45.51 ± 3.62	48.43	Tamers	-33.80 ± 0.2	41.20 ± 2.0	403
H-52a	-8.94 ± 0.38	-9.51	25.14 ± 0.66	27.35	Rev. F&G	-28.40 ± 0.2	35.20 ± 0.2	296
H-52b	-8.94 ± 0.38	-9.61	25.14 ± 0.66	28.33	Rev. F&G	-39.83 ± 0.72	7.87 ± 2.0	587

Table 4-4: Measured and computed isotopic data

The complexity of reactions increases in flowpath HTU-2. No match could be found by using Tamer´s model for A_0 determination. The revised Fontes & Garnier model for closed system isotope exchange was used instead. Reactions necessary for the inverse model include calcite dissolution and isotopic exchange (2 mmol L^{-1}), dolomite dissolution, sulphate reduction and methanogenesis as well as removal of ammonia (table 4-1). In order to keep the system in balance 3.78 mmol L^{-1} of CO_2 have to be removed from the system. Calculated radiocarbon values match measured values (Δ=0.96 pmC, p= 0.002) as well as $\delta^{13}C_{DIC}$ (Δ=0.57 ‰, p= 0.007) (table 4-4). The calculated flow path between H-32 and H-52 is 295 years.

Because this model suggests the formation of high amounts of methane, which was not observed in the aquifer (T. Behrendt, unpublished data), we ran a second model including more depleted values for TOC. These values were based on PLFA data from Schwab et al. (in prep), who measured ^{14}C activity and $\delta^{13}C$ of the main bacterial biomarker C16:0. Measured vales were -39.83 ± 0.72 ‰ for $\delta^{13}C$ and 7 ± 1 pMC for radiocarbon. Assuming this C source, model-estimated ^{14}C and $\delta^{13}C$ values agree less well with observations (Δ=3.69 pmC, p= < 0.01 and Δ=0.67 ‰, p= < 0.01 for $^{14}C_{DIC}$ and $\delta^{13}C_{DIC}$, respectively), but no methane production is required by the model. The computed radiocarbon age of the water is 587 years.

4.4 Discussion

4.4.1 Groundwater flow

DIC isotopes for the three different groundwater groups reflect both, differences in recharge characteristics as well as the evolution of waters as they flow through the aquifers.

The carbon isotopic composition of DIC of Group 1 waters suggest rapid recharge and minor exchange reactions due to rapid flow. $\delta^{13}C$ values are close to Tamer´s point, typical for fast water infiltration without isotopic exchange between DIC and CO_2 or carbonates in the soil (Han and Plummer, 2013). However, ^{14}C values of Group 1 wells are enriched compared to the preindustrial

atmosphere assumed for Tamer's point soil CO_2 end member (i.e. ^{14}C signature of 100 pmC for coil CO_2). Enrichment of ^{14}C can be caused by isotope exchange between soil CO_2 and DIC in the unsaturated zone (Fontes and Garnier, 1979; Han and Plummer, 2013). However, measured DIC values do not fall on line g in figure 4-6, which would be indicative for isotope exchange under open conditions in the soil. Enrichment of ^{14}C along arrow d in figure 4-6 indicates rather the presence of excess ^{14}C derived from nuclear bomb testing (Gillon et al., 2012). The presence of bomb carbon infers that soil CO_2 in the recharge zone is mainly derived from root respiration and mineralized organic matter in the topsoil (Richter et al., 1999). This is reasonable, because the soil groups in the recharge area of HTL are mainly rather shallow, belonging to Rendzic Leptosol or Cambisol soils, with presumably fast infiltration (Kohlhepp et al., 2016).

Radiocarbon dating of modern groundwater is difficult due to high model input uncertainty (Gillon et al., 2012). Recalculating initial ^{14}C activities of Group 1 wells assuming a Tamer´s like dilution by ^{14}C dead carbonates yields values of 110 pmC, 99 pmC, 120 pmC and 136 pmC for well H-31, H-41, H-51 and H-32, respectively. Initial ^{14}C values indicating predominance of bomb-derived radiocarbon as high as 136 pmC could be interpreted to suggest the time from the groundwater recharge area to the groundwater well in the range of years to decades. However an intense fracturing and karstification in the HTL aquifer with broad fractures, secondary porosity and even karst breccia within- and up to 4km away from the capture area (Kohlhepp et al., 2016), suggest that groundwater flow is more rapid than expected from the age model of this study. The radiocarbon signatures thus indicate variations of ^{14}C in soil CO_2 in the recharge area. For well H-51, there is also indication that ^{14}C values are influenced by mixing of waters of different radiocarbon concentration ((Bethke and Johnson, 2008; Cartwright et al., 2012). This is supported by the increase of SO_4^{2-} and Ca^{2+} concentrations in well H-51, caused most probably by convection of sulphate rich waters from the aquifer system below HTL. Mixing of waters and associated mixing corrosion can also explain the calcite dissolution suggested by NETPATH.

Group 2 waters representing wells H-42 and H-43 in the HTU aquifer complex also fall on the Tamer´s line for $\delta^{13}C$ but not for ^{14}C. ^{14}C values are more depleted than would be expected for a Tamer´s like dilution. Tamer´s model is also proposed by NETPATH to estimate initial ^{14}C in the recharge area, which – because it is lower (averaging 45.51 ± 3.62 pmC, equivalent to 403 ^{14}C years) than the current atmospheric $^{14}CO_2$ values in the year of sampling (~103 pmC) indicate the influence of CO_2 derived from decomposition of older organic matter. Depleted ^{13}C values in Group 2 wells do probably not represent lower flow dynamics and radioactive decay, but turnover of ^{14}C depleted carbon in Group 2 wells.

Isotope values of Group 3 cluster in a very different region than Groups 1 and 2. Enrichment in ^{13}C and depletion in ^{14}C is indicative for calcite dissolution. The best match of calculated and measured values was obtained by using the revised Fontes & Garnier model for isotope exchange between DIC and carbonates to correct for initial ^{14}C in the starting well H-32 (Han and Plummer, 2013). This indicates different recharge patterns or an alternative recharge area as well as enhanced water-rock interactions in this portion of the HTU aquifer complex.

An alternative recharge area for Group 3 wells is probably located in the agricultural area at the foot slope of the sub-catchment, where H-5 wells are situated. This would imply penetration of surface waters through more than 50 meters of low-permeable cap rocks (claystones, marlstones; Erfurt formation and Warburg formation) which is rather unlikely (Kohlhepp et al., 2016).

Both, Group 2 and Group 3 wells have radiocarbon ages of 403 and 296 or 587 years, respectively and are therefore not regarded as modern by NETPATH. Nevertheless, computed ages cannot be distinguished from modern waters within the model uncertainty.

4.4.2 Biogeochemical processes affecting DIC in Group 2 wells.

As indicated by the graphical method, DIC in Group 2 wells is influenced by oxidation of organic matter. However, that OM oxidation has to be performed under anoxic conditions present in these waters. According to the NETPATH

model, OM oxidation can be linked to iron and sulphate reduction. Both processes can also result in dissolution of carbonates and add OM-derived DIC according to:

$$C_6H_{12}O_6 + 24Fe^{3+} + 12H_2O \rightarrow 6HCO_3^- + 24Fe^{2+} + 30H^+ \quad (12)$$

and

$$CH_2O + SO_4^{2-} \rightarrow H_2S + 2HCO_3^- \quad (13)$$

$$H_2S + CaCO_3 \rightarrow HCO_3^- + Ca^{2+} + HS^- \quad (14)$$

A good correlation between sulphate concentrations and $\delta^{13}C$ of DIC supports an influence of sulphate reduction on DIC (figure 7). Moreover, *Desulfosporinus,* an endospore-forming strictly anaeorobic sulfate-reducing bacteria (Stackebrandt et al., 1997), was detected in H-43 (Group 2 well).

With the NETPATH model, the addition of oxidized OM with isotopic signatures identical to measured TOC matched observed DIC isotopic values reasonably well (table 4). This suggests that the carbon source is depleted in $\delta^{13}C$, with ^{14}C close to DIC values, i.e. older organic matter.

Autotrophic organisms can provide carbon that is characterized by the above-mentioned features. Chemolithoautotrophic microorganisms have been recognized to be important components of aquifer foodwebs, if sufficient electron donors are available (Alfreider et al., 2012; Hutchins et al., 2016; Kellermann et al., 2012).Chemolithoautotrophs can use six different metabolic pathways to fix DIC, of which the Calvin-Benson Cycle and the acetyl-CoA pathway are the two most important ones (Fuchs, 2011). Herrmann et al. (2015) found that up to 17 % of the microbial community in well H-43 has the potential for chemolithoautotrophic CO2 fixation via the Calvin-Benson Cycle. The Calvin Benson Cycle can function under anaerobic and aerobic conditions, whereas microorganisms using the acetyl-CoA cycle are restricted to anaerobic conditions (Berg, 2011; Fuchs, 2011). Both pathways fractionate against 13C

and may generate carbon that has 14C values

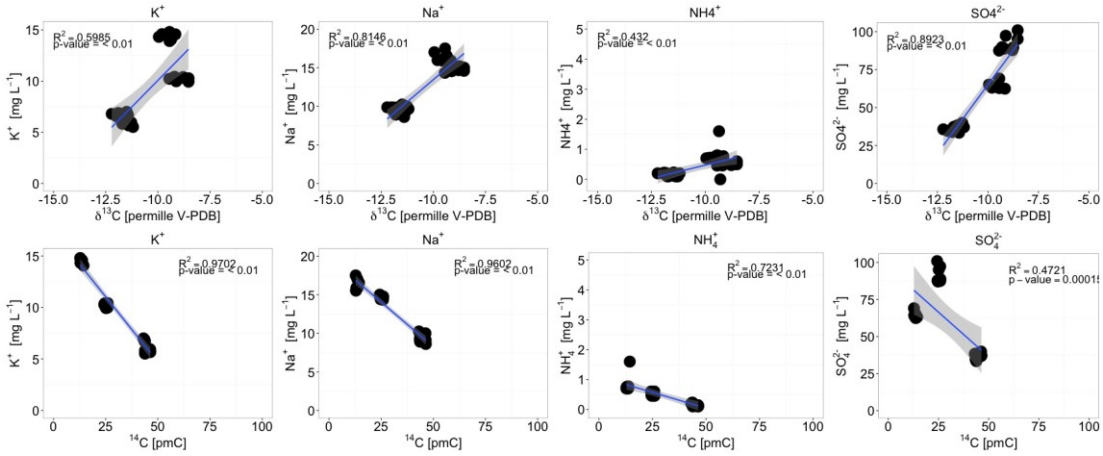

Figure 4-9: Correlations between elemental concentration and isotope values of DIC in group 2 and 3 wells

and measured $\delta^{13}C$ and ^{14}C values.close to DIC. Furthermore, autotrophic groups which oxidize iron under microaerophilic conditions (Gallionellaceae (Emerson et al., 2010)) were identified in Group 2 wells ; as well as autotrophic hydrogenoclastic methanogens.

According to mass fluxes calculated with NETPATH (0.77 mmol L^{-1}) C derived from oxidation of ^{13}C and ^{14}C depleted organic carbon would constitute 11 % of the DIC pool.

4.4.3 Biogeochemical processes affecting Group 3 wells

The Han-Plummer plot suggests that DIC in Group 3 wells is influenced by water rock interactions, including calcite and dolomite dissolution as well as isotopic exchange between DIC and calcite (Han and Plummer, 2016; Wigley, 1976).

Quantification of these fluxes by NETPATH estimates 1.57 mmol L^{-1} of calcite and 0.18 mmol L^{-1} of dolomite dissolution, with exchange of 2 mmol L^{-1} of carbon between DIC and carbonate rock.

Calcite dissolution/precipitation can be triggered by cation exchange of Ca^{2+} with Na^{+} and K^{+} or NH_4^{+} on clay minerals or organic matter (Coetsiers and Walraevens, 2009; van Breukelen et al., 2004). Decreasing Ca^{2+} concentrations can cause changes in $CaCO_3$ saturation indices and result in enhanced calcite

dissolution. The impact of cation exchange on DIC isotopic values in Group 3 wells is supported by good correlations with K^+, Na^+ and NH_4^+ concentrations in HTU (figure 7). Ammonia and K input into Group 3 wells could also be an indicator for surface derived nutrients from agricultural fields and highlight the potential impact of land use change on apparent groundwater ages.

In addition to abiotic exchanges with carbonate rocks, biotic processes also influence isotopic signatures of DIC in Group 3 wells. This is suggested by the Han-Plummer plot, as $\delta\,^{13}C$ values are more depleted than would be expected for solely isotopic exchange (figure 6a). NETPATH modelling suggests either involvement of methane or oxidation of organic matter that is depleted in $\delta\,^{13}C$ and ^{14}C compared to water equilibrated with surface soil CO_2 (Table 3).

Depending on isotopic input parameters, NETPATH indicates that either 1.33 mmol L^{-1} of methane or 1.82 mmol L^{-1} of ^{14}C depleted OM have to be oxidized to explain DIC isotopic signatures. However methane concentrations in Group 2 and 3 wells are low compared to what has been observed in other methanogenic aquifers, with values of ~ 0.1 µmol L^{-1} (T. Behrendt, unpublished data). Hence, oxidation of ^{13}C and ^{14}C depleted organic carbon seems a more plausible explanation, one that is further supported by the molecular data. Indeed, Bacteria of the family Ignavibacteriaceae, a major group in Group 3 wells, are chemoorganotrophs growing on carbohydrate fermentation (Iino et al., 2010).

A major carbon source that might provide ^{14}C depleted OM can be sedimentary organic matter (Aravena and Wassenaar, 1993; Coetsiers and Walraevens, 2009). Sedimentary organic matter might be released by carbonate dissolution, or be derived from marlstones that are interbedded with the fractured carbonate rocks (Kohlhepp et al., 2016). Bathyarchaeota, which are the second abundant archaeal group in Group 3 wells, are especially metabolically versatile and able to use different carbon sources (Lazar et al., 2016b).

^{13}C and ^{14}C depleted C for heterotrophic growth can also be (as in Group 2 wells) derived from chemolithoautotrophic microorganisms (Hutchins et al., 2016). Facultative chemolithoautotrophic bacteria like ammonia-oxidizing Nitrospirae or the thiosulfate-reducing *Sulfuritalea* (Kojima and Fukui, 2011) and the sulfur-oxidizing *Sulfuricurvum* (Kodama and Watanabe, 2004) were detected in well H-

52; as well as chemolithoauotrophic ammonia-oxidizing Thaumarcheota (Berg et al., 2014) which constitute 90 % of total archaeal reads.

An additional source of ^{14}C depleted carbon could also be input of old C from the soil. The NETPATH models predict distinct recharge areas for group 3 wells compared to group 2 and 1, and soils in areas recharging Group 3 wells may also have slower water infiltration (Küsel et al., 2016). During slow percolation of water through the soil, extensive recycling (either through sorption-desorption or fixation and oxidation in microbial C) might lead to input of DOC from subsoil horizons that is much more depleted in ^{14}C than in the shallow soils of the recharge area of Group 1 and 2 wells (Schiff et al., 1997). Also anthropogenic influences like land use change can lead to mobilization of old, ^{14}C depleted carbon from soils (Kalbitz et al., 2000).

Overall, while there is a range of possible sources for ^{13}C and ^{14}C depleted carbon that might contribute to the observed $^{13}C_{DIC}$ shift, it is clear that old organic matter is being oxidized to support a significant fraction of the microbial food web in Group 3 waters.

Variable carbon utilization by microorganisms has been shown already for deep surface communities (Simkus et al., 2016). Our data indicate similarly, a variable substrate utilization in shallow , surface near aquifers.

The timescales, on which biotic and abiotic processes act that influence DIC isotopic composition, remains uncertain. Radiocarbon ages calculated by the models have high uncertainties. Thus it is not possible to distinguish Group 3 water from modern waters. Water rock interactions like calcite precipitation or dissolution have been shown to act very rapidly (Matter et al., 2016; Miller et al., 2016), which is also supported by our data. However, without independent information (e.g. from hydrogeologic modelling) on water fluxes through the aquifers, we cannot estimate rates of transformation associated with changes in water chemistry between wells.

According to the NETPATH model, 1.82 mmol L^{-1} of OM were oxidized in Group 3 wells, which would account for more than 28 % of the total DIC pool.

4.5 Conclusions

The evaluation of DIC carbon isotopes by graphical and numerical methods revealed strikingly different abiotic and biotic processes influencing the DIC isotopic composition of groundwaters in our detailed study. The combination of the Han-Plummer plot and geochemical modelling yielded consistent results and allowed us to identify and quantify the different processes contributing to these large variations in DIC within a single sub-catchment.

As the residence time of groundwater in the aquifer assemblages is expected to be rather short, we attribute the observed differences in DIC in variations in recharge areas and subsequent biogeochemical processes. In HTL wells, the recharge waters (largely in forest) were equilibrated with CO_2 dominated by post-bomb C fixed from the atmosphere in the last years to decades. Subsequent evolution was largely dominated by abiotic processes, including carbonate dissolution and mixing with other waters.

In HTU wells, DIC isotopes reflected oxidation of organic matter from different sources in addition to abiotic water-rock interactions. Microbial communities in HTU wells are capable of using a range of C sources with very old ^{14}C concentrations (i.e. <50pmC), including inorganic carbon fixed through chemolithoautotrophy and/or heterotrophic oxidation of sedimentary organic matter. This metabolic versatility is also supported by bacterial and archeal DNA data.

As both aquifers studied are shallow and situated within a dynamic fractured setting, both biotic and abiotic processes appear to act on short timescales.

4.6 Acknowledgements

We thank Heiko Minkmar and Robert Lehmann for help with water sampling and on site logistics. We kindly acknowledge Petra Linke and Axel Steinhof and Heike Machts for measuring $\delta^{13}C$ and ^{14}C samples. Further, we would like to thank Christian Seifert and Sandy Laschke for assistance in sample preparation

for isotope analyses. We also kindly acknowledge Xiaomei Xu from the University of California Irvine for introduction in radiocarbon measurements of DIC. The study has been conducted in the Flux 3 project of the Collaborative Research Center AquaDiva. The work has been funded by the German Research Foundation (Deutsche Forschungsgemeinschaft, DFG) CRC 1076 "AquaDiva". MN was funded by the International Max-Planck Research School for Global Biogeochemical Cycles (IMPRS gBGC).

5 Concluding discussion

A common theme of the work conducted in this thesis is to quantify the role of CO_2 fixation in belowground carbon cycling. One objective was to demonstrate whether microbial CO_2 fixation contributes to soil organic matter formation. The origin of soil organic matter and factors leading to its stabilization are intensively discussed (Ekschmitt et al., 2008; Schmidt et al., 2011). Recently, (Gleixner, 2013) and (Miltner et al., 2012) suggested that organic constituents derived from microorganisms, like cell fragments, constitute the majority of soil organic matter. A major goal of this thesis was to explore the importance of CO_2 fixation in a number of different soils using C isotopes as tracers.

The unique setting of the mofette site provided an ideal opportunity to test the importance of CO_2 fixation as a source of organic matter, because the geogenic CO_2 exhaled at the mofette provided a naturally occurring tracer that allowed microbially-fixed (geogenic) to be distinguished from plant-fixed (atmospheric) carbon. Geochemical parameters, inlcuding low C/N ratios, already suggested that a large fraction of the carbon stored within the mofette soils might be derived from microorganisms (Wallander et al., 2003). Also the high number of 16S rRNA genes, which was higher than what is usually known from soils (Fierer et al., 2005), strongly indicated that microbially generated carbon is a strong contributor to the overall high organic matter stocks in the mofette soil. The combination of ^{14}C and ^{13}C isotopic tracers was a powerful tool to quantify proportions of plant and microbially derived carbon and this study was one of the few, which took advantage of such a dual isotope approach (Torn et al., 2013). This was particularly useful in the mofette setting, because the exhaling gas was enriched in ^{13}C and free of radiocarbon. Both isotopes could therefore be used for isotope mass balances. The study provides direct evidence that microbially derived carbon can constitute a high proportion of soil organic matter in a natural system.

Both isotopes also suggested that microbial CO_2 fixation plays a significant role in carbon cycling within the mofette and a high proportion of the microbial carbon was derived from CO_2 fixing microorganisms. This is reasonable, since the microbial community structure is adapted to high CO_2 concentrations and CO_2 fixation might be a favourable metabolic pathway in these ecosystems

(Beulig et al., 2014; Beulig et al., 2016). The isotope labelling experiment also demonstrated a higher activity of CO_2 fixing microorganisms in these soils compared to what was reported in soils from other studies (Liu and Conrad, 2011; Miltner et al., 2005; Wu et al., 2015b), potentially reflecting the adaptation of the microbial community to high CO_2 concentrations and a higher substrate availability. Beulig et al. (2016) showed that CO_2 fixation rates in mofette soils increased with increasing CO_2 concentrations.

The combination of rate measurements together with natural abundance isotope measurements and the quantification of functional genes was a powerful tool to elucidate the significance of CO_2 fixation for biogeochemical cycling in the mofette soils. The good correlation between functional genes and CO_2 uptake rates proved that the Calvin Benson cycle was one of the main metabolic cycles within the mofette soils which is in accordance with other studies (Wu et al., 2014; Yuan et al., 2012). Further, Beulig et al. (2016) showed that also the acetyl-CoA pathway plays a significant role within the mofette. The acetyl-CoA pathway has not yet been considered as an important pathway for CO_2 to be incorporated into soil organic matter, although it is energetically more favoured under anoxic conditions than the Calvin Benson cycle (Berg, 2011). Thus, more emphasis should be put on investigating the importance of the acetyl CoA pathway in soils, especially in poorly drained or wetland ecosystems (Ye et al., 2014).

The information about the main CO_2 fixation pathway is key for assessing the amount of organic matter derived from CO_2 fixation. Quantification of carbon derived from CO_2 fixation was already done in other studies, but solely on a lab incubation basis (Miltner et al., 2005; Wu et al., 2015b; Yuan et al., 2012). The present study not only allowed us to determine the amount of carbon derived from CO_2 fixation using a field-based approach in a natural system, but also permitted us to compare long-term soil processes to laboratory rate estimates.

Mofette soils are, irrespective the very high CO_2 concentrations in the soil atmosphere, natural analogues for wetland soils. They have a high carbon content ranging from 5 % to 25 % and are permanently depleted in oxygen, leading to anaerobic decomposition processes (Beulig et al., 2016). The finding that CO_2 fixation is a major pathway for incorporating carbon into soil organic

matter and that influences carbon isotopic signatures of soil organic matter, might therefore also have implications for other soils and ecosystems. Peat deposits are a crucial part of the global carbon cycle and store a significant amount of global soil carbon (Limpens et al., 2008). They provide excellent climate archives, whereas radiocarbon dating allows assessing former responses of peat to climate change (Blaauw and Christen, 2005). Recycling of CO_2 is a process that has been proposed to bias radiocarbon age dating of peat deposits. Kilian et al. (1995) suggested that recycling is related to oxidation of methane formed from old organic matter and fixation of this methane derived CO_2 by mycorrhizal fungi. However, there was no evidence from biomarker analyses for methanotrophic or fungal CO_2 uptake (Pancost et al., 2000). This thesis demonstrated that recycling of CO_2 can be accomplished by other organisms than methanotrophs or fungi, namely CO_2 fixing autotrophic microorganisms. Interestingly Pancost et al. (2000) estimated that around 20% of carbon in peat deposits can be derived from recycling of CO_2. This amount is similar to what was determined for the mofette soil and is a strong indicator for analogous processes in peat and mofette soils.

Another important finding from chapter two is the rate of CO_2 fixation measured in the reference soils. The high uptake in the topsoil emphasises the importance of CO_2 fixation for organic rich soils, since both reference soils used were characterized by high organic carbon contents in the first five centimetres. High uptake rates in organic rich soils were also observed by Yuan et al. (2012) and Wu et al. (2014), who inferred that phototrophic microorganisms were responsible. However, Wu et al. (2014) could only detect small or insignificant CO_2 uptake at lower depths, where carbon concentrations were much lower. In contrast, this thesis showed that microbial CO_2 fixation remains a relevant process for microbial communities in the subsoil, because uptake rates do not decrease with depth, if they are normalized to carbon content of the soil. Since microbial carbon has been generally suggested as an important source of organic matter in the subsoil (Rumpel and Kogel-Knabner, 2011), our data implies that also CO_2 fixing microbes can contribute to subsoil carbon cycling, which is the link to chapter 3.

One main finding in chapter 3 was the isotopic relationship between soil microbial biomass and soil organic matter. The gradual enrichment with depth highlights the importance of soil microbial biomass for organic matter formation, especially in the subsoil. A high contribution of microbial-derived carbon to organic matter in tropical forest soils has already been suggested by Rillig et al. (2001). The isotopic data presented in chapter 3 supports the concept that soil organic matter, especially in the deeper soil is mainly derived from microbial carbon (Kogel-Knabner, 2002; Miltner et al., 2012; Simpson et al., 2007)

Measured CO_2 uptake rates demonstrated that CO_2 fixing microorganisms are also active within tropical rainforest soils. The main pathway responsible for measured uptake rates at the surface was heterotrophic CO_2 fixation. Phototrophic microorganisms might also play a role under natural conditions, because they were detected by the 16S rRNA assay. However, they have likely not contributed to our measured uptake rates, as the samples were incubated in the dark.

Tropical rainforest soils show typically a strong enrichment in $\delta^{13}C$ with depth (Guillaume et al., 2015; Krull et al., 2002), which was also true for the investigated soils. Ehleringer et al. (2000) suggested that carboxylation processes might be responsible for the observed shift, if around 5 % of microbial biomass would be derived from CO_2 fixation. However, the measured CO_2 uptake rates revealed that the amount of fixed carbon was not sufficient and after a 90-day incubation the amount of fixed carbon was below 5 % in all soils. Therefore, heterotrophic CO_2 fixation is likely not the main controlling factor responsible for the enrichment of microbial biomass and soil organic matter with depth. However, the measured uptake rates are in a range that can cause a shift of radiocarbon signatures in the subsoil. Organic matter in the subsoil is an important part of soil carbon stocks (Rumpel and Kogel-Knabner, 2011). Similar to carbon concentrations, radiocarbon concentrations decrease with depth and turnover times of organic carbon become substantially larger than in the topsoil (Trumbore et al., 1995). Nevertheless, radiocarbon concentrations never become zero, even in soils that inherit some sedimentary carbon, which suggests a small contribution of a fast cycling modern radiocarbon pool at depth (Telles

et al., 2003; Torn et al., 2013). The study in chapter 3 emphasises that microbial CO_2 fixation can be a potential pathway for atmospheric radiocarbon into the subsoil, because CO_2 in the soil atmosphere has radiocarbon concentrations close to atmospheric values (Trumbore et al., 1995), which was also true in the investigated soils. Turnover times of carbon below 50 cm were on average on the timescale of millennia, whereas CO_2 fixation rates could potentially cycle carbon within timescales of centuries at this depth. Thus, if only small amounts of carbon fixed from CO_2 can get stabilized in the soil, CO_2 fixation might be a relevant process that contributes to shaping of $\Delta^{14}C$ depth profiles (Schrumpf et al., 2013). CO_2 can also diffuse into aggregates or the clay fraction in the deeper soil and might explain occurrence and turnover of carbon in soil fractions where recent plant carbon or dissolved constituents have no access (Kaiser and Kalbitz, 2012). The thesis highlights therefore that microbial CO_2 fixation might be a relevant process that contributes to belowground carbon cycling and that might influence radiocarbon depth profiles.

Another major finding of this thesis is that CO_2 fixation contributes to carbon cycling within aquifer ecosystems, where input of photosynthetically fixed carbon decreases with distance from the surface. DIC has been shown to be an integrative signal for carbon turnover in aquifers (Marfia et al., 2004). Measuring ^{13}C and ^{14}C of DIC is a powerful tool to elucidate different carbon pools and their contribution to carbon cycling as well as to distinguish between microbial and inorganic processes within groundwater systems (Han and Plummer, 2016). The study in chapter four combined for the first time a set of methods that allowed integrating water chemistry, isotopic data of different carbon compounds and microbiological data in order to get a comprehensive view about carbon turnover in groundwater ecosystems. The graphical method proposed by Han et al. (2012) allowed qualitative identification of the main processes that contributed to carbon turnover in the different aquifers assemblages, and distinguishing between different groups of groundwater, which was consistent with quantitative results obtained with NETPATH. Surprisingly, both aquifer assemblages showed strong variations in their geochemical, microbial and isotopic composition on a small spatial scale, which was the result of inorganic and organic processes acting in the system. Carbon

isotopes of DIC in combination with the modelling program NETPATH were suitable tools to elucidate sources contributing significantly to carbon cycling within the aquifer.

The finding that recycling of carbon derived from chemolithoautotrophic microorganisms is a significant carbon source within the aquifer is in line with recent information from other aquifer systems, where chemolithoautotrophes have been shown to contribute to aquifer foodwebs (Hutchins et al., 2016) and to be responsible for cycling of different elemental cycles (Jewell et al., 2016). The potential of chemolithoautotrophic microorganisms in aquifer systems has already been demonstrated e.g. by Alfreider et al. (2003), who investigated the diversity of cbbL genes in two groundwater systems, by Kellermann et al. (2012), who determined the potential for microbial CO_2 fixation in a tar oil contaminated aquifer by detection of the functional marker genes cbbL and cbbM and by Herrmann et al. (2015), who also found a high potential of CO_2 fixation via the Calvin Benson Cycle linked to the cycling of sulphur and nitrogen compounds. Compared to the other studies, this thesis provides a quantitative approach for determining how important CO_2 fixation is compared to other carbon sources like surface derived DOC or sedimentary organic matter, which are usually regarded as main source of carbon in aquifer systems (Aravena and Wassenaar, 1993; Mailloux et al., 2013). The study also showed that CO_2 fixation is mainly relevant in the anoxic parts of the aquifer, which is most probably related to the availability of reduced compounds for chemolithoautotrophic growth.

However, the study in chapter four also revealed that other sources, in particular sedimentary organic matter played an important role in the aquifer food web. This highlights that subsurface communities are not only dependent on surface related OM input (Mailloux et al., 2013), but that also subsurface derived OM can fuel microbial communities and sustain important biogeochemical cycles in shallow aquifer systems.

Utilization of different carbon sources has already been demonstrated for other groundwater systems (Aravena et al., 1995; Simkus et al., 2016). However, this thesis shows for the first time, that the microbial community of a shallow and dynamic limestone/marlstone and karst system can also use a set of different

carbon sources. Further it shows that both, biotic and abiotic processes affecting DIC act on short timescales.

Overall, this thesis shows that CO_2 fixation is a significant process contributing to belowground carbon cycling in a range of different natural settings. The activity of CO_2 fixing microorganisms is reflected in carbon isotopic ratios of soil organic matter and dissolved inorganic carbon in aquifer ecosystems.

In the high CO_2 environment of the mofette soils, CO_2 fixation contributed significantly to soil organic matter and caused a shift in carbon isotopic signatures, which in turn allowed quantifying its contribution.

CO_2 fixation also occurs in tropical rainforest soils, where the majority of the C fixed is due to heterotrophic CO_2 fixation in surface soils. Still to be done is to explore what microbial processes are responsible for CO_2 fixation in deeper soils. The amount of fixed CO_2 is not sufficient to explain enrichment of $\delta^{13}C$ with depth, as proposed by Ehleringer et al. (2000). Nevertheless, it is a process that provides a pathway for atmospheric radiocarbon into the subsoil and might therefore contribute to deviations of radiocarbon signatures of soil organic matter.

CO_2 fixation is also an important part of carbon cycling in aquifer systems, where it is accomplished mainly by chemolithoautotrophic microorganisms, that can act as an OM source for heterotrophic microbes.

6 Outlook

Future research should focus on combining more advanced molecular methods, like metatranscriptomic approaches with quantitative isotopic techniques. This would enhance the overall understanding of which CO_2 fixing pathway is dominating in which ecosystem. This might provide an overall better understanding about the significance of CO_2 fixation for carbon cycling in different ecosystems, especially wetlands. RNA-SIP would be a good approach to prove the importance of heterotrophic vs. autotrophic CO_2 fixation in soils. It is further important to assess the potential of CO_2 fixation in more soils and soil types in order to get a more comprehensive understanding how important this process is is on a global scale and to which extent it can contribute to mitigation of CO_2 from the atmosphere. There are numerous research questions remaining about CO_2 fixation in aquifer systems. So far research focused on few metabolic

pathways, especially the Calvin Benson Cycle. However, as has been shown, CO_2 fixation gets more pronounced under anoxic conditions. However, other, energetically more favourable pathways than the Calvin Benson cycle, like the acetyl CoA pathway should be used under these conditions, yet little is known about the role of this pathway for belowground carbon cycling. Metagenomic and metatranscriptomic approaches would help to overcome this research gap. Another crucial point is to determine CO_2 uptake rates and the activity of CO_2 fixing microbes in aquifers. So far there are no rate data from these environments, although we know CO_2 fixation can be an important process. It would be important to compare CO_2 fixation e.g. with oxidation of organic matter in aquifer systems to assess better the role of CO_2 fixation within the carbon cycle of aquifers.

7 Summary

Understanding belowground carbon cycling processes is of huge importance, because the terrestrial subsurface, especially soils, are a huge carbon reservoir, which in in exchange with the atmosphere. Soil microorganisms have recently been identified to contribute to soil organic matter formation. Their biomass gets continuously recycled and can be stabilized in the soil. Microbial CO_2 fixation is a process that can contribute to carbon recycling by assimilating respired CO_2 and converting it to organic molecules. Microbial CO_2 fixation has been demonstrated to act in soils and groundwater, however, little is known about its influence on carbon isotopic signatures of organic matter. Carbon isotopes of soil organic matter or dissolved inorganic carbon are important parameters that help to determine the cycling and residence time of carbon within the subsurface. The utilization of CO_2, its conversion into organic matter and its subsequent recycling can cause shifts in the isotopic composition of organic and inorganic carbon in soils or aquifers, because microbial CO_2 fixation is either accompanied with enzymatic fractionation processes or the assimilated CO_2 has another isotopic signature than other carbon sources. Microbial CO_2 fixation is therefore a little considered part of the belowground carbon cycle that might be responsible for shifts in carbon isotopic signatures.

The aim of this study is to use isotopic techniques in combination with molecular approaches in order to:

I) Prove the activity of CO_2 fixation along soil depth profiles.

II) To assess the potential of CO_2 fixation to contribute to soil organic matter formation.

III) To prove, if CO_2 fixation has the potential to alter isotope signatures of soil organic matter.

IV) To determine to which extent chemolithoautotrophic microorganisms contribute to carbon cycling in groundwater systems.

In chapter two, soils that were influenced by geogenic CO_2, so called mofettes, were investigated. The geogenic CO_2 was used as a naturally occurring tracer which allowed to distinguish plant carbon from microbially derived carbon. This was possible because the geogenic CO_2 was enriched in ^{13}C and depleted in ^{14}C compared to the atmosphere. Additionally, $^{13}CO_2$ labelling experiments were

conducted and functional genes encoding for RubisCO were quantified. The results showed that CO_2 fixation took place along the whole soil profile and uptake correlated with functional genes as well as deviations of isotope values of soil organic matter. This Information was used to assess the contribution of microbial CO_2 fixation to soil organic matter by isotope mass balances. Based on isotope mass balances, carbon derived from CO_2 fixation constituted 8 to 24 % of bulk soil carbon in the mofettes. The findings have implications for radiocarbon dating of peat deposits, where microbial CO_2 fixation might be responsible for reservoir effects due to recycling of CO_2.

In chapter three, tropical rainforest soils were investigated for their potential to fix CO_2. Tropical rainforest soils show a distinct enrichment of $\delta^{13}C$ with depth, which was hypothesised to be the result of heterotrophic carboxylation processes. Several pits were sampled up to 1 meter depth and $^{13}CO_2$ labelling experiments were conducted. Additionally, carbon isotopic signatures of microbial biomass, bulk soil organic matter as well as geochemical parameters were determined. The results showed that microbial biomass $\delta^{13}C$ values exhibited the same depth trend than bulk soil organic matter, highlighting the strong interrelationship between these two carbon pools.

CO_2 fixation occurred throughout the soil profile, however, the amount of fixed CO_2 was not sufficient to explain the shifts in $\delta^{13}C$ with depth. Nevertheless, CO_2 fixation can be a pathway that provides atmospheric radiocarbon to organic matter in subsoil horizons, because CO_2 in the soil pore space has radiocarbon values close to atmospheric signatures.

Chapter four investigates which biotic and abiotic factors influence the carbon isotopic signature of dissolved inorganic carbon. Special emphasis was put on determining the role of chemolithoautotrophic microorganisms for carbon cycling within two aquifer assemblages with different physicochemical properties. The study included isotopic measurements of DIC, DOC and POC. Further, a novel graphical evaluation method for DIC isotopes as well as geochemical modelling was applied, in order to elucidate processes that affect water chemistry and carbon isotopes within the aquifers. The results showed that both aquifer assemblages have dramatic differences in the biogeochemical evolution of their waters. Depletion of ^{14}C and ^{13}C in the upper aquifer over what

is expected from establishing equilibrium with carbonates results from a number of biotic and abiotic processes, including oxidation of ^{14}C depleted recycled microbial carbon derived from CO_2 fixation and sedimentary organic matter as well as water rock interactions. This proves utilization of different carbon sources, including autotrophic utilization of DIC as well as heterotrophic utilization of sedimentary organic carbon, within a shallow and dynamic aquifer system.

Overall this thesis shows that microbial CO_2 fixation is a ubiquitous process that contributes to carbon cycling within the subsurface and influences carbon isotopic signatures of organic matter.

8 Zusammenfassung

Zusammenhänge von Kohlenstoffkreisläufen im Untergrund zu verstehen ist von großer Bedeutung, da der terrestrische Untergrund, insbesondere bodenorganisches Material, ein großes Kohlenstoffreservoir darstellt, dass im permanenten Austausch mit der Atmosphäre steht. Aktuelle Studien zeigen, dass Bodenmikroorganismen eine wichtige Quelle für bodenorganisches Material sind. Ihre Biomasse wird ständig recycelt und kann im Boden stabilisiert werden. Mikrobielle CO_2 Fixierung ist ein Prozess, der zum Recycling von mikrobiellem Kohlenstoff beitragen kann, da respiriertes CO_2 assimiliert und in Organik umgewandelt wird. Obwohl mikrobielle CO_2 Fixierung in Böden und Grundwässern nachgewiesen wurde, ist wenig über deren Einfluss auf die Isotopensignatur von Kohlenstoffverbindungen bekannt. Kohlenstoffisotope von bodenorganischem Material oder gelöstem anorganischem Kohlenstoff sind wichtige Parameter um den Umsatz und die Verweildauer von Kohlenstoff im Untergrund zu bestimmen. Die Umwandlung von CO_2 in organisches Material sowie anschließendes Recycling kann Abweichungen in Kohlenstoff Isotopensignaturen verursachen, da mikrobielle CO_2 Fixierung zum einen mit enzymatischen Fraktionierungsprozessen einhergeht, zum anderen kann das assimilierte CO_2 eine unterschiedliche isotopen Signatur haben als andere Kohlenstoffquellen. Mikrobielle CO_2 Fixierung ist somit ein wenig beachteter Prozess, der für Änderungen in der Kohlenstoff-Isotopensignatur verantwortlich sein kann.

Diese Arbeit soll mithilfe von Isotopen Techniken und molekularen Methoden folgende Ziele erreichen:

I) Der Nachweis von CO_2 Fixierung in Bodentiefenprofilen
II) Der Nachweis, dass CO_2 Fixierung zur Bildung von bodenorganischem Material beiträgt
III) Prüfen, ob CO_2 Fixierung zu systematischen Änderungen des Isotopenverhältnisses von bodenorganischem Material beiträgt
IV) Abzuschätzen, inwieweit chemolithoautotrophe Mikroorganismen zum Kohlenstoffumsatz in Grundwasserleitern beitragen und isotopen Signaturen von gelöstem anorganischen Kohlenstoff beeinflussen.

In Kapitel zwei der Arbeit wurden Böden, die von geogenem CO_2 beeinflusst sind, so genannte Mofetten, untersucht. Das geogene CO_2 wurde als natürlich vorkommendes Markierungsmittel verwendet, um von Pflanzen abstammenden Kohlenstoff von mikrobiell gebildetem Kohlenstoff zu unterscheiden. Das war möglich, da das geogene CO_2 im Vergleich zur Atmosphäre angereichert in ^{13}C und abgereichert im Radiokarbon war. Zusätzlich wurden Experimente mit $^{13}CO_2$ Label durchgeführt sowie funktionelle Gene, die für RubisCO, das Schlüsselenzym des Calvin Benson Zyklus, enkodieren, quantifiziert.

Die Ergebnisse zeigten, dass CO_2 Fixierung im gesamten Bodenprofil stattfand und dass die Aufnahme mit den funktionellen Genen sowie Abweichungen in der Isotopensignatur des bodenorganischen Materials korrelierte. Diese Information wurde verwendet um den Anteil des von mikrobieller CO_2 Fixierung stammenden Kohlenstoffs mithilfe von Isotopenmassenbilanzen zu bestimmen. Der Anteil wurde auf 8 bis 27 % des gesamten Kohlenstoffs in den Mofetten berechnet. Die Ergebnisse lassen Schlussfolgerungen für Radiokarbon Datierungen in Mooren zu, wo mikrobielle CO_2 Fixierung für Reservoir Effekte aufgrund von CO_2 Recycling verantwortlich sein kann.

In Kapitel drei wurden tropische Regenwald Böden auf Ihr Potenzial CO_2 zu fixieren untersucht. Tropische Regenwald Böden zeigen eine klare Anreicherung im $\delta^{13}C$ Wert mit der Tiefe auf, wobei vermutet wurde, dass heterotrophe Karboxylasereaktionen dafür verantwortlich sein könnten. Mehrere Bodengruben wurden bis zu einem Meter tief beprobt und $^{13}CO_2$ labelling Experimente wurden durchgeführt. Zusätzlich wurden die Isotopensignatur der mikrobiellen Biomasse, des bodenorganischen Materials sowie geochemische Parameter der Böden bestimmt. Die Ergebnisse zeigten, dass die mikrobielle Biomasse den gleichen Tiefentrend in seiner ^{13}C Signatur aufwies wie das bodenorganische Material, was einen engen Zusammenhang zwischen mikrobieller Biomasse und bodenorganischem Material aufzeigt. CO_2 Fixierung konnte im gesamten Bodenprofil gemessen werden. Die Menge an fixiertem CO_2 war allerdings nicht ausreichend, um Verschiebungen im $\delta^{13}C$ Wert mit der Tiefe zu erklären. Trotzdem erwies sich CO_2 Fixierung als potenzieller Prozess, der einen Pfad von atmosphärischem CO_2 in den Unterboden ermöglicht, da CO_2

im Unterboden durch den Beitrag von Wurzelatmung atmosphärische Radiokarbonsignaturen aufweist.

In Kapitel vier wird untersucht, welche biotischen und abiotischen Faktoren die isotopen Signatur des gelösten anorganischen Kohlenstoffs in Grundwasserleitern beeinflussen. Ein Schwerpunkt lag auf der Untersuchung, inwieweit chemolithoautotrophe Mikroorganismen am Kohlenstoffumsatz in zwei sich in Ihren physikochemischen Eigenschaften unterscheidenden Grundwasserleitern beteiligt sind. Die Studie beinhaltete Messungen von gelöstem anorganischem und organischem sowie partikulärem Kohlenstoff. Ferner wurde eine neue graphische Methode für die Auswertung der DIC Isotopie angewandt und mit geochemischer Modellierung verknüpft. Die Ergebnisse zeigten, dass beide Aquifer Verbünde dramatische Unterschiede in ihrer geochemischen Entwicklung aufwiesen. Die Abreicherung von ^{14}C und ^{13}C jenseits von Werten, die über eine reine Gleichgewichtseinstellung mit Kalziumkarbonat hinauslaufen, war auf eine Vielzahl von biotischen und abiotischen Faktoren zurückzuführen. Faktoren waren u.a. die Oxidation von ^{14}C verarmtem Kohlenstoff, der von CO_2 Fixierung abstammt, von sedimentärem Kohlenstoff sowie Wasser - Gesteins Interaktionen. Somit konnte die Nutzung unterschiedlicher Kohlenstoff Quellen, wie gelöstem anorganischem und sedimentärem Kohlenstoff, in einem dynamischen, oberflächennahen Aquifersystem nachgewiesen werden.

Insgesamt wurde in der vorliegenden Arbeit gezeigt, dass CO_2 Fixierung ein signifikanter Prozess im unterirdischen Kohlenstoffkreislauf ist, der Verschiebungen in der Isotopensignatur von Kohlenstoffverbindungen verursachen kann.

9 Bibliography

1. Aeschbach-Hertig, W., Gleeson, T., 2012. Regional strategies for the accelerating global problem of groundwater depletion. Nature Geoscience 5, 853-861.
2. Akob, D.M., Küsel, K., 2011. Where microorganisms meet rocks in the Earth's Critical Zone. Biogeosciences 8, 3531-3543.
3. Alewell, C., Giesler, R., Klaminder, J., Leifeld, J., Rollog, M., 2011. Stable carbon isotopes as indicators for environmental change in palsa peats. Biogeosciences 8, 1769-1778.
4. Alfreider, A., Schirmer, M., Vogt, C., 2012. Diversity and expression of different forms of RubisCO genes in polluted groundwater under different redox conditions. FEMS Microbiology Ecology 79, 649-660.
5. Alfreider, A., Vogt, C., 2012. Genetic Evidence for Bacterial Chemolithoautotrophy Based on the Reductive Tricarboxylic Acid Cycle in Groundwater Systems. Microbes and Environments. 27, 209-214.
6. Alfreider, A., Vogt, C., Geiger-Kaiser, M., Psenner, R., 2009. Distribution and diversity of autotrophic bacteria in groundwater systems based on the analysis of RubisCO genotypes. Systematic and Applied Microbiology 32, 140-150.
7. Alfreider, A., Vogt, C., Hoffmann, D., Babel, W., 2003. Diversity of ribulose-1,5-bisphosphate carboxylase/oxygenase large-subunit genes from groundwater and aquifer microorganisms. Microbial Ecology. 45, 317-328.
8. Amha, Y., Bohne, H., Alsanius, B., 2012. Comparison of physiological and biochemical methods for assessing microbial activity and biomass of peats, Peat: Formation, Uses and Biological Effects, pp. 35-56.
9. Amundson, R., 2001. The carbon budget in soils. Annual Review of Earth and Planetary Sciences 29, 535-562.
10. Andreae, M.O., Acevedo, O.C., Araùjo, A., Artaxo, P., Barbosa, C.G.G., Barbosa, H.M.J., Brito, J., Carbone, S., Chi, X., Cintra, B.B.L., da Silva, N.F., Dias, N.L., Dias-Júnior, C.Q., Ditas, F., Ditz, R., Godoi, A.F.L., Godoi, R.H.M., Heimann, M., Hoffmann, T., Kesselmeier, J., Könemann, T., Krüger, M.L., Lavric, J.V., Manzi, A.O., Lopes, A.P., Martins, D.L., Mikhailov, E.F., Moran-Zuloaga, D., Nelson, B.W., Nölscher, A.C., Santos Nogueira, D., Piedade, M.T.F., Pöhlker, C., Pöschl, U., Quesada, C.A., Rizzo, L.V., Ro, C.U., Ruckteschler, N., Sá, L.D.A., de Oliveira Sá, M., Sales, C.B., dos Santos, R.M.N., Saturno, J., Schöngart, J., Sörgel, M., de Souza, C.M., de Souza, R.A.F., Su, H., Targhetta, N., Tóta, J., Trebs, I., Trumbore, S., van Eijck, A., Walter, D., Wang, Z., Weber, B., Williams, J., Winderlich, J., Wittmann, F., Wolff, S., Yáñez-Serrano, A.M., 2015. The Amazon Tall Tower Observatory (ATTO): overview of pilot measurements on ecosystem ecology, meteorology, trace gases, and aerosols. Atmospheric Chemistry and Physics 15, 10723-10776.

11. Aravena, R., Wassenaar, L.I., 1993. Dissolved Organic-Carbon and Methane in a Regional Confined Aquifer, Southern Ontario, Canada - Carbon-Isotope Evidence for Associated Subsurface Sources. Applied Geochemistry 8, 483-493.
12. Aravena, R., Wassenaar, L.I., Plummer, L.N., 1995. Estimating C-14 Groundwater Ages in a Methanogenic Aquifer. Water Resources Research 31, 2307-2317.
13. Assayag, N., Rivé, K., Ader, M., Jézéquel, D., Agrinier, P., 2006. Improved method for isotopic and quantitative analysis of dissolved inorganic carbon in natural water samples. Rapid Communications in Mass Spectrometry 20, 2243-2251.
14. Badger, M.R., Bek, E.J., 2008. Multiple Rubisco forms in proteobacteria: their functional significance in relation to CO(2) acquisition by the CBB cycle. Journal of Experimental Botany. 59, 1525-1541.
15. Balesdent, J., Mariotti, A., Guillet, B., 1987. Natural C-13 Abundance as a Tracer for Studies of Soil Organic-Matter Dynamics. Soil Biology & Biochemistry 19, 25-30.
16. Barns, S.M., Cain, E.C., Sommerville, L., Kuske, C.R., 2007. Acidobactetia phylum sequences in uranium-contaminated subsurface sediments greatly expand the known diversity within the phylum. Applied and Environmental Microbiology 73, 3113-3116.
17. Barth, J.A.C., Veizer, J., 1999. Carbon cycle in St. Lawrence aquatic ecosystems at Cornwall (Ontario), Canada: Seasonal and spatial variations. Chemical Geology 159, 107-128.
18. Batjes, N.H., Sombroek, W.G., 1997. Possibilities for carbon sequestration in tropical and subtropical soils. Global Change Biology 3, 161-173.
19. Benner, R., Fogel, M.L., Sprague, E.K., Hodson, R.E., 1987. Depletion of 13C in lignin and its implications for stable carbon isotope studies. Nature 329, 708-710.
20. Berg, C., Listmann, L., Vandieken, V., Vogts, A., Jürgens, K., 2014. Chemoautotrophic growth of ammonia-oxidizing Thaumarchaeota enriched from a pelagic redox gradient in the Baltic Sea. Frontiers in Microbiology 5, 786.
21. Berg, I.A., 2011. Ecological Aspects of the Distribution of Different Autotrophic CO2 Fixation Pathways. Applied and Environmental Microbiology 77, 1925-1936.
22. Berg, I.A., Kockelkorn, D., Buckel, W., Fuchs, G., 2007. A 3-hydroxypropionate/4-hydroxybutyrate autotrophic carbon dioxide assimilation pathway in archaea. Science 318, 1782-1786.
23. Berg, I.A., Kockelkorn, D., Ramos-Vera, W.H., Say, R.F., Zarzycki, J., Hugler, M., Alber, B.E., Fuchs, G., 2010a. Autotrophic carbon fixation in archaea. Nature Reviews Microbiology 8, 447-460.

24. Berg, I.A., Ramos-Vera, W.H., Petri, A., Huber, H., Fuchs, G., 2010b. Study of the distribution of autotrophic CO2 fixation cycles in Crenarchaeota. Microbiology-Sgm 156, 256-269.

25. Bernoux, M., Cerri, C.C., Neill, C., de Moraes, J.F.L., 1998. The use of stable carbon isotopes for estimating soil organic matter turnover rates. Geoderma 82, 43-58.

26. Bethke, C.M., Johnson, T.M., 2008. Groundwater age and groundwater age dating. Annual Review of Earth and Planetary Sciences 36, 121-152.

27. Beulig, F., Heuer, V.B., Akob, D.M., Viehweger, B., Elvert, M., Herrmann, M., Hinrichs, K.-U., Küsel, K., 2014. Carbon flow from volcanic CO2 into soil microbial communities of a wetland mofette. ISME Journal.

28. Beulig, F., Urich, T., Nowak, M., Trumbore, S.E., Gleixner, G., Gilfillan, G.D., Fjelland, K.E., Küsel, K., 2016. Altered carbon turnover processes and microbiomes in soils under long-term extremely high CO2 exposure. Nature Microbiology 1, 15025.

29. Biddle, A., Stewart, L., Blanchard, J., Leschine, S., 2013. Untangling the Genetic Basis of Fibrolytic Specialization by Lachnospiraceae and Ruminococcaceae in Diverse Gut Communities. Diversity 5, 627.

30. Blaauw, M., Christen, J.A., 2005. Radiocarbon peat chronologies and environmental change. Journal of the Royal Statistical Society Series C-Applied Statistics 54, 805-816.

31. Bol, R.A., Harkness, D.D., Huang, Y., Howard, D.M., 1999. The influence of soil processes on carbon isotope distribution and turnover in the British uplands. European Journal of Soil Science 50, 41-51.

32. Bräuer, K., Kämpf, H., Koch, U., Strauch, G., 2011. Monthly monitoring of gas and isotope compositions in the free gas phase at degassing locations close to the Novy Kostel focal zone in the western Eger Rift Czech Republic. Chemical Geology 290, 163-176.

33. Cartwright, I., Weaver, T.R., Cendon, D.I., Fifield, L.K., Tweed, S.O., Petrides, B., Swane, I., 2012. Constraining groundwater flow, residence times, inter-aquifer mixing, and aquifer properties using environmental isotopes in the southeast Murray Basin, Australia. Applied Geochemistry 27, 1698-1709.

34. Chadwick, K.D., Asner, G.P., 2016. Tropical soil nutrient distributions determined by biotic and hillslope processes. Biogeochemistry 127, 273-289.

35. Chambers, J.Q., Tribuzy, E.S., Toledo, L.C., Crispim, B.F., Higuchi, N., dos Santos, J., Araujo, A.C., Kruijt, B., Nobre, A.D., Trumbore, S.E., 2004. Respiration from a tropical forest ecosystem: Partitioning of sources and low carbon use efficiency. Ecological Applications 14, S72-S88.

36. Chasar, L.S., Chanton, J.P., Glaser, P.H., Siegel, D.I., Rivers, J.S., 2000. Radiocarbon and stable carbon isotopic evidence for transport and transformation of dissolved organic carbon, dissolved inorganic carbon,

and CH4 in a northern Minnesota peatland. Global Biogeochemical Cycles 14, 1095-1108.

37. Coetsiers, M., Walraevens, K., 2009. A new correction model for 14C ages in aquifers with complex geochemistry – Application to the Neogene Aquifer, Belgium. Applied Geochemistry 24, 768-776.
38. Conrad, R., 2005. Quantification of methanogenic pathways using stable carbon isotopic signatures: a review and a proposal. Organic Geochemistry 36, 739-752.
39. Coplen, T.B., Brand, W.A., Gehre, M., Gröning, M., Meijer, H.A.J., Toman, B., Verkouteren, R.M., 2006. New guidelines for delta13C measurements. Analytical Chemistry 78, 2439-2441.
40. Craig, H., 1957. Isotopic standards for carbon and oxygen and correction factors for mass-spectrometric analysis of carbon dioxide. Geochimica et Cosmochimica Acta 12, 133-149.
41. Dick, D.P., Goncalves, C.N., Dalmolin, R.S.D., Knicker, H., Klamt, E., Kogel-Knaber, I., Simoes, M.L., Martin-Neto, L., 2005. Characteristics of soil organic matter of different Brazilian Ferralsols under native vegetation as a function of soil depth. Geoderma 124, 319-333.
42. Drake, H.L., Küsel, K., Matthies, C., 2006. Acetogenic Prokaryotes. Prokaryotes: A Handbook on the Biology of Bacteria, Vol 2, Third Edition, 354-420.
43. Ehleringer, J.R., Buchmann, N., Flanagan, L.B., 2000. Carbon isotope ratios in belowground carbon cycle processes. Ecological Applications 10, 412-422.
44. Eichinger, L., 1983. A Contribution to the Interpretation of C-14 Groundwater Ages Considering the Example of a Partially Confined Sandstone Aquifer. Radiocarbon 25, 347-356.
45. Eichorst, S.A., Kuske, C.R., Schmidt, T.M., 2011. Influence of Plant Polymers on the Distribution and Cultivation of Bacteria in the Phylum Acidobacteria. Applied and Environmental Microbiology 77, 586-596.
46. Ekschmitt, K., Kandeler, E., Poll, C., Brune, A., Buscot, F., Friedrich, M., Gleixner, G., Hartmann, A., Kastner, M., Marhan, S., Miltner, A., Scheu, S., Wolters, V., 2008. Soil-carbon preservation through habitat constraints and biological limitations on decomposer activity. Journal of Plant Nutrition and Soil Science 171, 27-35.
47. El-Kadi, A.I., Plummer, L.N., Aggarwal, P., 2011. NETPATH-WIN: An Interactive User Version of the Mass-Balance Model, NETPATH. Ground Water 49, 593-599.
48. Emerson, D., Fleming, E.J., McBeth, J.M., 2010. Iron-Oxidizing Bacteria: An Environmental and Genomic Perspective. Annual Review of Microbiology 64, 561-583.
49. Feisthauer, S., Wick, L.Y., Kastner, M., Kaschabek, S.R., Schlomann, M., Richnow, H.H., 2008. Differences of heterotrophic (CO2)-C-13 assimilation by Pseudomonas knackmussii strain B13 and Rhodococcus

opacus 1CP and potential impact on biomarker stable isotope probing. Environmental Microbiology 10, 1641-1651.

50. Fierer, N., Jackson, J.A., Vilgalys, R., Jackson, R.B., 2005. Assessment of soil microbial community structure by use of taxon-specific quantitative PCR assays. Applied and Environmental Microbiology 71, 4117-4120.
51. Fontes, J.C., 1992. Chemical and Isotopic Constraints on C-14 Dating of Groundwater. Radiocarbon after Four Decades, 242-261.
52. Fontes, J.C., Garnier, J.M., 1979. Determination of the Initial C-14 Activity of the Total Dissolved Carbon - Review of the Existing Models and a New Approach. Water Resources Research 15, 399-413.
53. Friedlingstein, P., Cox, P., Betts, R., Bopp, L., Von Bloh, W., Brovkin, V., Cadule, P., Doney, S., Eby, M., Fung, I., Bala, G., John, J., Jones, C., Joos, F., Kato, T., Kawamiya, M., Knorr, W., Lindsay, K., Matthews, H.D., Raddatz, T., Rayner, P., Reick, C., Roeckner, E., Schnitzler, K.G., Schnur, R., Strassmann, K., Weaver, A.J., Yoshikawa, C., Zeng, N., 2006. Climate-carbon cycle feedback analysis: Results from the (CMIP)-M-4 model intercomparison. Journal of Climate. 19, 3337-3353.
54. Fuchs, G., 2011. Alternative Pathways of Carbon Dioxide Fixation: Insights into the Early Evolution of Life?, in: Gottesman, S., Harwood, C.S. (Eds.), Annual Review of Microbiology, Vol 65, pp. 631-+.
55. Gao, P., Xu, X., Zhou, L., Pack, M.A., Griffin, S., Santos, G.M., Southon, J.R., Liu, K., 2014. Rapid sample preparation of dissolved inorganic carbon in natural waters using a headspace-extraction approach for radiocarbon analysis by accelerator mass spectrometry. Limnology and Oceanography-Methods 12, 174-190.
56. Ge, T., Wu, X., Chen, X., Yuan, H., Zou, Z., Li, B., Zhou, P., Liu, S., Tong, C., Brookes, P., Wu, J., 2013. Microbial phototrophic fixation of atmospheric CO2 in China subtropical upland and paddy soils. Geochimica et Cosmochimica Acta 113, 70-78.
57. Ge, T.D., Liu, C., Yuan, H.Z., Zhao, Z.W., Wu, X.H., Zhu, Z.K., Brookes, P., Wu, J.S., 2015. Tracking the photosynthesized carbon input into soil organic carbon pools in a rice soil fertilized with nitrogen. Plant and Soil 392, 17-25.
58. Gelwicks, J.T., Risatti, J.B., Hayes, J.M., 1989. Carbon isotope effects associated with autotrophic acetogenesis. Organic Geochemistry 14, 441-446.
59. Gillon, M., Barbecot, F., Gibert, E., Plain, C., Corcho-Alvarado, J.A., Massault, M., 2012. Controls on C-13 and C-14 variability in soil CO2. Geoderma 189, 431-441.
60. Gleixner, G., 2013. Soil organic matter dynamics: a biological perspective derived from the use of compound-specific isotopes studies. Ecological Research 28, 683-695.
61. Gleixner, G., Poirier, N., Bol, R., Balesdent, J., 2002. Molecular dynamics of organic matter in a cultivated soil. Organic Geochemistry 33, 357-366.

62. Guillaume, T., Damris, M., Kuzyakov, Y., 2015. Losses of soil carbon by converting tropical forest to plantations: erosion and decomposition estimated by delta C-13. Global Change Biology 21, 3548-3560.

63. Hahn, V., 2004. Soil carbon sequestration and CO2 flux partitioning, Chemisch-Geowissenschaftliche Fakultät. Friedrich-Schiller-Universität, Jena.

64. Han, L.-F., Plummer, L.N., Aggarwal, P., 2012. A graphical method to evaluate predominant geochemical processes occurring in groundwater systems for radiocarbon dating. Chemical Geology 318–319, 88-112.

65. Han, L.F., Plummer, L.N., 2013. Revision of Fontes & Garnier's model for the initial C-14 content of dissolved inorganic carbon used in groundwater dating. Chemical Geology 351, 105-114.

66. Han, L.F., Plummer, L.N., 2016. A review of single-sample-based models and other approaches for radiocarbon dating of dissolved inorganic carbon in groundwater. Earth-Science Reviews 152, 119-142.

67. Hanson, P.J., Edwards, N.T., Garten, C.T., Andrews, J.A., 2000. Separating root and soil microbial contributions to soil respiration: A review of methods and observations. Biogeochemistry 48, 115-146.

68. Hart, K.M., Kulakova, A.N., Allen, C.C.R., Simpson, A.J., Oppenheimer, S.F., Masoom, H., Courtier-Murias, D., Soong, R., Kulakov, L.A., Flanagan, P.V., Murphy, B.T., Kelleher, B.P., 2013. Tracking the Fate of Microbially Sequestered Carbon Dioxide in Soil Organic Matter. Environmental Science and Technology 47, 5128-5137.

69. Hayes, J.M., 2001. Fractionation of carbon and hydrogen isotopes in biosynthetic processes. Reviews in Mineralogy and Geochemistry 43, 225-277.

70. Heimann, M., Reichstein, M., 2008. Terrestrial ecosystem carbon dynamics and climate feedbacks. Nature 451, 289-292.

71. Herrmann, M., Hädrich, A., Küsel, K., 2012. Predominance of thaumarchaeal ammonia oxidizer abundance and transcriptional activity in an acidic fen. Environmental Microbiology 14, 3013-3025.

72. Herrmann, M., Rusznyak, A., Akob, D.M., Schulze, I., Opitz, S., Totsche, K.U., Kusel, K., 2015. Large Fractions of CO2-Fixing Microorganisms in Pristine Limestone Aquifers Appear To Be Involved in the Oxidation of Reduced Sulfur and Nitrogen Compounds. Applied and Environmental Microbiology 81, 2384-2394.

73. Hornibrook, E.R.C., Longstaffe, F.J., Fyfe, W.S., Bloom, Y., 2000. Carbon-isotope ratios and carbon, nitrogen and sulfur abundances in flora and soil organic matter from a temperate-zone bog and marsh. Geochemical Journal 34, 237-245.

74. Hughen, K., Lehman, S., Southon, J., Overpeck, J., Marchal, O., Herring, C., Turnbull, J., 2004. C-14 activity and global carbon cycle changes over the past 50,000 years. Science 303, 202-207.

75. Hutchins, B.T., Engel, A.S., Nowlin, W.H., Schwartz, B.F., 2016. Chemolithoautotrophy supports macroinvertebrate food webs and affects diversity and stability in groundwater communities. Ecology, 97(6), 1530-42.

76. IAEA, 2009. Sampling Procedures for Isotope Hydrology. International Atomic Energy Agency, Vienna.

77. Iino, T., Mori, K., Uchino, Y., Nakagawa, T., Harayama, S., Suzuki, K.-i., 2010. Ignavibacterium album gen. nov., sp nov., a moderately thermophilic anaerobic bacterium isolated from microbial mats at a terrestrial hot spring and proposal of Ignavibacteria classis nov., for a novel lineage at the periphery of green sulfur bacteria. International Journal of Systematic and Evolutionary Microbiology 60, 1376-1382.

78. Imhoff, J.F., 2006. The Phototrophic Alpha-Proteobacteria, in: Dworkin, M., Falkow, S., Rosenberg, E., Schleifer, K.-H., Stackebrandt, E. (Eds.), The Prokaryotes: Volume 5: Proteobacteria: Alpha and Beta Subclasses. Springer New York, 41-64.

79. Jewell, T.N.M., Karaoz, U., Brodie, E.L., Williams, K.H., Beller, H.R., 2016. Metatranscriptomic evidence of pervasive and diverse chemolithoautotrophy relevant to C, S, N and Fe cycling in a shallow alluvial aquifer. ISME Journal 10, 2106-2117.

80. Jobbagy, E.G., Jackson, R.B., 2000. The vertical distribution of soil organic carbon and its relation to climate and vegetation. Ecological Applications 10, 423-436.

81. Kaiser, E.A., Mueller, T., Joergensen, R.G., Insam, H., Heinemeyer, O., 1992. Evaluation of methods to estimate the soil microbial biomass and the relationship with soil texture and organic matter. Soil Biology and Biochemistry 24, 675-683.

82. Kaiser, K., Kalbitz, K., 2012. Cycling downwards - dissolved organic matter in soils. Soil Biology & Biochemistry 52, 29-32.

83. Kalbitz, K., Geyer, S., Gehre, M., 2000. Land use impacts on the isotopic signature (C-13, C-14, N-15) of water-soluble fulvic acids in a German fen area. Soil Science. 165, 728-736.

84. Kämpf, H., Bräuer, K., Schumann, J., Hahne, K., Strauch, G., 2013. CO2 discharge in an active, non-volcanic continental rift area (Czech Republic): Characterisation (delta13C, 3He/4He) and quantification of diffuse and vent CO2 emissions. Chemical Geology 339, 71-83.

85. Kellermann, C., Selesi, D., Lee, N., Hügler, M., Esperschütz, J., Hartmann, A., Griebler, C., 2012. Microbial CO2 fixation potential in a tar-oil-contaminated porous aquifer. FEMS Microbiology Ecology 81, 172-187.

86. Kersters, K., De Vos, P., Gillis, M., Swings, J., Vandamme, P., Stackebrandt, E., 2006. Introduction to the Proteobacteria, in: Dworkin, M., Falkow, S., Rosenberg, E., Schleifer, K.-H., Stackebrandt, E. (Eds.), The Prokaryotes: Volume 5: Proteobacteria: Alpha and Beta Subclasses. Springer New York, pp. 3-37.

87. Kilian, M.R., VanDerPlicht, J., VanGeel, B., 1995. Dating raised bogs: New aspects of AMS C-14 wiggle matching, a reservoir effect and climatic change. Quaternary Science Reviews 14, 959-966.

88. Kodama, Y., Watanabe, K., 2004. Sulfuricurvum kujiense gen. nov., sp nov., a facultatively anaerobic, chemolithoautotrophic, sulfur-oxidizing bacterium isolated from an underground crude-oil storage cavity. International Journal of Systematic and Evolutionary Microbiology 54, 2297-2300.

89. Kogel-Knabner, I., 2002. The macromolecular organic composition of plant and microbial residues as inputs to soil organic matter. Soil Biology & Biochemistry 34, 139-162.

90. Kohlhepp, B., Lehmann, R., Seeber, P., Küsel, K., Trumbore, S.E., Totsche, K.U., 2016. Pedological and hydrogeological setting and subsurface flow structure of the carbonate-rock CZE Hainich in western Thuringia, Germany. Hydrology and Earth System Sciences Discussions 2016, 1-32.

91. Kojima, H., Fukui, M., 2011. Sulfuritalea hydrogenivorans gen. nov., sp nov., a facultative autotroph isolated from a freshwater lake. International Journal of Systematic and Evolutionary Microbiology 61, 1651-1655.

92. Kracht, O., Gleixner, G., 2000. Isotope analysis of pyrolysis products from Sphagnum peat and dissolved organic matter from bog water. Organic Geochemistry 31, 645-654.

93. Kramer, C., Gleixner, G., 2006. Variable use of plant- and soil-derived carbon by microorganisms in agricultural soils. Soil Biology and Biochemistry 38, 3267-3278.

94. Kramer, C., Gleixner, G., 2008. Soil organic matter in soil depth profiles: Distinct carbon preferences of microbial groups during carbon transformation. Soil Biology and Biochemistry 40, 425-433.

95. Krüger, J.P., Leifeld, J., Alewell, C., 2014. Degradation changes stable carbon isotope depth profiles in palsa peatlands. Biogeosciences 11, 3369-3380.

96. Krull, E.S., Bestland, E.A., Gates, W.P., 2002. Soil organic matter decomposition and turnover in a tropical Ultisol: Evidence from delta C-13, delta N-15 and geochemistry. Radiocarbon 44, 93-112.

97. Krull, E.S., Retallack, G.J., 2000. delta C-13 depth profiles from paleosols across the Permian-Triassic boundary: Evidence for methane release. Geological Society of America Bulletin 112, 1459-1472.

98. Küsel, K., Drake, H.L., 1995. Effects of environmental parameters on the formation and turnover of acetate by forest soils. Applied and Environmental Microbiology 61, 3667-3675.

99. Küsel, K., Totsche, K.U., Trumbore, S.E., Lehmann, R., Steinhäuser, C., Herrmann, M., 2016. How deep can surface signals be traced in the critical zone? Merging biodiversity with biogeochemistry research in a central German Muschelkalk landscape. Frontiers in Earth Science 4.

100. Lange, M., Eisenhauer, N., Sierra, C.A., Bessler, H., Engels, C., Griffiths, R.I., Mellado-Vázquez, P.G., Malik, A.A., Roy, J., Scheu, S., Steinbeiss, S., Thomson, B.C., Trumbore, S.E., Gleixner, G., 2015. Plant diversity increases soil microbial activity and soil carbon storage. Nature Communications 6, 6707.

101. Lazar, C., Wenke, S., Lehmann, R., Herrmann, M., Schwab, V., Totsche, K.U., Akob, D.M., Küsel, K., 2016a. Ecophysiology of uncultured Archaea in groundwater and carbonate rocks.

102. Lazar, C.S., Baker, B.J., Seitz, K., Hyde, A.S., Dick, G.J., Hinrichs, K.U., Teske, A.P., 2016b. Genomic evidence for distinct carbon substrate preferences and ecological niches of Bathyarchaeota in estuarine sediments. Environmental Microbiology 18, 1200-1211.

103. Le Quere, C., Moriarty, R., Andrew, R.M., Canadell, J.G., Sitch, S., Korsbakken, J.I., Friedlingstein, P., Peters, G.P., Andres, R.J., Boden, T.A., Houghton, R.A., House, J.I., Keeling, R.F., Tans, P., Arneth, A., Bakker, D.C.E., Barbero, L., Bopp, L., Chang, J., Chevallier, F., Chini, L.P., Ciais, P., Fader, M., Feely, R.A., Gkritzalis, T., Harris, I., Hauck, J., Ilyina, T., Jain, A.K., Kato, E., Kitidis, V., Goldewijk, K.K., Koven, C., Landschutzer, P., Lauvset, S.K., Lefevre, N., Lenton, A., Lima, I.D., Metzl, N., Millero, F., Munro, D.R., Murata, A., Nabel, J.E.M.S., Nakaoka, S., Nojiri, Y., O'Brien, K., Olsen, A., Ono, T., Perez, F.F., Pfeil, B., Pierrot, D., Poulter, B., Rehder, G., Rodenbeck, C., Saito, S., Schuster, U., Schwinger, J., Seferian, R., Steinhoff, T., Stocker, B.D., Sutton, A.J., Takahashi, T., Tilbrook, B., van der Laan-Luijkx, I.T., van der Werf, G.R., van Heuven, S., Vandemark, D., Viovy, N., Wiltshire, A., Zaehle, S., Zeng, N., 2015. Global Carbon Budget 2015. Earth System Science Data 7, 349-396.

104. Limpens, J., Berendse, F., Blodau, C., Canadell, J.G., Freeman, C., Holden, J., Roulet, N., Rydin, H., Schaepman-Strub, G., 2008. Peatlands and the carbon cycle: from local processes to global implications - a synthesis. Biogeosciences 5, 1475-1491.

105. Liu, F.H., Conrad, R., 2011. Chemolithotrophic acetogenic H-2/CO2 utilization in Italian rice field soil. Isme Journal 5, 1526-1539.

106. Ludwig, M., Achtenhagen, J., Miltner, A., Eckhardt, K.U., Leinweber, P., Emmerling, C., Thiele-Bruhn, S., 2015. Microbial contribution to SOM quantity and quality in density fractions of temperate arable soils. Soil Biology & Biochemistry 81, 311-322.

107. Lueders, T., Manefield, M., Friedrich, M.W., 2004. Enhanced sensitivity of DNA- and rRNA-based stable isotope probing by fractionation and quantitative analysis of isopycnic centrifugation gradients. Environmental Microbiology 6, 73-78.

108. Mailloux, B.J., Trembath-Reichert, E., Cheung, J., Watson, M., Stute, M., Freyer, G.A., Ferguson, A.S., Ahmed, K.M., Alam, M.J., Buchholz, B.A., Thomas, J., Layton, A.C., Zheng, Y., Bostick, B.C., van Geen, A., 2013. Advection of surface-derived organic carbon fuels microbial reduction in Bangladesh groundwater. Proceedings of the National Academy of Sciences of the United States of America 110, 5331-5335.

109. Malik, A., Gleixner, G., 2013. Importance of microbial soil organic matter processing in dissolved organic carbon production. Fems Microbiology Ecology 86, 139-148.

110. Marfia, A.M., Krishnamurthy, R.V., Atekwana, E.A., Panton, W.F., 2004. Isotopic and geochemical evolution of ground and surface waters in a karst dominated geological setting: A case study from Belize, Central America. Applied Geochemistry 19, 937-946.

111. Martinelli, L.A., Pessenda, L.C.R., Espinoza, E., Camargo, P.B., Telles, E.C., Cerri, C.C., Victoria, R.L., Aravena, R., Richey, J., Trumbore, S., 1996. Carbon-13 variation with depth in soils of Brazil and climate change during the quaternary. Oecologia 106, 376-381.

112. Matter, J.M., Stute, M., Snæbjörnsdottir, S.Ó., Oelkers, E.H., Gislason, S.R., Aradottir, E.S., Sigfusson, B., Gunnarsson, I., Sigurdardottir, H., Gunnlaugsson, E., Axelsson, G., Alfredsson, H.A., Wolff-Boenisch, D., Mesfin, K., Taya, D.F.d.l.R., Hall, J., Dideriksen, K., Broecker, W.S., 2016. Rapid carbon mineralization for permanent disposal of anthropogenic carbon dioxide emissions. Science 352, 1312-1314.

113. McCutchan, J.H., Lewis, W.M., Kendall, C., McGrath, C.C., 2003. Variation in trophic shift for stable isotope ratios of carbon, nitrogen, and sulfur. Oikos 102, 378-390.

114. Melzer, E., Oleary, M.H., 1987. Anapleurotic Co2 Fixation by Phosphoenolpyruvate Carboxylase in C-3 Plants. Plant Physiology 84, 58-60.

115. Miller, H.M., Matter, J.M., Kelemen, P., Ellison, E.T., Conrad, M.E., Fierer, N., Ruchala, T., Tominaga, M., Templeton, A.S., 2016. Modern water/rock reactions in Oman hyperalkaline peridotite aquifers and implications for microbial habitability. Geochimica Et Cosmochimica Acta 179, 217-241.

116. Miltner, A., Bombach, P., Schmidt-Brucken, B., Kastner, M., 2012. SOM genesis: microbial biomass as a significant source. Biogeochemistry 111, 41-55.

117. Miltner, A., Kopinke, F.D., Kindler, R., Selesi, D.E., Hartmann, A., Kastner, M., 2005. Non-phototrophic CO2 fixation by soil microorganisms. Plant and Soil 269, 193-203.

118. Miltner, A., Richnow, H.H., Kopinke, F.D., Kastner, M., 2004. Assimilation of CO2 by soil microorganisms and transformation into soil organic matter. Organic Geochemistry 35, 1015-1024.

119. Mook, W.G., Bommerso.Jc, Staverma.Wh, 1974. Carbon Isotope Fractionation between Dissolved Bicarbonate and Gaseous Carbon-Dioxide. Earth and Planetary Science Letters 22, 169-176.

120. Mook, W.G., van der Plicht, J., 1999. Reporting C-14 activities and concentrations. Radiocarbon 41, 227-239.

121. Nanba, K., King, G.M., Dunfield, K., 2004. Analysis of facultative lithotroph distribution and diversity on volcanic deposits by use of the

large subunit of ribulose 1,5-bisphosphate carboxylase/oxygenase. Applied and Environmental Microbiology 70, 2245-2253.

122. Nepstad, D.C., Decarvalho, C.R., Davidson, E.A., Jipp, P.H., Lefebvre, P.A., Negreiros, G.H., Dasilva, E.D., Stone, T.A., Trumbore, S.E., Vieira, S., 1994. The Role of Deep Roots in the Hydrological and Carbon Cycles of Amazonian Forests and Pastures. Nature 372, 666-669.

123. Nowak, M.E., Beulig, F., von Fischer, J., Muhr, J., Küsel, K., Trumbore, S.E., 2015. Autotrophic fixation of geogenic CO2 by microorganisms contributes to soil organic matter formation and alters isotope signatures in a wetland mofette. Biogeosciences 12, 7169-7183.

124. NRC, N.R.C., 2001. Basic research opportunities in earth science. National Academy Press, Washington DC.

125. Ogee, J., Peylin, P., Cuntz, M., Bariac, T., Brunet, Y., Berbigier, P., Richard, P., Ciais, P., 2004. Partitioning net ecosystem carbon exchange into net assimilation and respiration with canopy-scale isotopic measurements: An error propagation analysis with (CO2)-C-13 and (COO)-O-18 data. Global Biogeochemical Cycles 18.

126. Pancost, R.D., Damste, J.S.S., 2003. Carbon isotopic compositions of prokaryotic lipids as tracers of carbon cycling in diverse settings. Chemical Geology 195, 29-58.

127. Pancost, R.D., van Geel, B., Baas, M., Damste, J.S.S., 2000. delta C-13 values and radiocarbon dates of microbial biomarkers as tracers for carbon recycling in peat deposits. Geology 28, 663-666.

128. Parry, M.L., Canziani, O.F., Palutikof, J.P., Linden, v.d., Hansin, C.E., 2007. Contribution of Working Group II to the Fourth Assessment Report of the Intergovernmental Panel on Climate Change. Cambridge University Press, Cambridge, United Kingdom and New York, NY, USA.

129. Plummer, L.N., Prestemon, E.C., Parkhurst, D.L., 1992. Netpath - an Interactive Code for Interpreting Net Geochemical Reactions from Chemical and Isotopic Data Along a Flow Path. Water-Rock Interaction, Vols 1 and 2, 239-242.

130. Pratscher, J., Dumont, M.G., Conrad, R., 2011. Ammonia oxidation coupled to CO2 fixation by archaea and bacteria in an agricultural soil. Proceedings of the National Academy of Sciences of the United States of America 108, 4170-4175.

131. Quaiser, A., Ochsenreiter, T., Lanz, C., Schuster, S.C., Treusch, A.H., Eck, J., Schleper, C., 2003. Acidobacteria form a coherent but highly diverse group within the bacterial domain: evidence from environmental genomics. Molecular Microbiology 50, 563-575.

132. Quesada, C.A., Lloyd, J., Anderson, L.O., Fyllas, N.M., Schwarz, M., Czimczik, C.I., 2011. Soils of Amazonia with particular reference to the RAINFOR sites. Biogeosciences 8, 1415-1440.

133. Ragsdale, S.W., Pierce, E., 2008. Acetogenesis and the Wood-Ljungdahl pathway of CO2 fixation. Biochimica et Biophysica Acta-Proteins and Proteomics 1784, 1873-1898.

134. Rennert, T., Eusterhues, K., Pfanz, H., Totsche, K.U., 2011. Influence of geogenic CO2 on mineral and organic soil constituents on a mofette site in the NW Czech Republic. European Journal of Soil Science 62, 572-580.

135. Rethemeyer, J., Kramer, C., Gleixner, G., John, B., Yamashita, T., Flessa, H., Andersen, N., Nadeau, M.J., Grootes, P.M., 2005. Transformation of organic matter in agricultural soils: radiocarbon concentration versus soil depth. Geoderma 128, 94-105.

136. Richter, D.D., Markewitz, D., Trumbore, S.E., Wells, C.G., 1999. Rapid accumulation and turnover of soil carbon in a re-establishing forest. Nature 400, 56-58.

137. Rillig, M.C., Wright, S.F., Nichols, K.A., Schmidt, W.F., Torn, M.S., 2001. Large contribution of arbuscular mycorrhizal fungi to soil carbon pools in tropical forest soils. Plant and Soil 233, 167-177.

138. Risk, D., Nickerson, N., Phillips, C.L., Kellman, L., Moroni, M., 2012. Drought alters respired delta(CO2)-C-13 from autotrophic, but not heterotrophic soil respiration. Soil Biology & Biochemistry 50, 26-32.

139. Robinson, J.J., Scott, K.M., Swanson, S.T., O'Leary, M.H., Horken, K., Tabita, F.R., Cavanaugh, C.M., 2003. Kinetic isotope effect and characterization of form II RubisCO from the chemoautotrophic endosymbionts of the hydrothermal vent tubeworm Riftia pachyptila. Limnology and Oceanography 48, 48-54.

140. Rumpel, C., Kogel-Knabner, I., 2011. Deep soil organic matter-a key but poorly understood component of terrestrial C cycle. Plant and Soil 338, 143-158.

141. Saini, R., Kapoor, R., Kumar, R., Siddiqi, T.O., Kumar, A., 2011. CO2 utilizing microbes - A comprehensive review. Biotechnology Advances 29, 949-960.

142. Sanderman, J., Amundson, R., 2008. A comparative study of dissolved organic carbon transport and stabilization in California forest and grassland soils. Biogeochemistry 89, 309-327.

143. Santana, R.H., Catao, E.C.P., Lopes, F.A.C., Constantino, R., Barreto, C.C., Kruger, R.H., 2015. The Gut Microbiota of Workers of the Litter-Feeding Termite Syntermes wheeleri (Termitidae: Syntermitinae): Archaeal, Bacterial, and Fungal Communities. Microbial Ecology. 70, 545-556.

144. Santruckova, H., Bird, M.I., Elhottova, D., Novak, J., Picek, T., Simek, M., Tykva, R., 2005. Heterotrophic fixation of CO2 in soil. Microbial Ecology. 49, 218-225.

145. Scheibe, A., Krantz, L., Gleixner, G., 2012. Simultaneous determination of the quantity and isotopic signature of dissolved organic

matter from soil water using high-performance liquid chromatography/isotope ratio mass spectrometry. Rapid Communications in Mass Spectrometry 26, 173-180.

146. Schiff, S.L., Aravena, R., Trumbore, S.E., Hinton, M.J., Elgood, R., Dillon, P.J., 1997. Export of DOC from forested catchments on the Precambrian Shield of Central Ontario: Clues from C-13 and C-14. Biogeochemistry 36, 43-65.

147. Schimel, J., Schaeffer, S.M., 2012. Microbial control over carbon cycling in soil. Frontiers in Microbiology 3.

148. Schmidt, M.W.I., Torn, M.S., Abiven, S., Dittmar, T., Guggenberger, G., Janssens, I.A., Kleber, M., Kogel-Knabner, I., Lehmann, J., Manning, D.A.C., Nannipieri, P., Rasse, D.P., Weiner, S., Trumbore, S.E., 2011. Persistence of soil organic matter as an ecosystem property. Nature 478, 49-56.

149. Schrumpf, M., Kaiser, K., Guggenberger, G., Persson, T., Kogel-Knabner, I., Schulze, E.D., 2013. Storage and stability of organic carbon in soils as related to depth, occlusion within aggregates, and attachment to minerals. Biogeosciences 10, 1675-1691.

150. Schulten, H.R., Gleixner, G., 1999. Analytical pyrolysis of humic substances and dissolved organic matter in aquatic systems: structure and origin. Water Research 33, 2489-2498.

151. Schwab, V., Roth, V.-N., Gleixner, G., Lehmann, R., Pohnert, G., Trumbore, E.S., Küsel, K., Totsche, K.U., 2016. Functional diversity of microbial communities in pristine aquifers: phospholipid fatty acid distribution and d13C values related to substrate utilization patterns (submitted).

152. Selesi, D., Pattis, I., Schmid, M., Kandeler, E., Hartmann, A., 2007. Quantification of bacterial RubisCO genes in soils by cbbL targeted real-time PCR. J Microbiological Methods 69, 497-503.

153. Selesi, D., Schmid, M., Hartmann, A., 2005. Diversity of green-like and red-like ribulose-1,5-bisphosphate carboxylase/oxygenase large-subunit genes (cbbL) in differently managed agricultural soils. Applied and Environmental Microbiology 71, 175-184.

154. Simkus, D.N., Slater, G.F., Lollar, B.S., Wilkie, K., Kieft, T.L., Magnabosco, C., Lau, M.C.Y., Pullin, M.J., Hendrickson, S.B., Wommack, K.E., Sakowski, E.G., van Heerden, E., Kuloyo, O., Linage, B., Borgonie, G., Onstott, T.C., 2016. Variations in microbial carbon sources and cycling in the deep continental subsurface. Geochimica Et Cosmochimica Acta 173, 264-283.

155. Simpson, A.J., Simpson, M.J., Smith, E., Kelleher, B.P., 2007. Microbially Derived Inputs to Soil Organic Matter: Are Current Estimates Too Low? Environmental Science and Technology 41, 8070-8076.

156. Six, J., Conant, R.T., Paul, E.A., Paustian, K., 2002. Stabilization mechanisms of soil organic matter: Implications for C-saturation of soils. Plant Soil 241, 155-176.

157. Smith, K.S., Jakubzick, C., Whittam, T.S., Ferry, J.G., 1999. Carbonic anhydrase is an ancient enzyme widespread in prokaryotes. P Natl Acad Sci USA 96, 15184-15189.

158. Sombroek, W.G., Nachtergaele, F.O., Hebel, A., 1993. Amounts, Dynamics and Sequestering of Carbon in Tropical and Subtropical Soils. Ambio 22, 417-426.

159. Stackebrandt, E., Sproer, C., Rainey, F.A., Burghardt, J., Pauker, O., Hippe, H., 1997. Phylogenetic analysis of the genus Desulfotomaculum: Evidence for the misclassification of Desulfotomaculum guttoideum and description of Desulfotomaculum orientis as Desulfosporosinus orientis gen. nov., comb. nov. Int J Syst Bacteriol 47, 1134-1139.

160. Stein, S., Selesi, D., Schilling, R., Pattis, I., Schmid, M., Hartmann, A., 2005. Microbial activity and bacterial composition of H-2-treated soils with net CO2 fixation. Soil Biology & Biochemistry 37, 1938-1945.

161. Steinhof, A., Adamiec, G., Gleixner, G., van Klinken, G.J., Wagner, T., 2004. The new C-14 analysis laboratory in Jena, Germany. Radiocarbon 46, 51-58.

162. Tamers, M.A., Stipp, J.J., Weiner, R., 1975. Radiocarbon Ages of Ground-Water as a Basis for Determination of Safe Limits of Aquifer Exploitation. Environ Res 9, 250-264.

163. Telles, E.D.C., de Camargo, P.B., Martinelli, L.A., Trumbore, S.E., da Costa, E.S., Santos, J., Higuchi, N., Oliveira, R.C., 2003. Influence of soil texture on carbon dynamics and storage potential in tropical forest soils of Amazonia. Global Biogeochemical Cycles 17.

164. Tolli, J., King, G.M., 2005. Diversity and structure of bacterial chemolithotrophic communities in pine forest and agroecosystem soils. Applied and Environmental Microbiology 71, 8411-8418.

165. Torn, M.S., Kleber, M., Zavaleta, E.S., Zhu, B., Field, C.B., Trumbore, S.E., 2013. A dual isotope approach to isolate soil carbon pools of different turnover times. Biogeosciences 10, 8067-8081.

166. Torn, M.S., Trumbore, S.E., Chadwick, O.A., Vitousek, P.M., Hendricks, D.M., 1997. Mineral control of soil organic carbon storage and turnover. Nature 389, 170-173.

167. Trumbore, S., 2000. Age of soil organic matter and soil respiration: Radiocarbon constraints on belowground C dynamics. Ecol Appl 10, 399-411.

168. Trumbore, S., 2006. Carbon respired by terrestrial ecosystems - recent progress and challenges. Global Change Biology 12, 141-153.

169. Trumbore, S., 2009. Radiocarbon and Soil Carbon Dynamics. Annu Rev Earth Pl Sc 37, 47-66.

170. Trumbore, S., Da Costa, E.S., Nepstad, D.C., De Camargo, P.B., Martinelli, L.I.Z.A., Ray, D., Restom, T., Silver, W., 2006. Dynamics of fine root carbon in Amazonian tropical ecosystems and the contribution of roots to soil respiration. Global Change Biology 12, 217-229.

171. Trumbore, S.E., Czimczik, C.I., 2008. Geology - An uncertain future for soil carbon. Science 321, 1455-1456.

172. Trumbore, S.E., Davidson, E.A., Decamargo, P.B., Nepstad, D.C., Martinelli, L.A., 1995. Belowground Cycling of Carbon in Forests and Pastures of Eastern Amazonia. Global Biogeochemical Cycles 9, 515-528.

173. Trumbore, S.E., Sierra, C.A., Hicks Pries, C.E., 2016. Radiocarbon Nomenclature, Theory, Models, and Interpretation: Measuring Age, Determining Cycling Rates, and Tracing Source Pools, in: Schuur, A.G.E., Druffel, E., Trumbore, E.S. (Eds.), Radiocarbon and Climate Change: Mechanisms, Applications and Laboratory Techniques. Springer International Publishing, Cham, pp. 45-82.

174. van Breukelen, B.M., Griffioen, J., Röling, W.F.M., van Verseveld, H.W., 2004. Reactive transport modelling of biogeochemical processes and carbon isotope geochemistry inside a landfill leachate plume. Journal of Contaminant Hydrology 70, 249-269.

175. Vance, E.D., Brookes, P.C., Jenkinson, D.S., 1987. An extraction method for measuring soil microbial biomass-C. Soil Biology & Biochemistry 19, 703-707.

176. Wallander, H., Nilsson, L.O., Hagerberg, D., Rosengren, U., 2003. Direct estimates of C:N ratios of ectomycorrhizal mycelia collected from Norway spruce forest soils. Soil Biology and Biochemistry 35, 997-999.

177. Werth, M., Kuzyakov, Y., 2010. C-13 fractionation at the root-microorganisms-soil interface: A review and outlook for partitioning studies. Soil Biology & Biochemistry 42, 1372-1384.

178. Whiticar, M.J., 1999. Carbon and hydrogen isotope systematics of bacterial formation and oxidation of methane. Chemical Geology 161, 291-314.

179. Wigley, T.M.L., 1976. Effect of Mineral Precipitation on Isotopic Composition and C-14 Dating of Groundwater. Nature 263, 219-221.

180. Wood, H.G., Werkman, C.H., Hemingway, A., Nier, A.O., 1941. Heavy carbon as a tracer in heterotrophic carbon dioxide assimilation. Journal of Biological Chemistry 139, 365-376.

181. Wu, X., Ge, T., Wang, W., Yuan, H., Wegner, C.E., Zhu, Z., Whiteley, A.S., Wu, J., 2015a. Cropping systems modulate the rate and magnitude of soil microbial autotrophic CO_2 fixation in soil. Frontiers in Microbiology 6.

182. Wu, X.H., Ge, T.D., Wang, W., Yuan, H.Z., Wegner, C.E., Zhu, Z.K., Whiteley, A.S., Wu, J.S., 2015b. Cropping systems modulate the rate and magnitude of soil microbial autotrophic CO_2 fixation in soil. Frontiers in Microbiology 6.

183. Wu, X.H., Ge, T.D., Yuan, H.Z., Li, B.Z., Zhu, H.H., Zhou, P., Sui, F.G., O'Donnell, A.G., Wu, J.S., 2014. Changes in bacterial CO2 fixation with depth in agricultural soils. Applied Microbiology and Biotechnology 98, 2309-2319.

184. Yakir, D., Sternberg, L.D.L., 2000. The use of stable isotopes to study ecosystem gas exchange. Oecologia 123, 297-311.

185. Ye, R.Z., Jin, Q.S., Bohannan, B., Keller, J.K., Bridgham, S.D., 2014. Homoacetogenesis: A potentially underappreciated carbon pathway in peatlands. Soil Biology & Biochemistry 68, 385-391.

186. Young, I.M., Crawford, J.W., 2004. Interactions and Self-Organization in the Soil-Microbe Complex. Science 304, 1634.

187. Yuan, H.Z., Ge, T.D., Chen, C.Y., O'Donnell, A.G., Wu, J.S., 2012. Significant Role for Microbial Autotrophy in the Sequestration of Soil Carbon. Applied and Environmental Microbiology 78, 2328-2336.

10 Selbstständigkeitserklärung

Ich erkläre, dass ich die vorliegende Arbeit selbständig und unter Verwendung der angegebenen Hilfsmittel, persönlichen Mitteilungen und Quellen angefertigt habe.

Jena,

Martin Nowak

11 Curiculum vitae

Name: Martin Nowak
Date of birth: 10.09.1983
Place of birth: Mikołow, Poland

Education

06/2013 - 12/2016	PhD student: Department for Biogeochemical Processes, Max Planck Institute for Biogeochemistry, Jena, Germany
02/2009 - 09/2009	Study abroad at AGH University of Science and Technology Cracow
10/2005 - 05/2011	Study of Geology and Palaeontology at Friedrich Alexander University Erlangen/Nürnberg
09/1995 - 07/2004	High School Franz Ludwig Gymnasium Bamberg

Working Experience

02/2012 - 05/2013	Scientific Staff member at Geocentre of Northern Bavaria Erlangen Nürnberg in the CCS Project CO_2MAN
06/2011 - 02/2012	Geologist for Gesellschaft für Internationale Zusammenarbeit in Saudi Arabia

Awards and Grants

06/2013 - 12/2016	Associated PhD student at the International Max Planck Research School on Global Biogeochemical Cycles (IMPRS-gBGC)
06/2013 - 03/2016	DFG Fellowship for PhD in the research training group “Alternation and element mobility at the microbe-mineral interface”.

Martin Nowak

Publications:

Nowak, M., Myrttinen, A., Van Geldern, R., Becker, V., Mayer, B., Barth, J. A. C., 2013. A brief overview of isotope measurements carried out at various CCS pilot sites worldwide, in Hou, M.Z., Xie, H., Were, P. (Eds.), Clean Energy Systems in the Subsurface: Production, Storage and Conversion. Springer, New York, pp. 75-87

Nowak, M., Myrttinen, A., Van Geldern, R., Becker, V., Mayer, B., Barth, J. A. C., 2013. A brief overview of isotope measurements carried out at various CCS pilot sites worldwide, in Hou, M.Z., Xie, H., Were, P. (Eds.), Clean Energy Systems in the Subsurface: Production, Storage and Conversion. Springer, New York, pp. 75-87.

Nowak, M., Myrttinen, A., Zimmer, M., Wiese, B., Barth, J.A.C., 2013. Well-based geochemical leackage monitoring of an aquifer immediately above a CO_2 storage reservoir by stable carbon isotopes at the Ketzin pilot site, Germany. Energy Procedia 40, 346-354

Wiese, B., Zimmer, M., Nowak, M., Pellizzari, L., and Pilz, P.: Well-based hydraulic and geochemical monitoring of the above zone of the CO2 reservoir at Ketzin, Germany, Environmental Earth Sciences, 70, 3709-3726, 2013.

Nowak, M. E., van Geldern, R., Myrttinen, A., Zimmer, M., and Barth, J. A. C.: High-resolution stable carbon isotope monitoring indicates variable flow dynamic patterns in a deep saline aquifer at the Ketzin pilot site (Germany), Applied Geochemistry, 47, 44-51, 2014.

van Geldern, R., Nowak, M. E., Zimmer, M., Szizybalski, A., Myrttinen, A., Barth, J. A. C., and Jost, H. J.: Field-Based Stable Isotope Analysis of Carbon Dioxide by Mid-Infrared Laser Spectroscopy for Carbon Capture and Storage Monitoring, Anal Chem, 86, 12191-12198, 2014.

Nowak, M. E., Beulig, F., von Fischer, J., Muhr, J., Küsel, K., and Trumbore, S. E.: Autotrophic fixation of geogenic CO_2 by microorganisms contributes to soil organic matter formation and alters isotope signatures in a wetland mofette, Biogeosciences, 12, 7169-7183, 2015.

Barth, J. A. C., Nowak, M. E., Zimmer, M., Norden, B., and van Geldern, R.: Monitoring of cap-rock integrity during CCS from field data at the Ketzin pilot site (Germany): Evidence from gas composition and stable carbon isotopes, International Journal of Greenhouse Gas Control, 43, 133-140, 2015.

Beulig, F., Urich, T., Nowak, M., Trumbore, S. E., Gleixner, G., Gilfillan, G. D., Fjelland, K. E., and Küsel, K.: Altered carbon turnover processes and microbiomes in soils under long-term extremely high CO2 exposure, Nature Microbiology, 1, 15025, 2016.